SKB

# TECHNICAL REPORT 87-21

## Hydrochemical investigations in crystalline bedrock in relation to existing hydraulic conditions: Klipperås test-site, Småland, Southern Sweden

John Smellie[1]
Nils-Åke Larsson[1]
Peter Wikberg[3]
Ignasi Puigdomènech[4]
Eva-Lena Tullborg[2]

[1]Swedish Geological Company, Uppsala
[2]Swedish Geological Company, Göteborg
[3]Royal Institute of Technology, Stockholm
[4]Studsvik Energiteknik AB, Nyköping

September 1987

**SVENSK KÄRNBRÄNSLEHANTERING AB**
*SWEDISH NUCLEAR FUEL AND WASTE MANAGEMENT CO*

BOX 5864 S-102 48 STOCKHOLM
TEL 08-665 28 00 TELEX 13108-SKB

# HYDROCHEMICAL INVESTIGATIONS IN CRYSTALLINE BEDROCK IN RELATION TO EXISTING HYDRAULIC CONDITIONS

## KLIPPERÅS TEST-SITE, SMÅLAND, SOUTHERN SWEDEN

John Smellie[1]
Nils-Åke Larsson[1]
Peter Wikberg[3]
Ignasi Puigdomenech[4]
Eva-Lena Tullborg[2]

1987-09-18

1 Swedish Geological Company, Uppsala
2 Swedish Geological Company, Göteborg
3 Royal Institute of Technology, Stockholm
4 Studsvik Energiteknik AB, Nyköping

CONTENTS Page

ABSTRACT

From a total of 14 cored boreholes drilled at the Klipperås test-site area, three were selected for hydrochemical characterisation; boreholes Kl 1, Kl 2 and Kl 9. From these holes, 7 conductive borehole sections were isolated and sampled, one each from Kl 1 and Kl 9, and the remaining 5 from Kl 2. The location and extension of the conductive fracture zones were greatly facilitated by borehole tubewave (borehole Kl 2) and radar (boreholes Kl 1, Kl 2 and Kl 9) techniques.

Of these 7 borehole sections sampled, the water budget calculations predicted that four should result in representative groundwaters, one possible representative groundwater, and two unrepresentative groundwaters. Groundwaters which are here considered representative are defined as those which show no evidence of mixing with other water sources, whether from drilling water, younger, near-surface water, or other deeper groundwaters. Taking into consideration the groundwater chemistry and available isotopic data, it was possible to support the water budget calculations for 3 of the 4 representative sections; inadequate pumping time to remove all the residual drilling water was the most obvious reason for the unacceptance of the remaining section. What all 3 representative levels have in common is a positive head deviation and moderate hydraulic conductivities between $7 \times 10^{-10}$ to $9 \times 10^{-8}$ m/s. Those horizons, characterised by high conductivity but negative head, may eventually yield a representative sample, but only after considerably longer pumping intervals than the periods usually employed for sampling purposes.

Plugging of borehole Kl 2 to minimise open-hole effects during the time-lag between drilling and sampling, which in this case amounted to 3-6 months, was considered worthwhile for some of the sampled sections, especially those of moderate conductivity (and low negative head) characteristics. Plugging of all zones, and especially high-conductive zones, has to be carried out rapidly in order to be in any way effective.

Two groundwater types are indicated: groundwaters of near-surface origin, and of intermediate origin. No deep saline varieties were encountered. In comparison with the near-surface waters, the itermediate type contains slightly enhanced contents of Na, Cl, Br and F, and reduced amounts of Ca and $HCO_3$; slightly higher pH is also suggested. The overall reducing nature of the groundwaters is indicated by the consistently negative redox potential values (-360 to -270 mV) and supported by most of the analysed total iron being in the ferrous state. Geochemical modelling of the representative groundwaters showed that: a) the groundwaters are nearly saturated with respect to calcite and other carbonate minerals, b) both $Fe^{3+}$ and $Al^{3+}$ ions appear to be saturated with their hydroxides ($Fe(OH)_3$ (amorph.) and gibbsite respectively), and c) the uranium concentration levels for some samples are regulated by the precipitation of $UO_2$ (amorph) whilst others indicate saturation with some secondary uranium mineral (possibly uranophane). These findings are to some extent supported by mineralogical studies of the sampled fracture zones.

The absence of any marked redox trends, together with the relatively little chemical variation in the groundwaters, bearing in mind that sampling has been systematically conducted to considerable depths, underlines the caution necessary when sampling is mainly carried out within highly active, relatively isolated hydraulic fracture systems, which traverse through the bedrock. Much of the sampled water has undoubtedly originated at substantially higher levels than those depths actually sampled, and their presence at greater depths is due to downward hydraulic gradients along active fracture zones, many of which have been shown through drilling to be mainly sub-vertical in orientation through the bedrock.

# HYDROCHEMICAL INVESTIGATIONS IN CRYSTALLINE BEDROCK IN RELATION TO EXISTING HYDRAULIC CONDITIONS; KLIPPERÅS TEST-SITE, SMÅLAND, SOUTHERN SWEDEN

## 1. INTRODUCTION

Earlier integration studies of geology, hydrology and hydrochemistry from the SKB test-site areas have been reported by Smellie et al (1985). A noteable omission in this report was the geochemical modelling of the respective hydrogeological environments. This was partly due to a dearth of reliable groundwater samples, a general absence of fracture mineralogical data, and also the unavailability of a suitable data program. At that time only some preliminary data were available for the Klipperås test-site area, and this was restricted to one borehole. Subsequent investigations, which have included fracture mineralogy, borehole tubewave and radar measurements, on site groundwater analysis using the mobile laboratory, in addition to the normal full-scale geological and hydrological programmes, have resulted in a considerable amount of information (see, for example, Stenberg, 1984; Olkiewicz et al, 1984; Stenberg and Olsson, 1985; Olkiewicz and Stejskal, 1986; Stenberg, 1986; Sehlstedt and Stenberg, 1986; Gentzschein, 1986; Tullborg, 1986; Carlsten et al, 1987). From the Klipperås test-site therefore, there is the possibility of providing a much more quantitative appraisal of the bedrock environment in relation to the conditions required for a suitable waste respository.

This report of the Klipperås test-site area (Fig. 1.1) has been structured to allow a full discussion of all the component procedures employed during the study, and to evaluate their respective use in such a site specific programme. For example, the suitability of the sampled groundwaters, in terms of representative compositions for the hydrogeological environment sampled, are thoroughly assessed before their use in the geochemical modelling procedures.

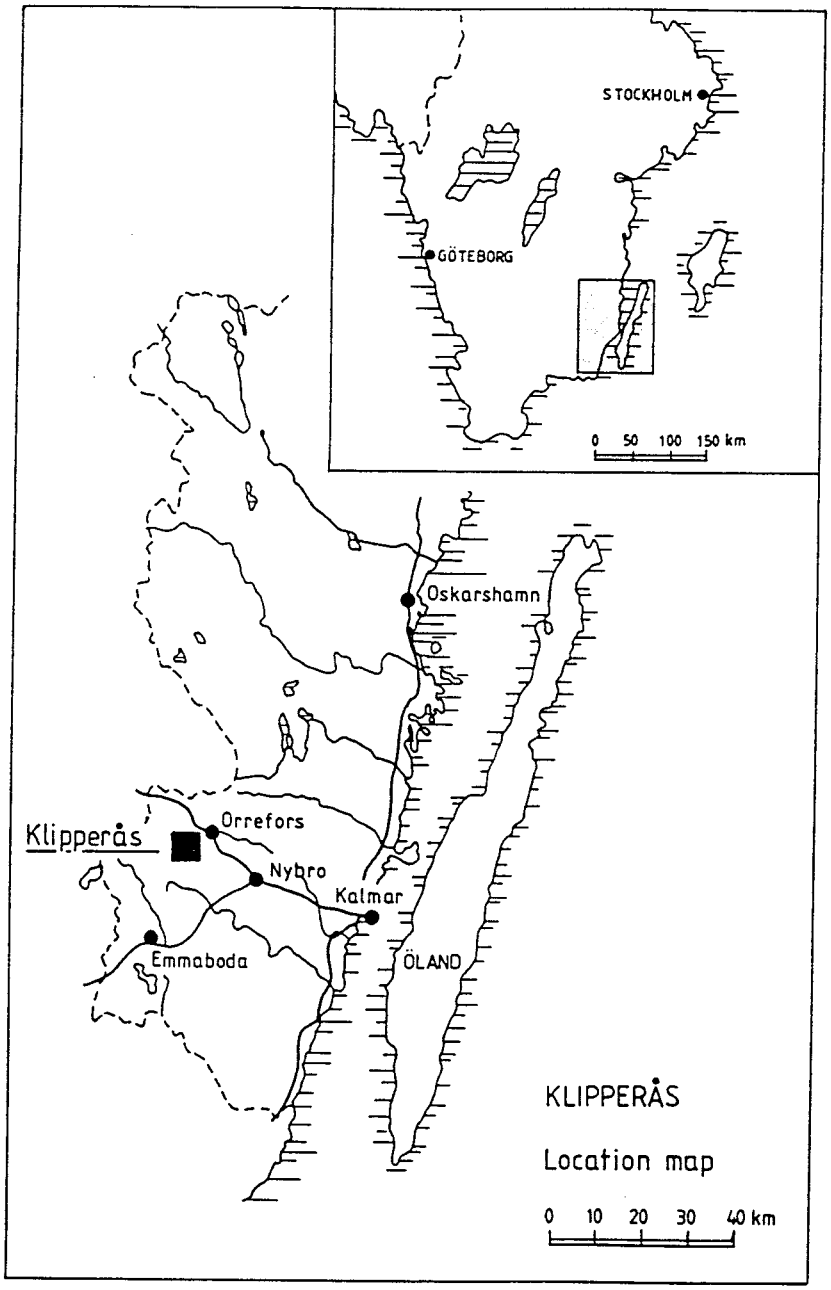


Figure 1.1: Location of the Klipperås test-site.

# 2. PARAMETERS CONSIDERED

The major hydrologic and chemical parameters considered for the Klipperås area are similar to those previously described for the other sites (Smellie et al, 1985; Section 2, p. 3-28). Respectively, these parameters referred to: 1) hydraulic conductivity and hydraulic head, 2) the pH and carbonate contents of the groundwaters, 3) the sodium, calcium and chloride contents of the groundwaters, 4) the groundwater redox-sensitive parameters, 5) the uranium geochemistry, and
6) the environmental isotopic characteristics of the groundwaters. For the Klipperås site area additional borehole measurements using tubewave and radar techniques have been carried out, and the application of geochemical modelling to the groundwater data has been attempted.

## 2.1 Borehole Tubewave Measurements

The investigation of the tubewave method for the identification of permeable fracture zones in crystalline rock was initiated by Huang and Hunter (1981) and subsequently applied to the Swedish Programme (Stenberg and Olsson, 1985). The objectives of the application were:

- to determine to what extent tubewaves are generated by fracture zones of different permeabilities
- to determine whether a quantitative measure of hydraulic conductivity can be obtained from the tubewave data

The theoretical background, application procedures and instrumentation are described by Stenberg and Olsson (op. cit.). The tubewave method is a seismic method whereupon tubewaves propagate up and down a borehole with very little attenuation along the interface between the borehole wall and the borehole fluid. They are registered using a multiple hydrophone array lowered into the borehole (Fig. 2.1). Essentially, when the compressional wave energy from a surface explosive source impinges onto a fracture zone, the fracture is compressed and the water contained in this zone is squeezed out into the borehole. This gene-

rates a tubewave which travels up and down the borehole. (Fig. 2.2).

In practice, a small dynamite charge is detonated in a shallow shothole (usually drilled some 2-6 m into the bedrock and completely filled with water for the best energy transfer to the rock formation), with an offset distance which varies from 20-40 m from the borehole entrance (Fig. 2.1). After each shot, the hydrophone array is lowered to a new position in the borehole with some overlap with the previous array position; normally steps of 10.6 m are used until the complete borehole length is measured.

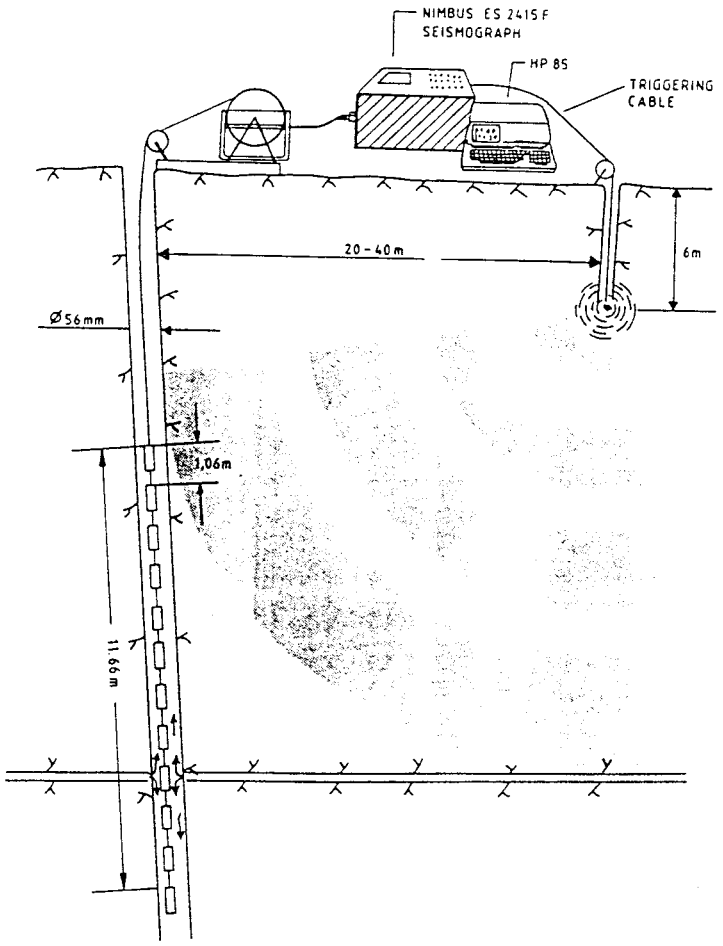


Figure 2.1: Principle of the tubewave method using a multiple hydrophone array lowered into the borehole.

Tubewave studies are considered to provide data relating:

- to a measure of the elastic properties of a large volume of rock
- to the detection of borehole sections of high or increased hydraulic conductivity. In general terms, it appears that tubewaves may be detected from zones with a hydraulic conductivity exceeding $10^{-10}$ m/s. The detection limit depends on the background hydraulic conductivity and also on the packer spacing used for the hydraulic tests, with which the tubewave data are compared.
- to the detection of impermeable fracture zones filled with clay. Tubewaves from clay-filled zones have, in general, smaller amplitude than tubewaves obtained from hydraulically conductive zones.

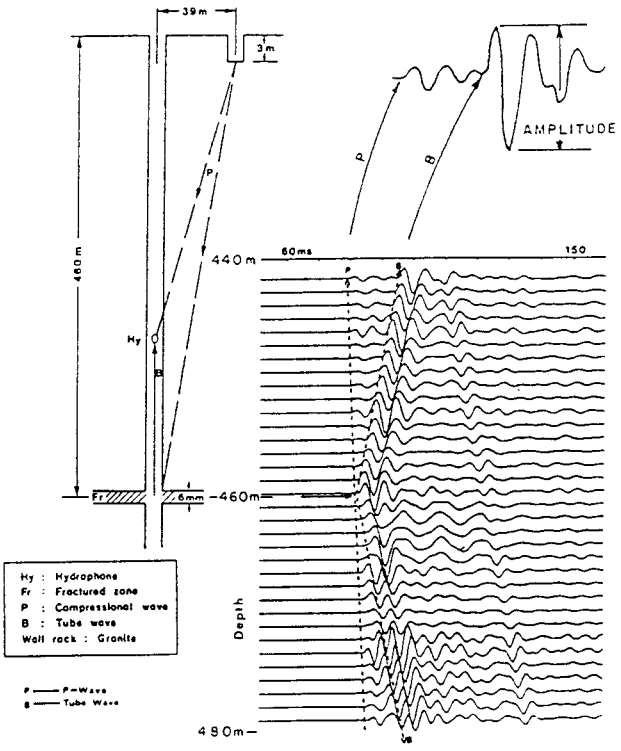


Figure 2.2: Mechanism for the generation of tubewaves in a borehole (after Huang and Hunter, 1981).

## 2.2 Borehole Radar Measurements

Detailed descriptions of the background theory to radar measurements, and the instrumentation employed, is presented by Olsson et al (1983) and Olsson and Sandberg (1984); application to the Klipperås area is described by Carlsten et al (1987). Essentially, the radar system can be considered as a short pulse system which means that the length of the pulse transmitted into the rock will be approximately one wavelength. During operation, a short current pulse is fed to the transmitter antenna thus generating a radar pulse which propagates through the rock (Fig. 2.3). The reflected pulse is made as short as possible to obtain a high resolution. If a reflecting structure (i.e. an intersecting fracture plane) is present in the bedrock, the pulse is reflected and collected by the same type of antenna on a receiver. The pulse is amplified and registered as a function of time. The receiver may be located in the same borehole as the transmitter or in any other borehole. Thus, the borehole radar system can register the distance (travel time) from the transmitter to a reflector, the strength of the reflex, and the attentuation and delay of the direct wave between transmitter and receiver (Olsson et al, 1985).

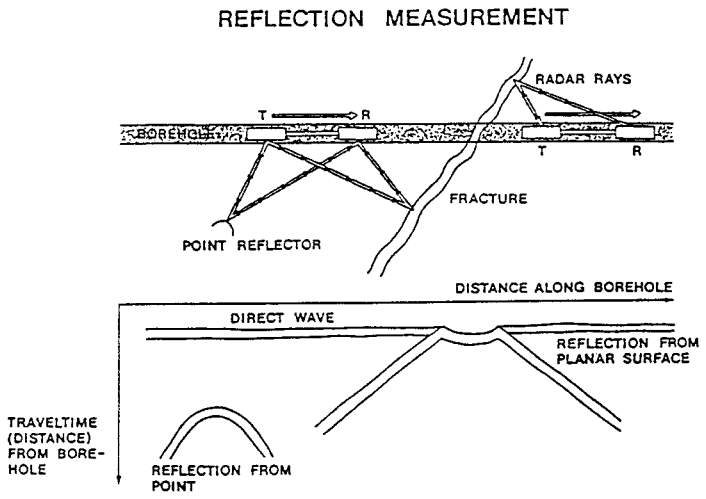


Figure 2.3: Principle of the borehole reflection radar and the patterns generated by plane and point reflectors.

The distance to a reflecting object is determined by measuring the difference in arrival time between the transmitted and reflected pulse. As the radar is pushed step by step into the borehole the time difference will vary in a manner characteristic of the reflector. Two basic pulse patterns are produced (Fig. 2.3): point reflectors and planar reflectors which characterise fracture zones. The planar reflector works like a mirror and is therefore the most efficient type, and the only one likely to be observed at large ranges.

Besides the characteristic pulse patterns produced by the geometry of the planar fracture zones intersecting the borehole at varying angles, the energy of the radar pulse is dependent on the electrical properties of the host bedrock. Highly fractured zones are characterised by increased porosity and a significant change in resistivity, which influences both the reflection coefficient and the energy of the primary pulse.

As dipole antennae are used for these measurements, the observed radar reflections are cylindrically symmetric around the borehole. Consequently a complete orientation of a fracture plane cannot be determined by measurements in a single borehole. However, the orientation can be obtained by combining results from several boreholes, assuming that the same fracture zone has been intersected by two or more boreholes. Future development of directional antennae may result in fracture plane orientation from a single borehole.

In practice, for single hole reflection measurements, the transmitter and receiver are put into the same hole and the distance between the probes is kept constant. The transmitter-receiver array is moved stepwise down the hole and measurements are made at 1m intervals. In the 22 MHz measurements performed at Klipperås the probes were separated by 10 m of glass fibre rods, which gives a total separation of 15 m between the midpoints of the antennae (Fig. 2.4). In the 60 MHz range, the probes were separated by 4 m which gave a total separation of 9 m.

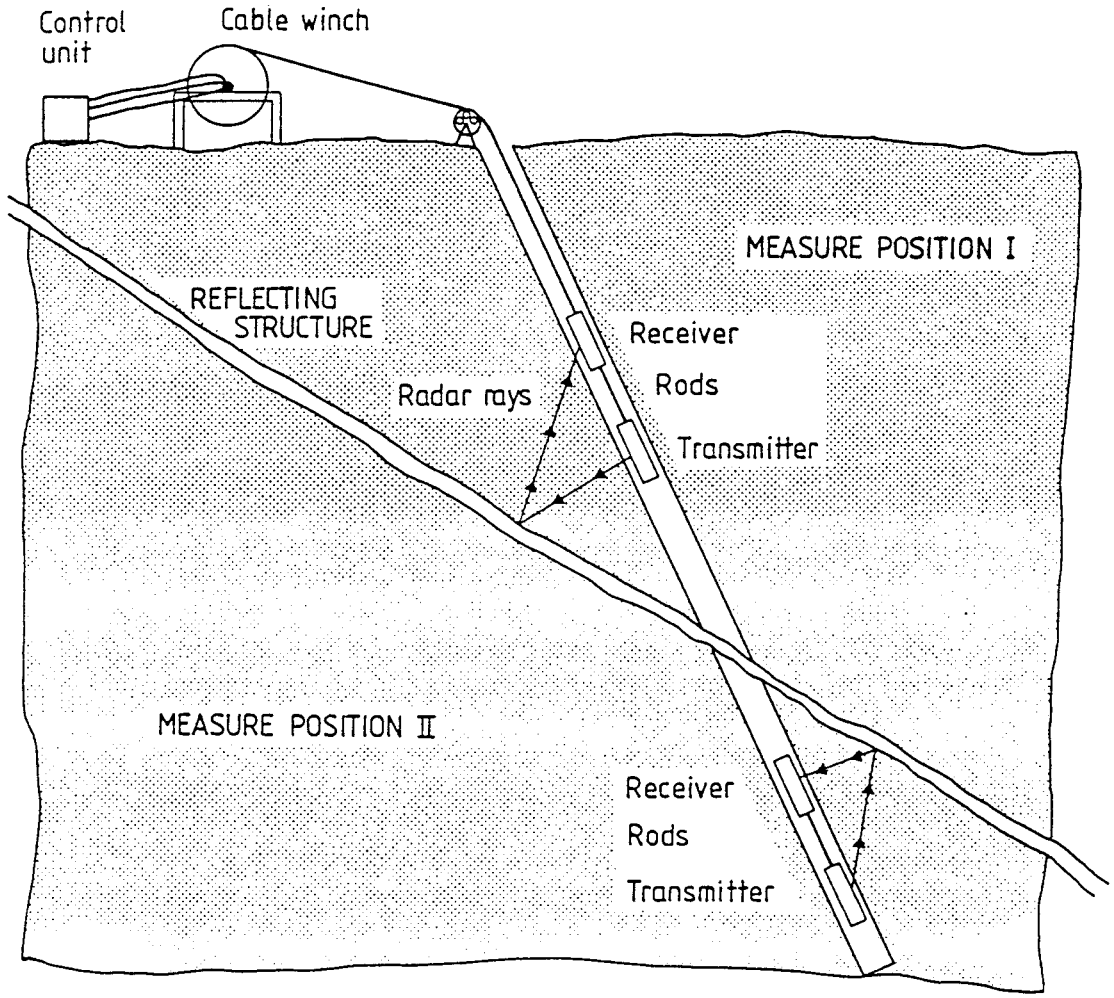


Figure 2.4: Principle of single hole reflection measurement.

Radar measurements can thus result in:

- the ability to detect structural (or lithological, such as dykes) patterns (orientation and extension) within the host bedrock outside (or between) the measured boreholes, thus providing a two- or three-dimensional detailed construction of the tectonic characteristics or the bedrock. The more holes available, the better the construction.

- a general picture of the anisotropy of the total rock mass.
- the identification of structures seen outside the borehole which do not intersect or should intersect the extension of the borehole.

## 2.3 Chemical Equilibrium Modelling

Previous geochemical studies of groundwater data from the Swedish test-site areas (Smellie et al, 1985) made little use of computer codes to model the geochemical parameters of the water samples obtained. For groundwater in general, and now specifically for the Klipperås area, the work falls naturally into two categories: redox groundwater characterisation, and geochemical interpretation of the analytical data (aqueous speciation and solution-mineral equilibria).

Several processes influence the chemical composition of natural waters in geological environments. These processes determine the maximum solubility levels for actinide metal ions (present in spent nuclear fuel) and affect the stability of barriers like metal canister, concrete, etc. A good understanding of these processes is also necessary in order to determine in which way the water chemistry, mineralogy, and trace metal concentrations will respond to natural changes and perturbations.

The processes to take into account include chemical reactions in solution (e.g. metal cation hydrolysis and complexation, redox reactions etc.), mineral - water reactions (e.g. precipitation, sorbtion, ion exchange, etc.), and mass

transport (groundwater movement through the fracture network in the rock).

A large number of parameters (or numerical variables) and equations must be included in any mathematical model of natural waters, because several hundred aqueous species (and even more mineral types) have to be considered simultaneously. The use of a computer program is then clearly necessary.

For the Klipperås data a chemical equilibrium model has been used. Although neither the mass transport (water movement) nor mass transfer (precipitation or dissolution reactions) have been included, the saturation state of minerals has been calculated.

A large number of computer programs have been reported in the literature (Nordstrom and Ball, 1984). However, the quality of any model for natural waters depends both on its thermodynamic data base, and on its model for activity coefficient corrections. The computer program used in this report is EQ3NR (Wolery, 1979, 1983, program version: 3243c90, with thermodynamic data base 3245c47) and was selected for the quality and documentation of its thermodynamic data base.

The EQ3NR model uses as input the chemical analysis of the sampled waters, and using the pertinent parameters and equations included in its data base, it determines the equilibrium state of the sampled groundwaters. The results of the calculations include the concentrations of all species in the aqueous solution (metal complexes etc.), the redox potentials according to all chemical couples, mineral saturations, and gas fugacities.

# 3. INFLUENCE ON GROUNDWATER CONDITIONS BY BOREHOLE AND BOREHOLE ACTIVITIES

According to Ask and Carlsson (1984) the following activities are considered to be the main causes of influence on the groundwater:

- borehole drilling
- gas-lift pumping
- hydraulic injection tests
- water sampling
- open-hole effect
- drilling debris

These have been discussed in detail by Smellie et al (1985) and consequently will only be summarised below.

A borehole drilled in crystalline bedrock inevitably influences the groundwater conditions. In addition, the actual drilling of the borehole, followed by gas-lift pumping and hydraulic testing, influence both the hydraulic and chemical conditions of the groundwater. The two main sources of influence found are those of drilling and the open-hole effect.

Based on values of drilling rate, drilling water pressure and flow-rate, and the hydraulic conductivity of the borehole, a very rough estimate can be made on the amount of water injected into the bedrock during drilling. It has been calculated that more than 100 $m^3$ of drilling water is injected into the bedrock under certain circumstances. The drilling water has a chemical composition normally diverging from the natural groundwater at each respective groundwater level traversed. During gas-lift pumping, only a small part (12-20 %) of the drilling water is flushed out; consequently most of it remains in the bedrock.

The long-term influence of the open-hole effect can be illustrated by numerical modelling of a generic site (Smellie et al, 1985). Depending on the occurrence of different

hydraulic units such as fracture zones, and different assumptions as to the variation of hydraulic conductivity with depth, the amount of water circulating in a borehole might be several hundreds of $m^3$ per year.

During hydraulic testing additional water is injected into the bedrock, although this amount is very small compared to the amount injected during drilling. A second gas-lifting operation performed prior to water sampling flushes out some additional amounts (8-15 %) of the remaining drilling water. The final procedure to take place is water sampling, during which a somewhat smaller volume of water is removed from the borehole than during the cleaning operation. However, the major part of the injected drilling water is still left in the bedrock.

In Figure 3.1, representing two investigated horizons from the Fjällveden study site (Smellie et al, 1985), the calculated amount of water entering and leaving the bedrock surrounding boreholes Fj2 and Fj4 (disregarding the open-hole effect) is presented. The figure also shows the water budget estimations for the sampled level 123 m (borehole length) in Fj 2. In this case the long-term importance of the open-hole effect is clearly illustrated.

The numerical calculations presented also show that the fracture zones, i.e. zones of higher hydraulic conductivity, are of major importance. Short-circuiting by a borehole will eventually result in the drilling water being replaced by fresh groundwater. This replacement might be caused by the flow of drilling water from the rock to the borehole (recharge zone). In this case the fresh groundwater is likely to be from the hydraulic zone itself and thus representative for the level. When replacement is in the other direction (discharge zone), i.e. an inflow of water from the borehole to the rock, it is likely that the drilling water will be replaced by groundwater emanating from other parts of the rock than the actual zone. If the borehole is left for a long time, without the most conductive zones being sealed off by packers, the short-circuiting might seriously affect the naturally existing groundwater conditions at the site area.

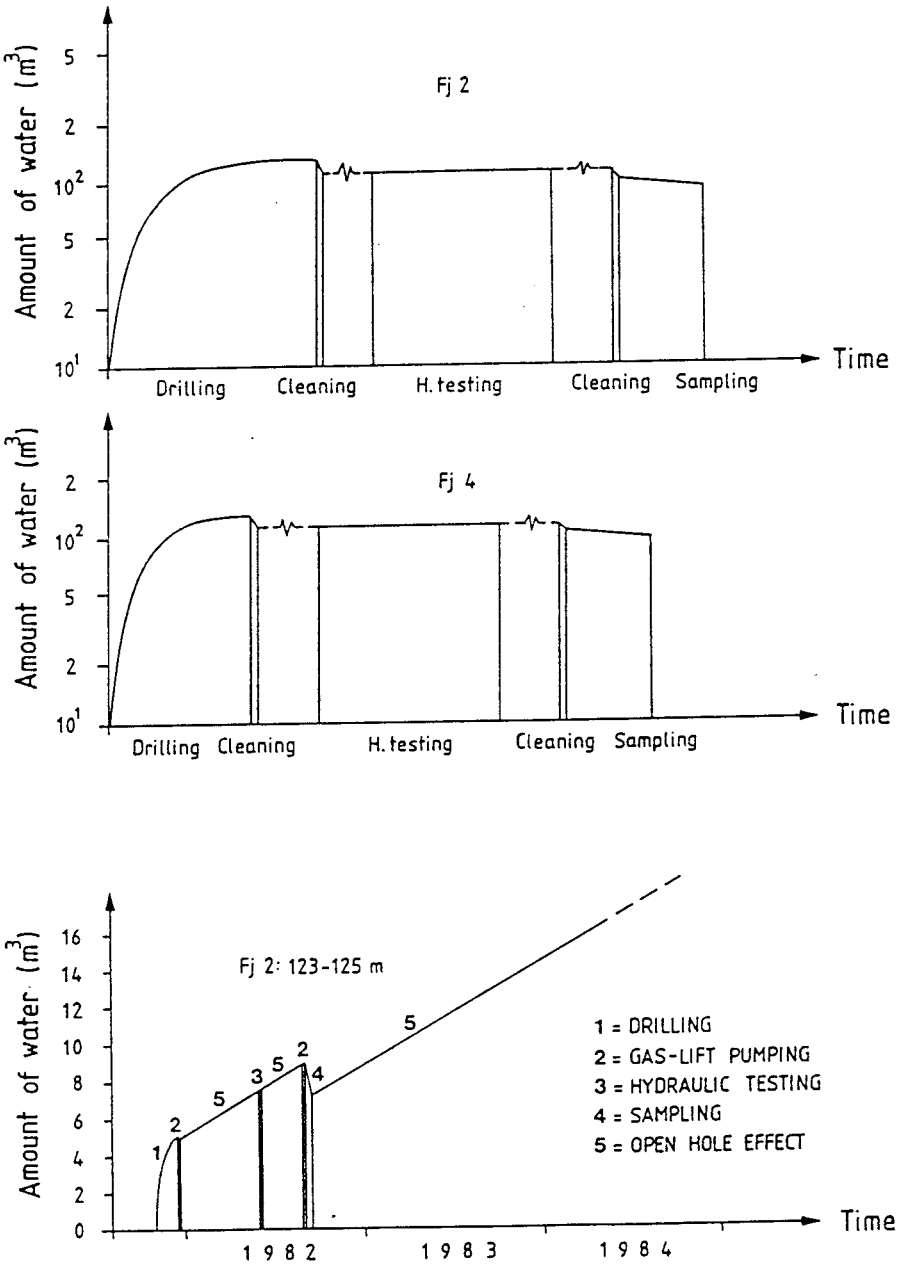


Figure 3.1: Estimated water budget during different activities for boreholes Fj2 and Fj4 disregarding the open-hole effect. The bottom diagram illustrates the water budget for section 123-126 m within borehole Fj2.

The time elapsed before sampling is conducted in the borehole will influence the quality of the sampled water. The kind of influence depends on whether the sampled section of the borehole represents borehole recharge or borehole discharge zone. If sampling is carried out in a recharge zone, all the drilling water once injected into the zone may have been replaced by fresh groundwater and thus the sample will consist of up to 100 % groundwater representative for the actual level. If, in contrast, sampling is carried out in a discharge zone, the water sample may be up to 100 % drilling water or fresh groundwater unrepresentative for the actual level. Consequently, depending on the hydraulic head, the hydraulic conductivity of the sampled zone, and on the time elapsed since completion of the core drilling, the sampled water may consist of anything between 100% drilling water and 100% fresh groundwater.

# 4. GROUNDWATER SAMPLING AND ANALYSIS

During the earlier site investigations reported by Smellie et al (1985) it became increasingly obvious that improvement of sampling and analysis of certain important chemical parameters was necessary, and that a more rapid feed-back of analytical data would help to implement immediate changes in the investigation protocol to suit local bedrock and hydrological conditions. These requirements resulted in the design and construction of a mobile laboratory to meet the following criteria:

- the immediate analysis of the main groundwater constituents. These data would be used to direct the on-going drilling and sampling programme.
- the on-site analysis of the redox-sensitive trace elements.
- the in situ measurement of the redox potential (Eh) of the groundwaters.

These criteria have been successfully achieved through the mobile laboratory (for the analysis of main constituents and the redox-sensitive trace elements), and by a down-hole measuring sond (equipped with electrodes for Eh, pH and pS measurements); the sond is connected to a pump and packer system through an umbilical hose and a downhole gas sampling unit. This integrated equipment is described by Almén et al (1986) and is schematically illustrated in Figure 4.1

The groundwater is pumped directly to the mobile field laboratory whereupon the water can be analysed free from contact with the atmosphere. This is particularly important for the redox-sensitive trace constituents which have to be analysed immediately to avoid reactions between atmospheric oxygen and the reducing elements in the groundwater (e.g. Fe(II) and S). It is also important for the measurement of Eh, pH and pS values which are obtained via flow-through cells housed in the laboratory; dissolved oxygen and conductivity are also measured in-line. The cells are placed in a refrigerator which is kept at the same temperature as in the downhole sampling section.

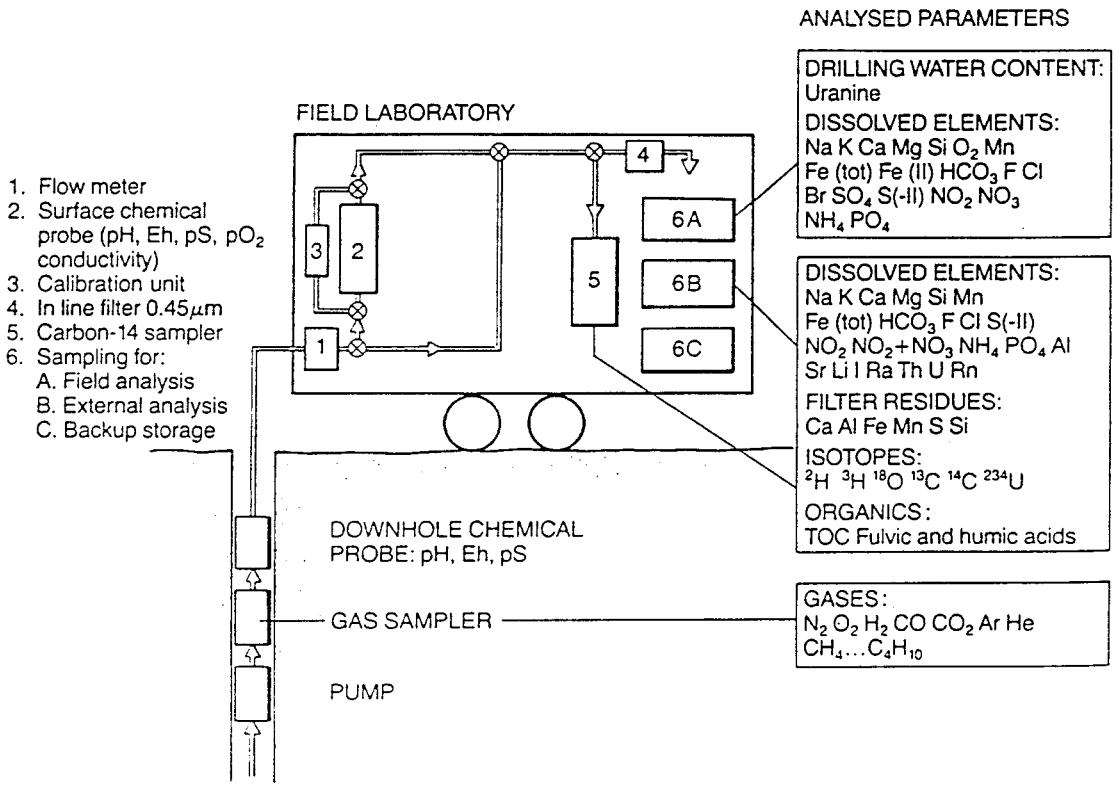


Figure 4.1: The water-flow system from borehole to analysis.

Downhole sampling (5 m sections) from specific conductive horizons is possible using packers consisting of rubber sleeves which are inflated and pressed outwards towards the walls of the borehole. In contrast to earlier investigations, the packer system has been modified to a 5 m packer spacing compared to 2.7 m previously. The pump and packer systems are hydraulically operated through pressure tubings in an umbilical hose. An important addition has been the construction of a downhole flow-through cell with an electrode system capable of measuring the various groundwater potentials (i.e. Eh, pH and pS) and transmitting the signal to a surface computer. Such values should be free from any accidental contamination by oxygen during transportation to or at the surface. Any such effects can be detected by comparison with the values measured within the field unit at the bedrock surface.

The water samples are routinely analysed for uranine which is used as a tracer in the drilling water. In this way contamination within the borehole section under investigation can be traced down to concentrations of less than one per mil in the sampled groundwater.

Field analysis are carried out using an ion chromatograph, a spectrophotometer, and titration techniques. The methods employed, the elements analysed, and the levels of detection, are summarised in Table 4.1; Table 4.2 lists the more specialised analysis carried out by external laboratories.

Table 4.1: Methods and detection limits of the analyses performed in the field laboratory.

| Method | Element | Detection limit (mg/l) |
|---|---|---|
| IC | Na | 0.1 |
| IC | K | 0.1 |
| IC/SP | $NH_4$ | 0.1/0.005 |
| IC | $NO_3$ | 0.05 |
| IC/SP | $NO_2$ | 0.05/0.001 |
| IC | F | 0.1 |
| IC | Cl | 0.1 |
| IC | Br | 0.05 |
| IC/SP | $PO_4$ | 0.2/0.002 |
| IC | $SO_4$ | 0.05 |
| SP | $Fe_{tot}/Fe^{2+}$ | 0.005 |
| SP | Mn | 0.01 |
| SP | $SiO_2$ | 1 |
| SP | $S^{2-}_{tot}$ | 0.01 |
| Tit | Ca | 2 |
| Tit | Mg | 0.4 |
| Tit | $HCO_3$ | 0.6 |
| SF | uranine | <0.1% drilling water |

IC = ion chromatograph
SP = spectrophotometer
Tit= titrations
SF = spectrofluorimeter

Table 4.2: Trace elements, isotopes and gases sampled for external analysis.

| Element | Sample volume | Method |
|---|---|---|
| Al | | |
| B | 250 ml | AA/AE |
| Ba | | |
| Sr | | |
| TOC | 1 l | |
| U | | |
| Ra | 10 l | |
| Rn | | activation analyses |
| Th | | |
| $^{2}H$ | 100 ml | MS |
| $^{3}H$ | 1 l | natural decay |
| $^{13}C$ | | MS |
| $^{14}C$ | 130 l | natural decay |
| $^{18}O$ | 100 ml | MS |
| $^{234}U/^{238}U$ | 5 l | |
| gases | 50-200 ml | gaschromatograph |
| fulvic and humic acids | | chemical characterization |

AA = atomic absorption
AE = atomic emission
MS = mass spectrometry

# 5. RESULTS AND DISCUSSION FROM THE KLIPPERÅS TEST-SITE INVESTIGATIONS.

The results from the investigated test-site are presented in Tables 5.2 to 5.11 and Figures 5.1 to 5.24. The hydrogeological data used for calculation purposes are based on hydraulic measurements carried out along 20 m sections (25 m sections for Kl 1) of the boreholes (except for the total volume of water removed during the sampling period which is measured directly). The calculated hydraulic conductivity values for the 20 m sections are then linearly extrapolated to 5 m lengths. Usually there is a wide distribution of fracture type and frequency within such a 20 m section, and as only a small percentage of these fractures will be sampled for water (i.e. the 5 m section), the question arises as how representative are the hydrological data for the actual fracture or fracture zone being sampled?

Linear extrapolation of the data to 5 m sections gives a true picture of the water budget if the hydraulic conductivity is uniformly spread along the 20 m length of borehole. However, in the event that the conductive horizon is contained solely within the 5 m section, the amount of contaminating water injected and removed due to drilling, hydraulic testing, open-hole effects and gas-lift pumping, will be about four times larger (i.e. max 20/5). This problem is partly resolved for those sampled sections where more detailed measurements (i.e. 5 m) have been performed. Furthermore, the selected levels for water sampling have in most cases high hydraulic conductivity, thus having a dominating influence on the piezometric head.

In addition, the amount of water removed by the gas-lift pumping is considered to be 100 percent of the drilling water. In practice, however, the drilling water is mixed with groundwater from different levels in the borehole so that the portion of drilling water may vary from 10 to 100 percent of the water which is removed by the gas-lift pumping. The amount of drilling water removed is then a factor of 0.1 to 1 times the amount of the total water removed.

Table 5.1: Probable compositional ranges of non-saline groundwaters in Swedish crystalline bedrock. The concentrations are given in mg/l. (Source: KBS-3).

| | | | |
|---|---|---|---|
| pH | 7 - 9 | $Ca^{2+}$ | 10 - 40 |
| Eh, V | 0 - (-0.45) | $Mg^{2+}$ | 2 - 10 |
| $HCO_3^-$ | 90 - 275 | $Na^+$ | 10 - 100 |
| $SO_4^{2-}$ | 0.5 - 15 | $K^+$ | 1 - 5 |
| $HPO_4^{2-}$ | 0.01 - 0.2 | $Fe^{2+}$ | 0.02 - 5 |
| $NO_3^-$ | 0.01 - 0.05 | $Mn^{2+}$ | 0.1 - 0.5 |
| $F^-$ | 0.5 - 4 | $NH_4^+$ | 0.05 - 0.2 |
| $Cl^-$ | 4 - 15 | $SiO_2$ (tot) | 3 - 14 |
| $HS^-$ | 0 - 0.5 | TOC | 1 - 8 |

Regarding the following presentation of the water chemistry, mention is made of non-saline groundwaters characteristic of crystalline bedrock environments in Sweden. For reference Table 5.1 presents the ranges of the most common chemical species from such groundwaters analysed within the SKB hydrochemial programme.

## 5.1 The Klipperås Test-site Area

The Klipperås test-site is located in SE Sweden approximately 300 km south of Stockholm (Fig. 1.1). The topography of the region is characteristically flat with an almost complete moraine cover which makes geological interpretation extremely uncertain; only a few weakly discerned lineaments are indicated. The surface expression of the geological features is therefore reliant mostly on ground geophysics and aerial/ satellite photography together with borehole extrapolation.

Investigations in the Klipperås area started in 1982 with reconnaissance studies for the selection of the site and geological mapping of the area. During 1982-83 tentative surface geophysical investigations were performed within an

area of 14 $km^2$. Sub-surface investigations commenced in April 1983 with the first cored and percussion drillcores. During 1984 a detailed ground surface geophysical investigation was conducted resulting in the selection of an area of approximately 4-8 $km^2$. From June to April 1985 a total of 13 cored boreholes and 13 percussion boreholes were drilled which subsequently underwent geophysical and hydrogeological investigations.

### 5.1.1 Geological features

The regional geology of the Klipperås area has been previously described by Holst (1876; 1893), the Swedish Geological Survey (1960) and Åberg (1978). As a result of the above-mentioned SKB investigations carried out in the years 1982-1985, the detailed geology of the area has been described by Olkiewicz et al (1984) and Olkiewicz and Stejskal (1986).

The extremely flat nature of the topography is illustrated in Figure 5.1; the maximum altitude difference over a distance of 35 km (which includes the site area) from east to west is approximately 30 m, due to a gradual slope towards the east. The highest and lowest points are 206 m and 160 m above sea-level respectively.

Because of the virtual absence of outcrop in the area (those that do exist occur mostly in the western part) no detailed geological maps are available. However, based on geophysical interpretation and the drilling programme, the present state of the known geology is illustrated in Figures 5.2 and 5.3. The rock-types which dominate the region are magmatic and two main varieties exist: the Småland granite and porphyry. These have been dated by Åberg (1978) to 1690Ma for the granite and 1645Ma for the porphyry; there is a possibility that the porphyry at Klipperås may be somewhat older. Here the granite has intruded the porphyry and normally the contact between the two is parallel to the volcanic layering and schistosity within the porphyry; occasionally the granite has penetrated through the structural alignement. The porphyry is composed mainly of lava

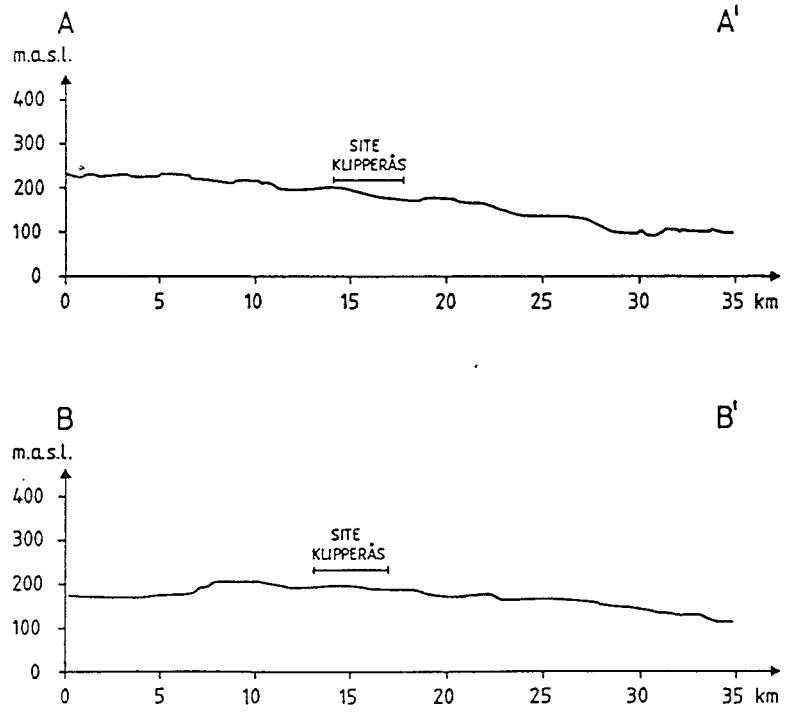


Figure 5.1: Two respective physiographic profiles trending NE-SE (A-A´) and NE-SW (B-B´) across and including the Klipperås site.

of variable acidity, together with intercalations of volcanoclastic sediment. As mentioned above, it is strongly sheared and the volcanoclastic fragments have been deformed parallel to the regional structural trend. The granite, in contrast, is coarse-grained and massive, showing only a sporadic strong deformation fabric.

Within the study area itself (Fig. 5.3), greenstones are second to granite in occurrence. They have variable chemical compositions and represent a number of originally different rock-types. Some occur as xenoliths in the granite; others can be observed intruding the granite, i.e. respectively older and younger. The latter greenstone occurrences are often associated with dyke porphyries as composite dykes, and tend to be younger in age.

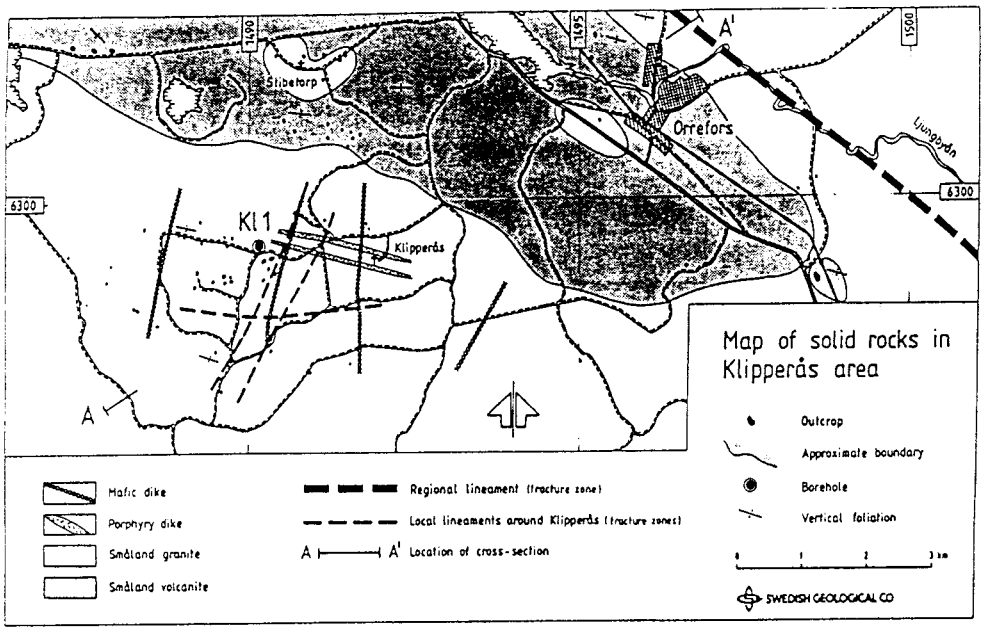


Figure 5.2: Map of solid rocks in the Klipperås test-site and surroundings.

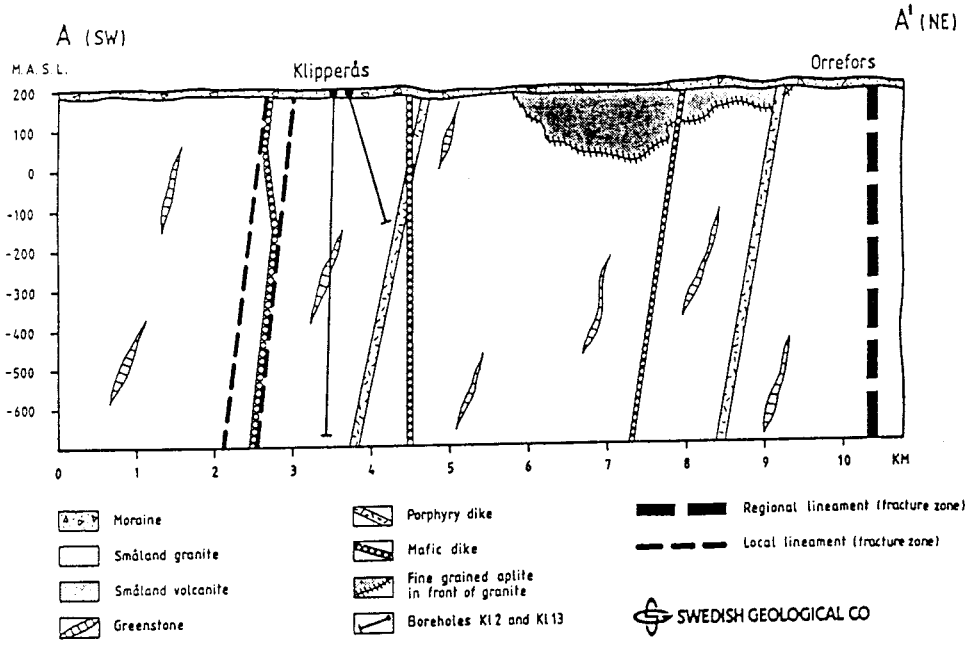


Figure 5.3: Schematic vertical cross section of the Klipperås test-site and surroundings.

The youngest rocks in the area are dykes of mafic composition and dated by Lundqvist (1979) to range from 960-980 Ma. They generally have well-preserved textures and magnetic properties. Their width varies from some metres to almost 10 m; one dyke detected by geophysical measurements indicates a width of up to 100 m. They tend to strike from N-S to NE-SW and are steeply dipping.

Detailed descriptions of the Klipperås rock-types, their textures, mineralogy and chemistry, is presented in Olkiewicz and Stejskal (1986).

Fracture fillings have been mapped and are reported by Olkiewicz and Stejskal (op. cit.). A more detailed study has been carried out by Tullborg (1986) using microscopy, XRD identification, and analysis of the stable isotopes of oxygen and carbon. The dominating fracture filling minerals in the Klipperås area are chlorite, epidote, hematite, calcite, muscovite/illite, quartz, andularia and pyrite. Smectite, together with calcite, also occur within the metabasites and dolerites.

### 5.1.2 Tectonic features

A regional lineament interpretation (over an area of 626 $km^2$) from aerial photography is presented in Figure 5.4. In the chosen site area only two of the large regional lineaments are included, both trending NW-SE and positioned 5 km NE and 9 km SW respectively from the Klipperås site area; the position of the former is marked on Figures 5.2 and 5.3. Within the test-site area itself (Fig. 5.5) only a few morphologically weak marked lineaments are present. This is due to the fact that the test-site is located on the Precambrian peneplane which is extremely flat and covered by till. In most cases, therefore, interpretation is uncertain. The western part of the area exhibits the highest frequency of lineaments; the central part, where all the boreholes are sited, is practically devoid of lineament features. The length of the lineaments never exceeds 1 km and most are shorter than 500 m.

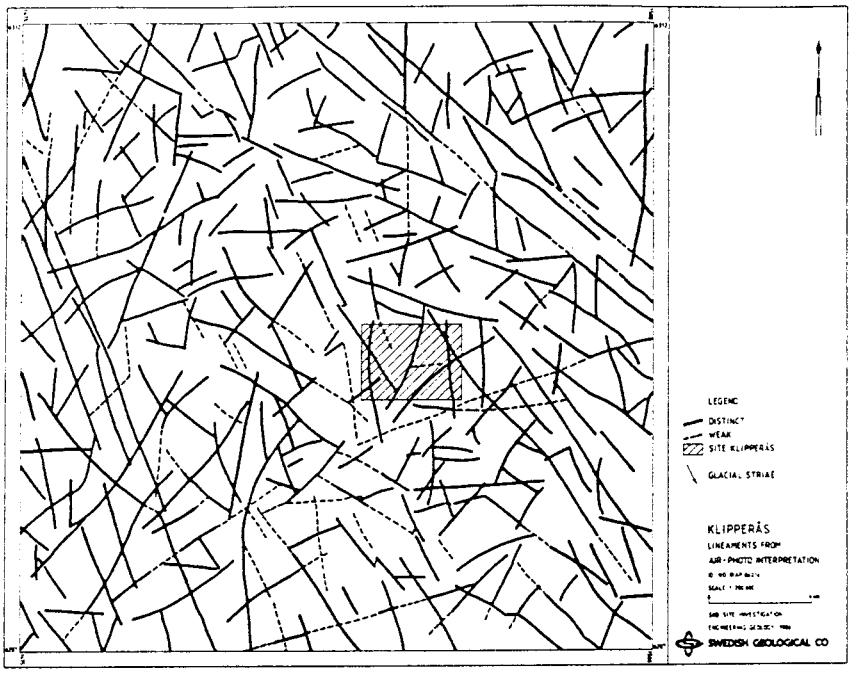


Figure 5.4: Lineament interpretation map of an area of 626 $km^2$.

As a result of the geophysical surface investigations and drilling programme, a much more complicated tectonic pattern emerges when compared with the aerial interpretation. The major discontinuities trend mainly N-S and NE-SW; some are open and highly conductive, others are sealed by secondary minerals or by dykes of different rock compositions. Of the 14 boreholes drilled in the Klipperås area, all those positioned with respect to the discontinuities have proved the existence of either a fracture zones or dyke (Fig. 5.6).

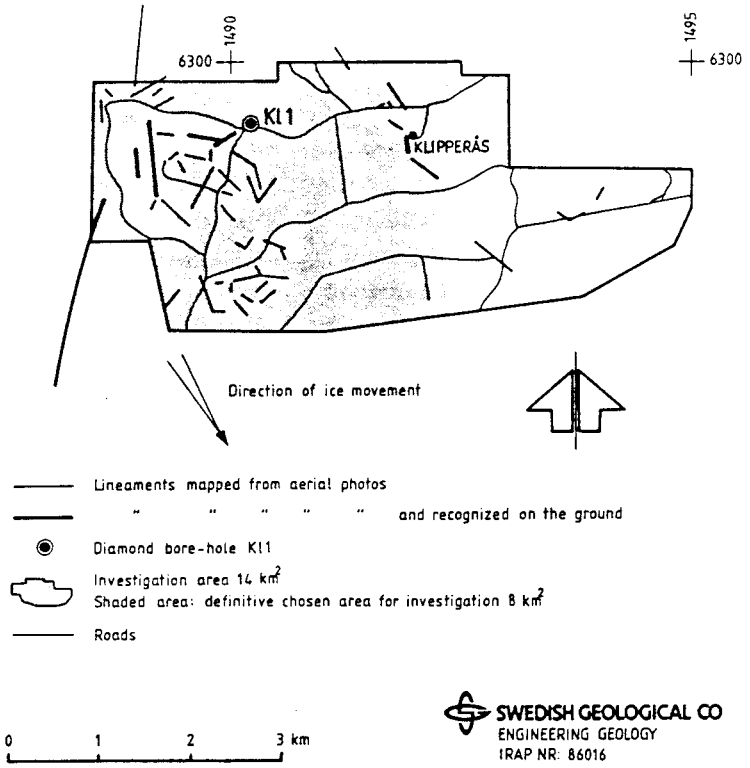


Figure 5.5: Lineament interpretation of the Klipperås test-site.

In all, some 12 fracture zones are indicated in the test-site area (Fig. 5.6). The width of the fracture zones vary: generally it can be stated that the width of 50% are between 20-30 m and the remaining 50% between 10-15 m. Due to zone undulation, the fracture width is often variable along its own length. From the drillcores these fracture zones are recognised by increased fracture frequency, crushed rock, clay alteration and hematisation of the feldspars. All of the fracture zones (apart from three) are associated with greenstones; in four cases porphyry dykes together with greenstones (as composite dykes) are present.

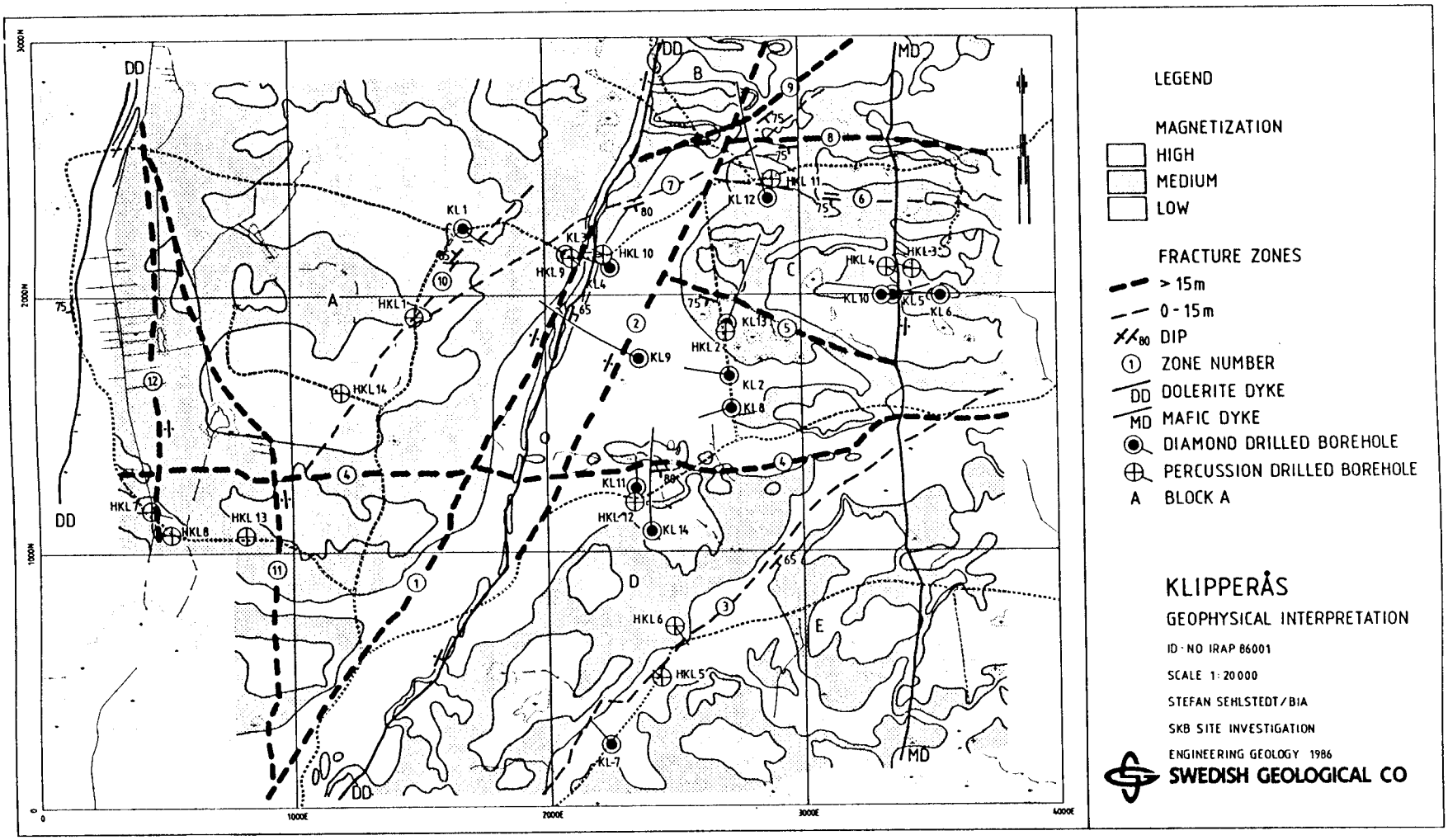


Figure 5.6: Fracture zones and dykes within the Klipperås test-site (after Sehlstedt and Stenberg, 1986)

The distribution of bedrock magnetic properties has revealed some very interesting features in the Klipperås area. These, illustrated in Fig. 5.6, show large areas of low magnetisation which, in some cases, tend to follow both sides of the fracture zones. One outstanding example is the demagnetised area between Zones 1 and 2 which indicates high tectonic activity. Another feature is the generally higher magnetism in the area west of Zone 1 than that to the east. These data have been interpretated as indicating the existence of large-scale blocks which have undergone vertical displacement relative to each other; the magnitude and direction of the vertical movement is uncertain (Sehlstedt and Stenberg, 1986). A horizontal displacement is demonstrated by a number of magnetic porphyry dykes in the NE part of the area. Here the dykes are cut by Zone 2 and rotated by about $15^{o}$ from their original direction.

### 5.1.3 Surficial hydrological features

The Quaternary deposits consist primarily of moraine which is covered by overlying peat bogs in the depressions. In the western part of the site moraine with a high frequency of large boulders dominate. The boulder size decreases towards the central part of the site area, in the east the moraine consists mainly of small boulders and gravel. The soil depth, measured in connection with the drilling of the 28 boreholes within the site, varies between 0.5 and 11 m, with a mean value of 4.2 m.

There are a number of eskers in the region adjacent to the Klipperås test-site. The largest of these is Nybroåsen which extends along Orrefors and Nybro in a SE direction down to Ljungbyholm, where it connects with another esker from the north (Fig. 5.7).

With regard to land use, the Klipperås site and near-vicinity comprises a productive coniferous forest; a few farms are also located in the area. Close to the site is sparsely populated but within a radius of 30 km from Klipperås there are several municipalities which get their water from wells drilled either in the Quaternary deposits or in the bedrock (Pousette et al, 1981).

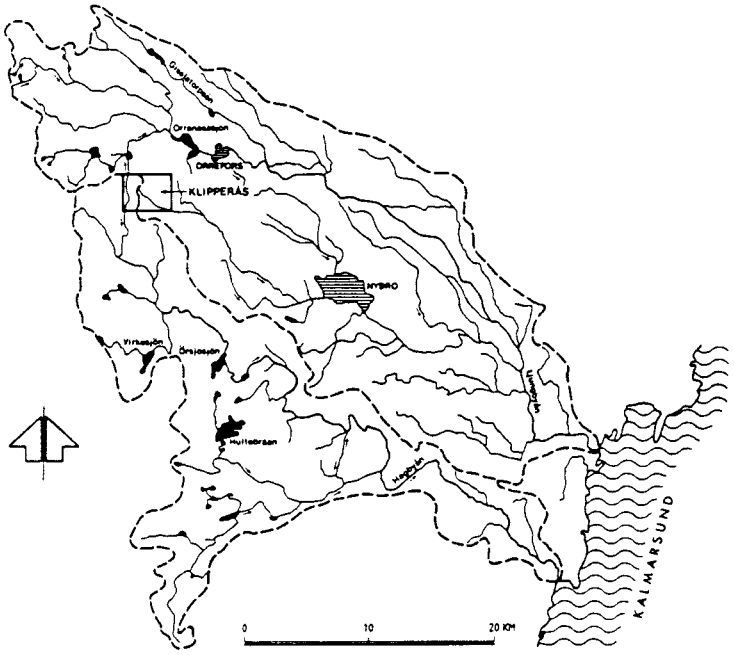


Figure 5.7: Drainage areas of the two streams Ljungbyån and Hagbyån.

The Klipperås site area is situated on the water divide between two drainage systems (Fig. 5.7). The eastern part, which includes all the diamond drilled boreholes, is drained by the Ljungbyån stream and the western part drained by the Hagbyån stream. The Ljungbyån drainage area covers 750 $km^2$ with a lake portion of 0.8% and the Hagbyån drainage area covers 447 $km^2$ with a lake portion of 3.6% (the largest lakes are smaller than 2 $km^2$). The two streams flow into the Baltic after covering a distance of 40 km and 50 km respectively. The location of the study site on a water divide indicates that it constitutes a recharge area. Low-lying parts of the area are local discharge areas for superficial groundwater. There are only three small meres which together comprise an area of less than 0.01 $km^2$. Usually the depressions contain peat bogs which constitute 3.4% of the site area (Gentzschein, 1986).

The water balance of the site area during the period 1951-1980, based on data from the SE of Sweden, has been roughly calculated to:

| | |
|---|---|
| Adjusted precipitation | 760 mm/year |
| Potential evaporation | 580 mm/year |
| Actual evaporation | 510 mm/year |
| Run-off | 250 mm/year |

Most of the precipitation falls during the late Summer (July - 87 mm; August - 82 mm) and decreases slightly from Autumn to Spring. Of the annual precipitation 15 percent falls as snow and the snow cover exists on average 126 days of the year (Nov. 25 to March 30). Greatest evaporation naturally coincides with the highest air temperatures (May to July); the annual mean temperature is approx. 6°C.

The run-off varies considerably over the year. The main water volume is discharged during the Spring snow thaw and during the late Autumn rains; this results in discharge peaks in April and November respectively.

The seasonal variation of the groundwater level in this part of Sweden generally shows a single minimum and maximum value during the year. The minimum value coincides with late Summer and the main period of groundwater recharge is during the Autumn; this is prolonged by the short mild winter so that the maximum levels occur in Spring. The annual mean temperature of the groundwater ranges from 6.5-7°C (Knutsson and Fagerlind, 1977).

During the short period of groundwater table observations (8 months) the water level in the high altitude boreholes usually fluctuated between 0.5 and 5 m below the ground surface. In the lower situated areas the groundwater table varied between 0.1-1.2m below ground surface. The altitude of the groundwater table varied during the observation period (May 1984 - Jan 1985) from 172-196 m above sea-level. The morphology of the groundwater table at Klipperås (and generally in Sweden as a whole), with its humid climate, topographical and geological

conditions, is a close reflection of the topographic relief, although on a much smoother scale. Thus, the groundwater table profile at the Klipperås site (and region) is characterised by poor relief with a general dip from west to east and consequently an eastward directed large-scale groundwater flow. This implies that there is a low hydraulic gradient in the bedrock, which also has been confirmed by piezometric head measurements in the boreholes. Out of 241 measurements 240 recorded a head difference of less than 5 m of water.

### 5.1.4 Borehole Kl 1

Borehole Kl 1 was drilled at $80^{o}$ to a vertical depth of approx. 555 m (borehole length 563.95 m) to make a preliminary evaluation of the bedrock geology, (Fig. 5.8).

The dominant rock-type encountered is a medium- to coarse-grained homogeneous granite, red in colour and forms part of the so-called Växjö granite type. This is a quartz-rich microcline granite with varying amounts of plagioclase and little mafic content. Along the total length of the drillcore this granite accounts for 82 % followed by dolerite/ greenstone (10 %), intermediate to acid volcanite (8 %) and lastly aplite (<1 %). The tectonic influence on the granite is observed as: 1) microfracturing of the granite, 2) alteration of feldspar to an iron-oxide fine-grained aggregate; complete alteration of the mafic constituents, 3) strongly mylonitised zones accompanied by a reduction in grain size and deformation of individual grains parallel to the regional foliation.

The volcanites are subdivided, on the basis of colour and macroscopic properties, into greenstone and intermediate to acid varieties. The acid type is dark-grey to grey-brown in colour, and is characterised by a dense matrix devoid of any noteable phenocrysts. The greenstones are considered to be altered varieties of intermediate to basic volcanite. Occurring occasionally within the bedrock are fine-grained aplite dykes (up to 1.5 m wide) which show sharp contacts with the medium grained granite.

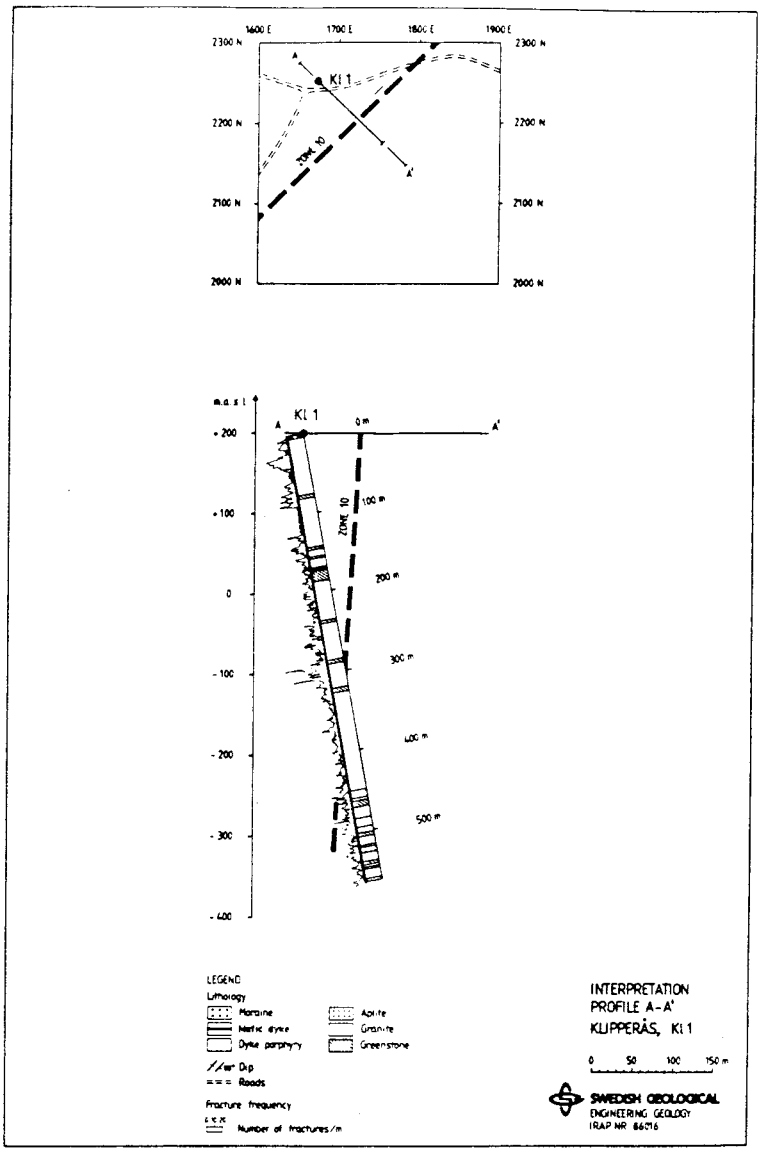


Figure 5.8: Schematic lithology and fracture frequency with interpretation of the borehole Kl 1.

Investigations of the fracture distributions within the borehole have revealed two distinct types of bedrock tectonics (Fig. 5.8; 5.9a). Above 300 m the bedrock is characterised by horizontal to sub-horizontal fractures which are stress-release in origin. This contrasts with the lower borehole section which is dominated by steeply inclined fractures ($0\text{-}30^{o}$). The fracture zone at 280-310 m (Zone 10) thus represents the boundary between two tectonic blocks of different character. This is also supported by sharp changes in hydraulic conductivity discussed below. Using 5 m sections the

Table 5.2: Measured hydraulic parameters and calculated water budget values of the various influences due to borehole activities at the water sampled levels in borehole Kl 1, Kl 2 and Kl 9.

| Bh/level (m hole length) | K-value (m/s) | Head deviation (m) | Flow direction | Drilling water (+) ($m^3$) | Gas-lift pumping (-) ($m^3$) | Hydraulic testing (+) ($m^3$) | Open-hole effect before sampling(±) ($m^3$) | Sampled water before analysis (-) ($m^3$) | Notes Σ wb | Notes year |
|---|---|---|---|---|---|---|---|---|---|---|
| Kl 1/406- | $3.2 \cdot 10^{-11}$** | >0 | ↑ | 0.023 | <0.001 | <0.001 | $-0.032 \cdot \Delta H$ | 1.9/0.86 | - | 1983/1985 |
| Kl 1/433-438* | $6.6 \cdot 10^{-10}$ | +0.35 | ↑ | 0.023 | <0.001 | <0.001 | -0.008 | 1.9 | -1.89 | 1983 |
| Kl 1/433-438* | $6.6 \cdot 10^{-10}$ | +0.35 | ↑ | 0.023 | <0.001 | <0.001 | -0.063 | 0.86 | -2.80 | 1985 |
| Kl 2/326-331 | $4.7 \cdot 10^{-10}$ (20m) | +0.6 | ↓ | (0.039) | (0.003) | (<0.001) | (-0.017) | 1.5 | (-1.48) | 1984 |
| | $1.9 \cdot 10^{-9}$ ( 5m) | +0.9 | ↓ | 0.15 | 0.010 | 0.001 | -0.100 | | -1.46 | |
| Kl 2/623-628 | $5.5 \cdot 10^{-10}$ | -2.8 | ↓ | 0.050 | 0.006 | <0.001 | +0.080 | 0.26 | -0.13 | 1984 |
| Kl 2/741-746 | $1.1 \cdot 10^{-8}$ (20m) | -2.5 | ↓ | (0.14) | (0.057) | (0.008) | (+0.546) | 1.4 | -0.77 | 1984 |
| | $8.2 \cdot 10^{-9}$ ( 5m) | -2.6 | ↓ | 0.10 | 0.044 | 0.006 | +0.424 | | -0.92 | |
| Kl 2/761- | $1.2 \cdot 10^{-7}$** | -2.2 | ↓ | 28.4 | 22.2 | 3.43 | +154.0 | 2.2 | +158 | 1984 |
| Kl 2/777- | $1.3 \cdot 10^{-7}$** | -2.2 | ↓ | 28.0 | 21.3 | 3.34 | +132.4 | 2.1 | +137 | 1984 |
| Kl 2/860- | $3.2 \cdot 10^{-10}$** | <0 | ↓ | 0.13 | 0.03 | 0.005 | $+0.695 \cdot \Delta H$ | 1.9 | - | 1985 |
| Kl 2/865-870* | $6.9 \cdot 10^{-9}$ | -2.0 | ↓ | 0.12 | 0.03 | 0.005 | +1.520 | 1.9 | -0.29 | 1985 |
| Kl 9/696-701 | $9.4 \cdot 10^{-8}$ | +3.7 | ↑ | (2.0) | (0.025) | (0.068) | (-35.309) | 6.9 | -40.2 | 1985 |

* Proposed location of sampled groundwater

** Meanvalue of existing K-values

( ) Data calculated by 0.25 x K (20m), i e as if no detailed information from 5m-sections existed

ΔH Head deviation (m of water)

recorded fracture frequency generally falls around 5 fractures/ metre for the borehole as a whole. There are, however, three sections of high fracture frequency; at 25-30 m, 280-295 m and 450-564 m. In the uppermost zone iron-oxides and chlorite dominate as fracture filling minerals; there is a noteable absence of calcite. In the intermediate zone chlorite and calcite dominate although iron-oxide does sporadically occur, and in the lowermost zone only chlorite and calcite occur.

The hydraulic conductivity is very high down to about 300 m whereupon it decreases markedly (Fig. 5.9b). The piezometric head (Fig. 5.9c) in the upper conductive part of the borehole shows small deviation from the hydrostatic head (197 m above sea-level) in the borehole. The two sections exhibiting the highest excess pressure at depth are probably overestimated due to the uncertainty in determining the piezometric head at low K-values. The excess pressure (+1.05 m) in section 431-456 m is further supported by the detailed testings in the 5m sections. The local fracture Zone 10 penetrates the borehole at 280-310 m and has a calculated K-value of $9.3 \times 10^{-7}$ m/s.

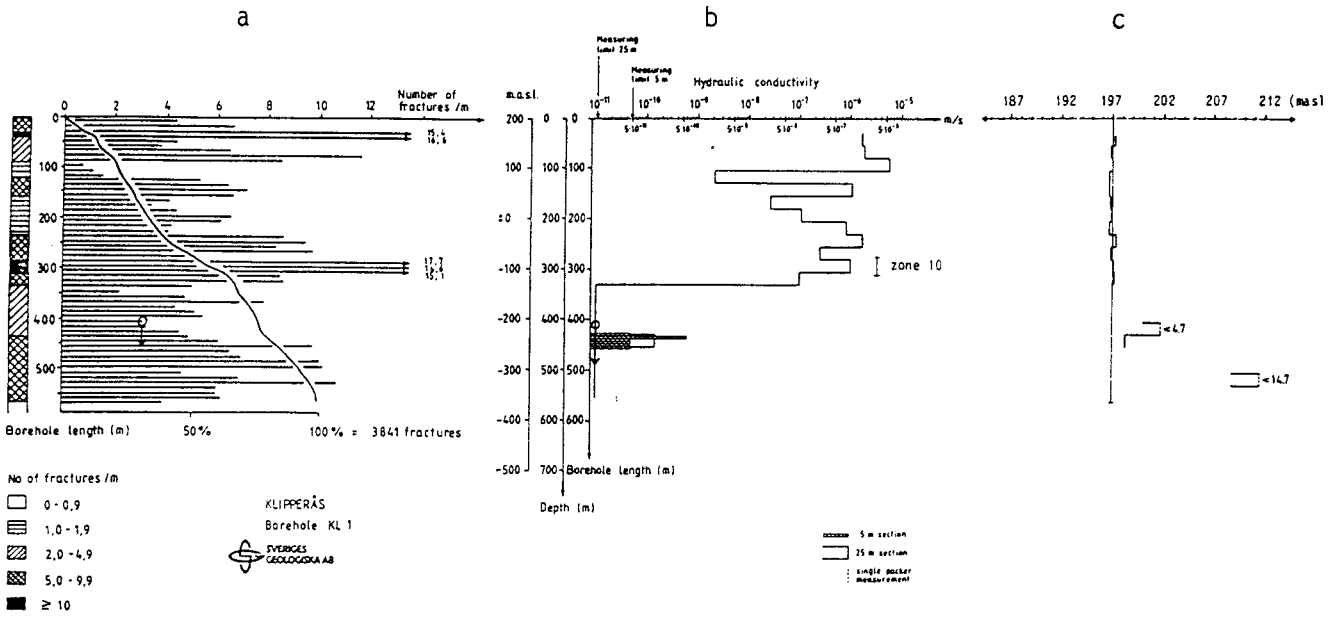


Figure 5.9: Hydrogeological characteristics of borehole Kl 1.
a) Fracture frequency (for 10m sections)
b) Hydraulic conductivity
c) Piezometric head distributions and hydrostatic head in the borehole

Tubewave and radar measurements were carried out subsequent to hydraulic and hydrochemical investigations at Klipperås. Borehole Kl 1 was not, however, subject to tubewave measurements. The radar measurements for borehole Kl 1 were recorded for both 22 MHz and 60 MHz; the former are illustrated in Figure 5.10 together with the geophysical loggings for correlation purposes. The number of interpretated radar reflecting structures intersecting the borehole in the 22 MHz measurement is 15 and these are listed and correlated in Table 5.3. Of the 15, greenstone constitutes 6, aplite 3, porphyry 2 and other structures 4. The number of reflectors not intersecting the borehole is 7.

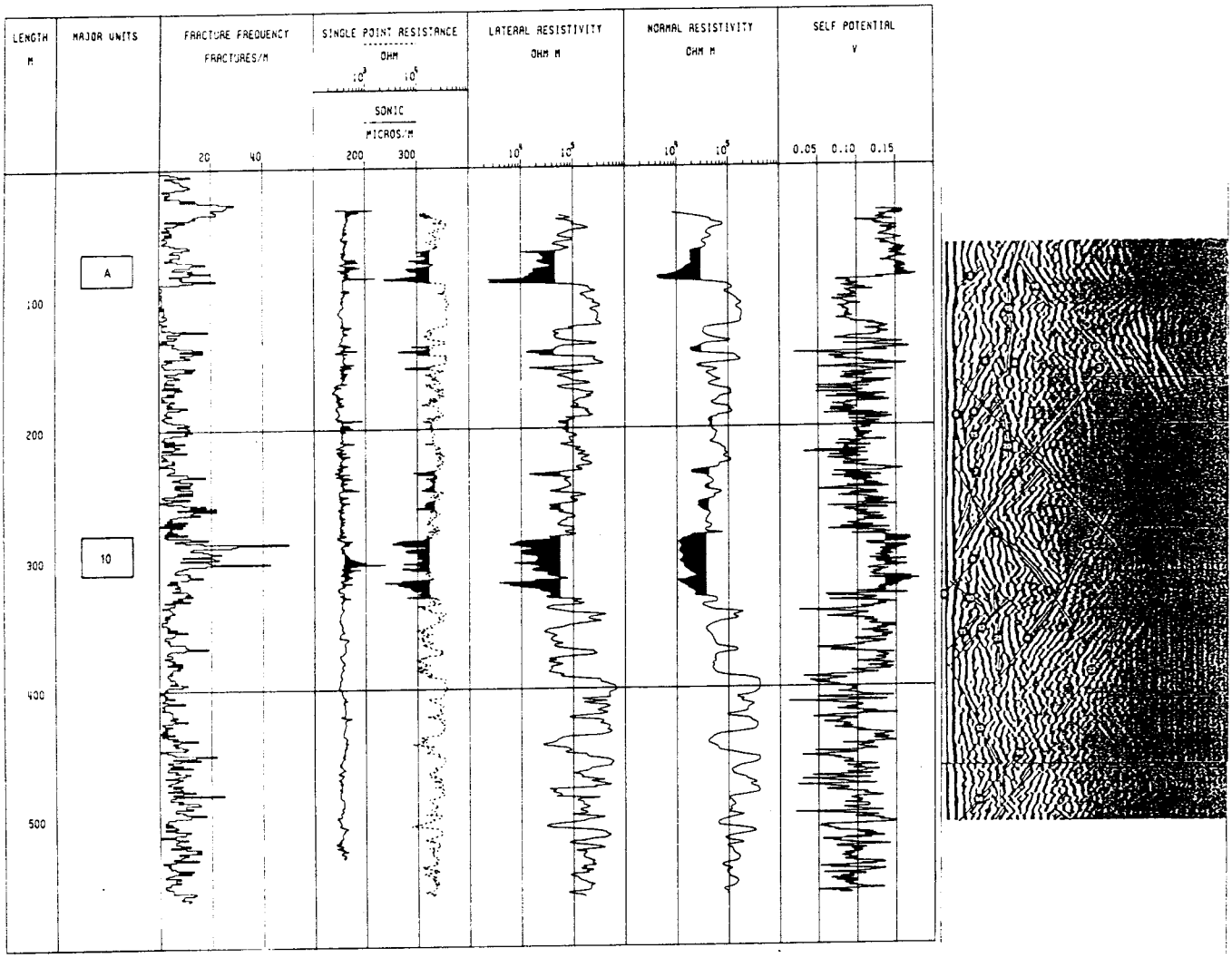


Figure 5.10: Composite plot of borehole K1 1 allowing comparison of the fracture occurrences (interpreted from geophysical logging methods) and radar measurements at 22 MHz.

The most prominent radar reflecting structures in the 22 MHz radar map from the borehole are no. 1 (greenstone, low resist.), no. 3 (fracture zone 10, low resist.), no. 4 (porphyry) and no. 6 (high fracture frequency, low resist.). These prominent reflectors can be traced over 200 m along the borehole and at a distance of 75 m outside the borehole. Most reflectors in this borehole have an acute angle to the borehole which indicates that the structures interpreted from this near vertical borehole are vertical or subvertical. The reflected structures also exhibit a somewhat undulating character. The other interpreted reflectors are mainly short compared to the prominent reflectors. Loss of pulse energy occurs between 77-91 m (fractured) and 309-328 m (Zone 10).

Table 5.3: Radar reflecting structures identified from the borehole Kl 1 (22 MHz).

Radar reflecting structures intersecting the borehole.

| Position (m) | Reflector | Angle Upper/Lower | Geological structure | Comments |
|---|---|---|---|---|
| 94 m | 2 | 40/ | Greenstone(86) | |
| 128 m | 6 | /35 | Fractured | Resist.anom. |
| 194 m | 1 | /25 | Greenstone l.s. | Somewhat low resistivity |
| 217 m | 5 | 18/ | Aplite(218) | Gamma anom. |
| 219 m | 8 | 27/ | (222) | |
| 238 m | 15 | 25/ | Greenstone l.s. (236) | Somewhat low resistivity. |
| 294 m | 10 | /45 | Zone 10 | Change of resist. within zone. |
| 310 m | 3 | 25/ | Zone 10 l.s. fractured.(305) | Resist.anom. |
| 315 m | 7 | 13/ | Greenstone u.s. (316) | Resist.anom. Gamma anom. |
| 326 m | 9 | 35/ | Greenstone l.s. (325) | Resist.anom. |
| 345 m | 13 | /18 | Aplite(344) | |
| 375 m | 11 | 30/ | | Rapid decrease in |
| 393 m | 12 | 28/ | Greenstone(391) | Resist.anom. |
| 456 m | 4 | 25/ | Porphyry l.s.(460) | |
| 515 m | 14 | 35/ | Contact(518) porphyry/aplite | Magnet.anom. Gamma anom. |

Table 5.4: Physico-chemical parameters of groundwaters from borehole Kl 1 (406 m - hole bottom).

| Level/ sample | Depth below surface (metres) | Sampling duration (days) | pH | Eh (mV) | Cond. (mS/m) | $Na^+$ (mg/l) | $K^+$ (mg/l) | $Ca^{2+}$ (mg/l) | $Mg^{2+}$ (mg/l) | $Al^{3+}$ (mg/l) | $Mn^{2+}$ (mg/l) | Fe (tot) (mg/l) | Fe(II) (mg/l) | $HCO_3^-$ (mg/l) | $Cl^-$ (mg/l) | $F^-$ (mg/l) | $Br^-$ (mg/l) | $I^-$ (mg/l) | $PO_4^{3-}$ (mg/l) | $SO_4^{2-}$ (mg/l) | $S^{2-}$ (mg/l) | TOC (mg/l) | $Si^{4+}$ (mg/l) | Drilling water (%) |
|---|---|---|---|---|---|---|---|---|---|---|---|---|---|---|---|---|---|---|---|---|---|---|---|---|
| Kl 1 | 406-hole bottom (398) | 1 | - | - | - | 45 | 0.9 | 14 | 2.6 | - | 0.05 | 0.013 | 0.012 | 73 | 42 | 3.3 | 32 | - | 0.001 | 2.3 | 0.01 | - | 4.1 | 0.03 |
| | | 3 | - | -303* | 28.8 | 46 | 0.9 | 14 | 2.2 | - | 0.04 | 0.021 | 0.021 | 77 | 43 | 3.6 | 34 | - | 0.001 | 2.3 | 0.01 | - | 4.1 | - |
| | | 3 | 8.2 | -303* | 30.2 | 46 | 1.1 | 14 | 2.6 | 0.01 | 0.04 | 0.016 | 0.012 | 78 | 43 | 3.8 | 38 | 0.006 | 0.001 | 1.8 | 0.15 | 3.7 | 4.2 | 0.02 |
| | | 4 | 8.3 | -311* | 31.0 | 47 | 0.9 | 14 | 2.3 | - | 0.03 | 0.006 | 0.002 | 80 | 45 | - | 39 | - | 0.001 | 1.5 | 0.11 | - | 4.4 | 0.02 |
| | | 5 | 8.3 | -314* | 31.6 | 48 | 0.9 | 14 | 2.3 | - | 0.04 | 0.010 | 0.007 | 80 | 48 | - | 40 | - | 0.001 | 1.3 | 0.13 | - | 4.3 | 0.02 |
| | | 10 | 8.4 | -303 | 31.8 | 48 | 1.1 | 14 | - | 0.04 | 0.03 | - | - | 79 | - | 3.9 | - | 0.008 | 0.001 | - | 0.09 | - | 4.3 | - |

Tritium: < 3 TU
Carbon-14: 28375 years
Oxygen-18: -12.11 ‰
Deuterium: -86.5 ‰
Uranium: 0.68 ppb (0.01 ppb)
$^{234}U/^{238}U$ ratio: 5.9

* measurements made in a flow-through cell located at ground surface.

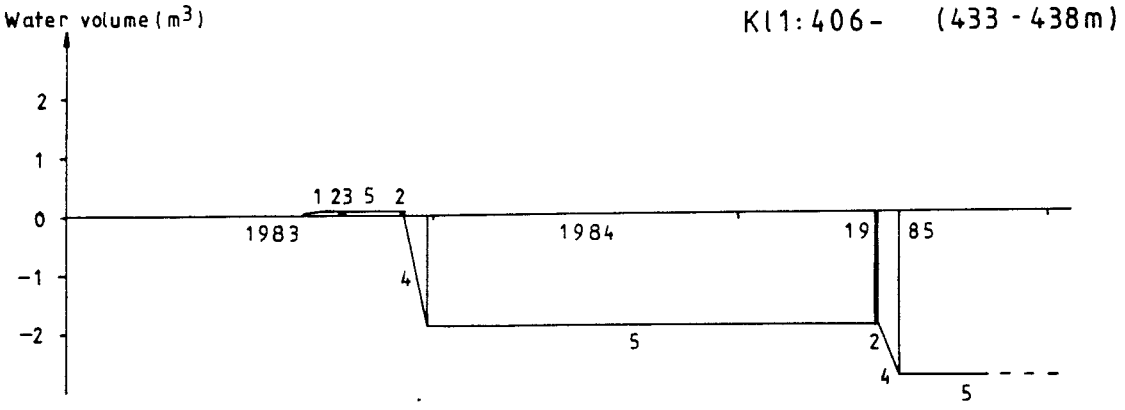


Figure 5.11: Schematic illustration of the calculated water budget for level 406 m - hole bottom in borehole Kl 1.
1 = Drilling water; 2 = Gas-lift pumping;
3 = Hydraulic testing; 4 = Sampling;
5 = Open-hole effect.

5.1.4.1 Level 406 m - hole bottom

The borehole length is characterised by roughly 50% medium-grained, grey to red microcline granite, and the remaining 50% is comprised of acid porphyry and greenstone horizons with thin zones of pegmatite and aplite intrusions. Generally the fracture frequency is low (Fig. 5.9a) with an average of about 5 fractures/metre. The main infilling minerals are calcite, chlorite, epidote, muscovite and minor kaolinite; possible gibbsite and stilbite have been detected from levels 329-365 m and 438-480 m respectively.

Hydrology

It is clearly evident from Figure 5.9b that the most conductive section of the borehole is located at approximately 433-438 m depth. This is characterised by a K-value $6.6 \times 10^{-10}$ m/s (measured along a 5 m length) and a positive piezometric head of +0.35 m (Table 5.2). Otherwise the borehole section sampled records K-values which are below the limit of measurement. The mean K-value for the sampled borehole length is $3 \times 10^{-11}$ m/s. From the water budget (Fig. 5.11) the sampled groundwater should be representative for both Dec. 1983 and June 1985, the two sampling occasions. For example, in Dec. 1983 the pumped volume was 1.9 $m^3$, which is almost five times the borehole volume of the packed-off section. Similarly in 1985, 0.86 $m^3$ were removed, which should also have secured a representative sample.

Water geochemistry

The sampled water (Table 5.4) is characterised by a pH of 8.3; of the major cations, Na, K and Mg are all present in appreciable but normal amounts for non-saline groundwater representative for Swedish crystalline rocks, likewise for the major anions $HCO_3$, Cl, F, Br and $SO_4$ (Table 5.1). S and TOC are also present in appreciable amounts; I and $PO_4$ are very low. The percentage of drilling water component is almost negligible.

Redox-sensitive parameters

Both Fe(II) and S(-II) are present, but only in very small amounts. A reducing groundwater environment is indicated by negative Eh values (mean -307 mV) and that most of the iron present is in the ferrous form.

Isotope geochemistry

This level is characterised by $\delta^{18}O$ and $\delta^{2}H$ values (-12.11 ppt and -86.5 ppt respectively) representative of a meteoric water source. No younger near-surface derived water is present (<3TU) and this is supported by a very old $^{14}C$ value (28375 yrs).

Uranium geochemistry

A uranium content of 0.68 ppb by alpha-spec. and a high $^{234}U/^{238}U$ activity ratio of 5.9 support a strongly reducing groundwater with a long residence time to account for the build-up of the excess $^{234}U$ by alpha-recoil processes.

5.1.4.2 Borehole summary and discussion

Even though the groundwater sampling was carried out along the borehole length extending from approximately 406-564m, hydrological considerations point to only one conducting level of any major importance. This is represented by a fracture zone which intersects the borehole at 433-438 m depth. This registers a hydraulic conductivity of $6.6 \times 10^{-10}$ m/s compared to the mean conductivity of the sampled borehole length of $3 \times 10^{-11}$ m/s. This, together with registering a positive piezometric head (+0.35 m), indicates that the main portion of the sampled groundwater has originated from this fracture zone intersection. Water budget considerations show that this water is representative and should be free from contamination resulting from drilling water and other younger-derived sources.

The chemistry of the groundwater conforms to an intermediate non-saline water of a strongly reducing character. The water budget prediction has been supported by the isotopic chemistry which indicates a very old groundwater with an absence of any young surface or near-surface component. Furthermore, the absence of drilling water is indicated by the almost negligible uranine content. During the sampling period of 10 days no variation of the measured and analysed parameters occurred. This is further evidence that the sampled water is from the same reservoir, and therefore representative for the major conducting zone at 433-438 m depth.

### 5.1.5 Borehole Kl 2

Borehole Kl 2 was drilled at $78^{o}$ to a vertical depth of approx. 947 m (borehole length of 958.60 m) to further investigate the measured presence of a weak electromagnetic anomaly in an otherwise homogeneous bedrock (Fig 5.6).

The main rock type characterising the drillcore is a grey or reddish medium- to coarse-grained granite, with the very subordinate presence of aplitic dyke material (Fig. 5.12). Within the granite, as inclusions or xenoliths, occurs greenstone and dolerite dyke material; these account for some 10% of the penetrated rock mass. In total, along the length of the drillcore, the granite accounts for 86.46 % followed by the greenstone (9.13 %), the mafic dolerite material (0.96 %) and finally aplite (<0.1 %). The granite is massive and, on a macroscopic scale, quite homogeneous apart from localised narrow zones of cataclastis and bands of mylonite. The greenstones tend to occur as steeply dipping tabular slabs within the granite. Their distribution is irregular along the drillcore; thicknesses range from decimetres to metres in width. Prominent greenstone horizons occur at 100-130 m, 586-618 m and at 680 m. Macroscopically the greenstones are massive and slightly schistose, whilst contacts to the granite are always indicated by a strong schistosity.

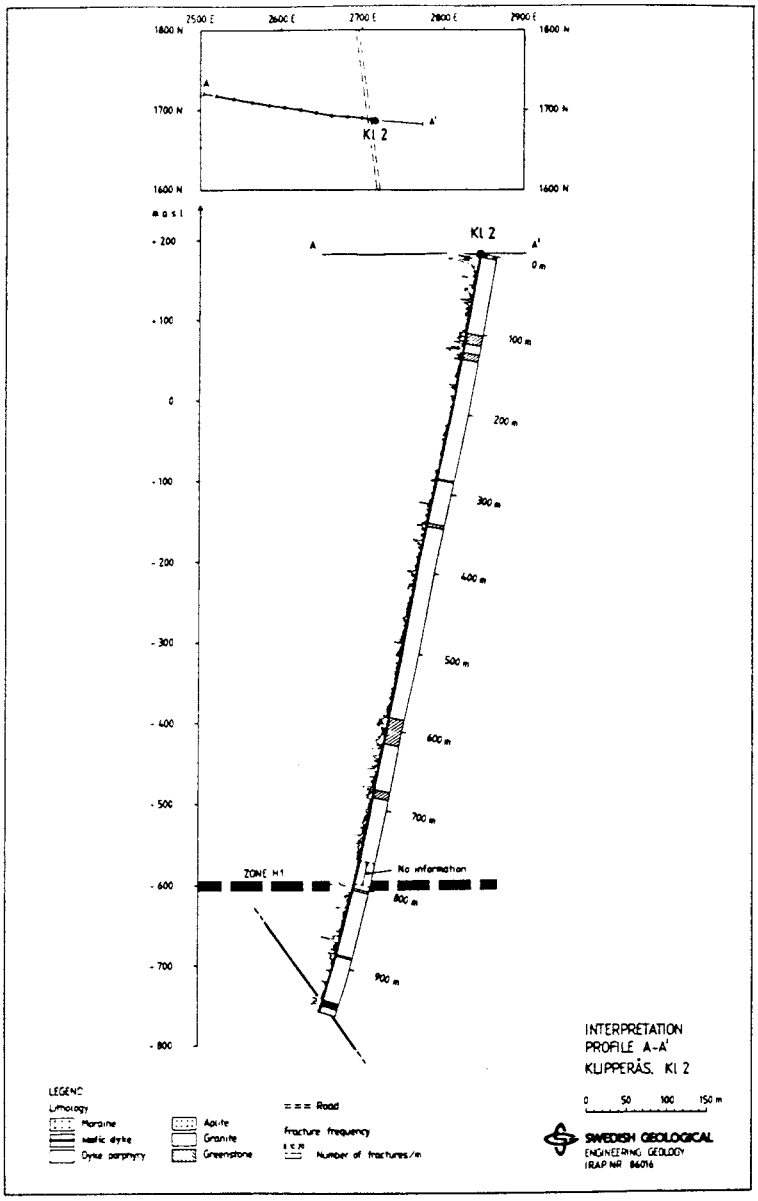


Figure 5.12: Schematic lithology and fracture frequency of borehole Kl 2.

As illustrated by Figure 5.12, the borehole is intersected by a local horizontal fracture zone (Zone H1) from 792-804 m depth. Unfortunately the core within and adjacent to this zone was lost; a residual 8 m length consists of highly fractured granite mixed with compressed greenstone material. The crushed portion accounts for 50% of the length. In addition the rocks show slight alteration with the fracture surfaces coated with hydroxy iron-oxides; a sealed breccia matrix at around 802m contained appreciable calcite and epidote. Because no further correlation with adjoining boreholes has been successful, this zone is considered horizontal to sub-horizontal in nature, a feature supported by the borehole radar measurements.

Investigations of the fracture distributions (Fig. 5.13a) have revealed a mean fracture density of 2.79 fractures/m. In relation to rock type, the greatest fracture frequency is associated with the mafic/dolerite material (8.74 fractures/m) followed by the greenstones (6.70), aplite (2.50) and finally granite (2.31). The granite generally shows a low but irregular joint distribution along the drillcore. In places there exist unfractured sections up to 4 m in length; adjacent to the greenstone contacts there is a marked increase in fracture frequency.

The dominant fracture-infilling phases are calcite, chlorite, epidote, hematite, andularia and muscovite; some kaolinite and possibly talc have been identified from approx. 625 m depth.

Hydrologically, the borehole shows an unusual distribution of hydraulic conductivity (Fig. 5.13b). High K-values characterise a broad sector between 740-810 m, contrasting with relatively low conductivity values in the uppermost part of the hole. Between these two sectors most measured 20m sections are characterised by K-values at or below the limit of measurement ($1 \times 10^{-11}$ m/s); some exceptions do occur achieving values of up to $1 \times 10^{-9}$ m/s. The highest conductivity ($1.2 \times 10^{-6}$ m/s) is associated with the sub-horizontal fracture Zone H1 at 792-804 m depth, which has a calculated hydraulic conductivity of $2 \times 10^{-6}$ m/s (Table 5.2).

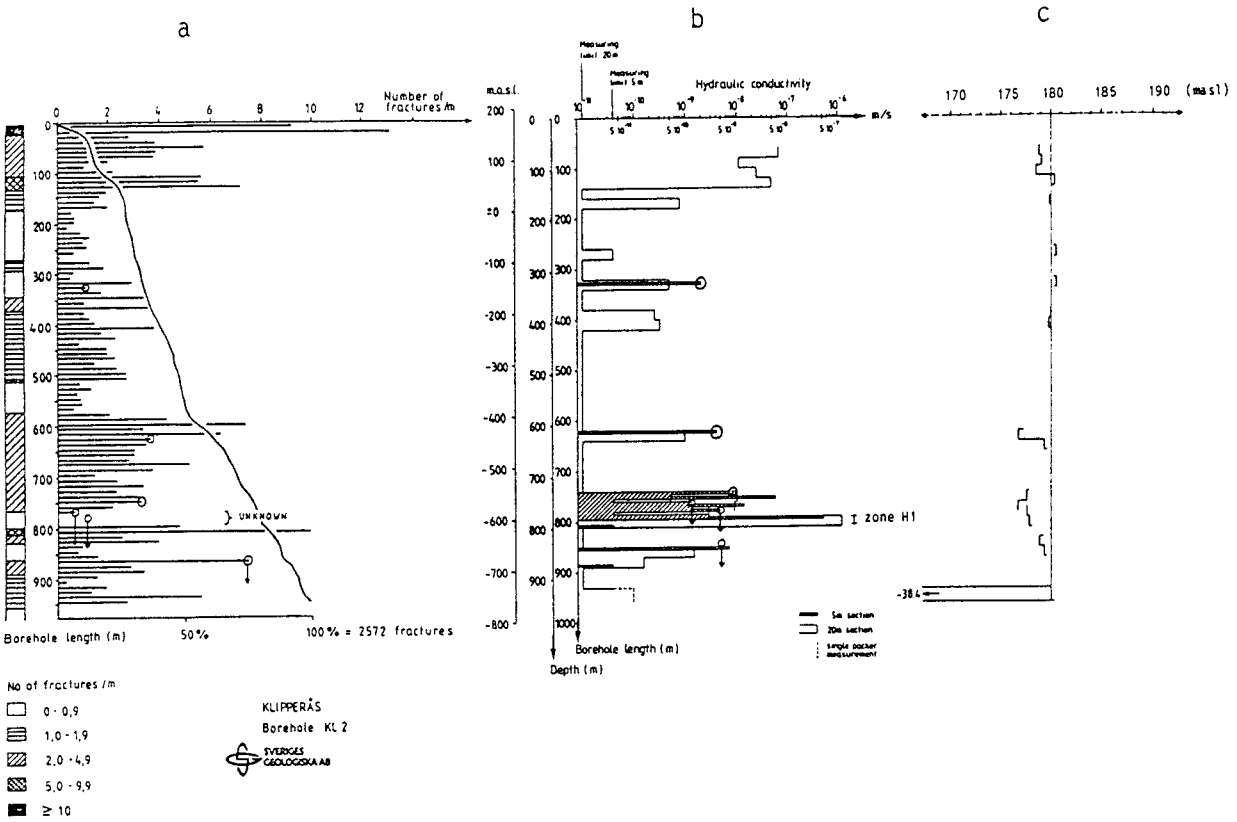


Figure 5.13: Hydrogeological characteristics for borehole Kl 2.
a) Fracture frequency (for 10 m sections).
b) Hydraulic conductivity.
c) Piezometric head distribution and hydrostatic head in the borehole.

The piezometric head along the borehole (Fig. 5.13c) is known only sporadically because of the low K-values and the short duration of the hydraulic tests (2 hours). The available data, however, show a clear downward movement of the groundwater flow. For example, within the 760m-hole bottom section, a rough estimate of the hole-to-bedrock outflow indicates that 4.5 $m^3$ / day flows into the bedrock, which is about 2.4 times the water volume in the above borehole portion. Most of this flow is considered to enter the bedrock via fracture Zone H1 (i e highly conductive in combination with a negative head) rather than at the 930m-hole bottom section, which indicates a very negative head but low conductivity. This head value is probably grossly underestimated due to the very low K-value in that actual section (see Figs. 5.13b and c).

An important aspect of borehole Kl 2, which will have had a great bearing on open-hole effects and therefore the water budget calculations presented below, was the fact that it was plugged subsequent to drilling but prior to groundwater sampling. Borehole Kl 2 was drilled from 27 April to 28 June 1984 and then plugged from 15 July to 19 September of the same year. Following tubewave measurements conducted at the beginning of October, groundwater sampling commenced on 18 October at level 777 m. Every subsequent level above this depth was systematically sampled until completion in 11 December 1984. The deepest level at 860 m was sampled after a break of 5-6 months (18 May to 15 June 1985) during which time the hole remained open. Plugging of the hole during the above-mentioned period effectively sub-divided the hole into the following sections: bedrock surface to 350 m, 350-720 m, 720-800 m, 800-860 m and from 860-hole bottom.

Borehole Kl 2 was also used as an experimental hole for tubewave measurements which, as mentioned above, were conducted prior to groundwater sampling. The recorded tubewave measurements are illustrated in Figure 5.14, together with the relative tubewave amplitude from each source point, the measured temperature, the temperature gradient, the hydraulic conductivity (as measured between packers with a spacing of 20 m), and the fracture frequency per 5m section.

In borehole Kl 2, tubewaves are generated in the uppermost 125 m. The hydraulic conductivity in this region exceeds $10^{-8}$ m/s. The fracturing in this section causes a significant decrease in the amplitude of upward propagating tubewaves generated between 270-300 m.

In the section between 125-170 m no tubewaves are generated. This is consistent with a very low fracture frequency and also a hydraulic conductivity below the measuring limit ($10^{-11}$ m/s). An exception is the section between 160-180 m where the hydraulic conductivity exceeds $5\ 10^{-10}$ m/s, but no tube waves are generated here.

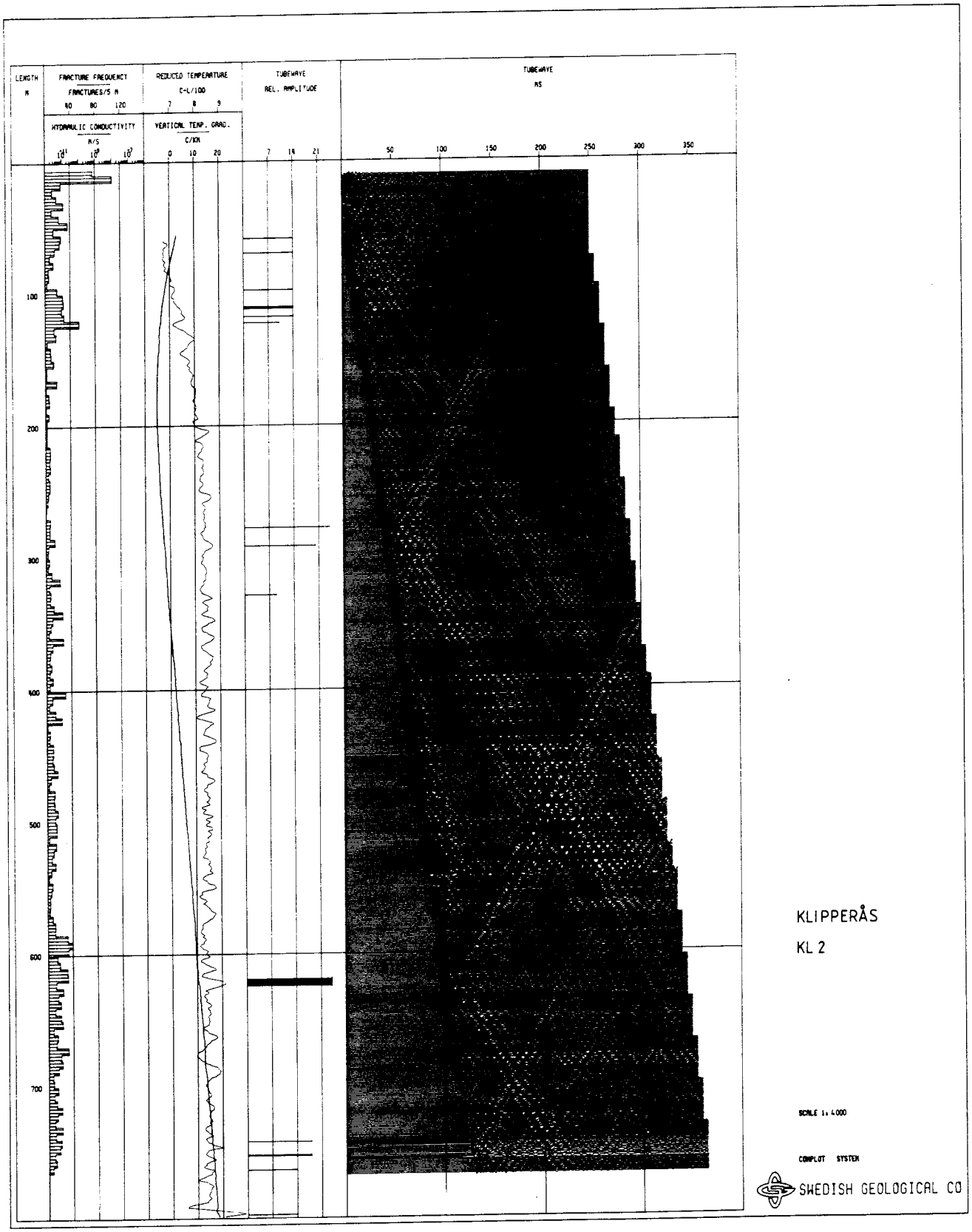


Figure 5.14: Tubewave record from borehole Kl 2 allowing comparison with several geophysical parameters and hydraulic conductivity.

In the section 270-300 m, large amplitude waves are generated, but water injection tests indicate only a small increase in hydraulic conductivity in the section between 260-280 m. It is interesting to observe that there is no attentuation or reflection of the tubewaves generated above 125 m at this relatively strong source of tubewaves. In many cases, both reflection and a decrease in amplitude of both downward and upward propagating tubewaves are observed in connection with single fractures open to fluid flow.

In the section between 320-340 m, an increase in measured hydraulic conductivity ($>10^{-9}$ m/s) is observed, and this corresponds to a weak tubewave propagating downwards.

In the section between 340-620 m no significant tubewaves are generated. This is consistent with the water injection tests, which indicate a measured hydraulic conductivity below the measuring limit ($<10^{-11}$ m/s). However, again there is an exception. In the section between 380-420 m a small increase in hydraulic conductivity ($>2\ 10^{-10}$ m/s) is observed. However, no tubewaves are generated within these sections.

In the section between 620-640 m, large amplitude tubewaves are generated, propagating both upwards and downwards along the borehole. In the water injection tests, an increase in hydraulic conductivity is observed (near $10^{-9}$ m/s). Only small reflections and a small decrease in amplitude of upward and downward propagating tubewaves are observed in connection with this tubewave source.

In the section between 640-740 m, no tubewaves are generated and the hydraulic conductivity of this section is less than the measuring limit of the equipment ($<10^{-11}$ m/s). Below 740 m, large amplitude tubewaves are generated at a major fracture zone, with a hydraulic conductivity exceeding $10^{-9}$ m/s.

The tubewave measurements were followed after sampling was completed by borehole radar measurements. The results are presented in Table 5.5 and Figure 5.15, together with the geology and geophysical logs sensitive to lithological

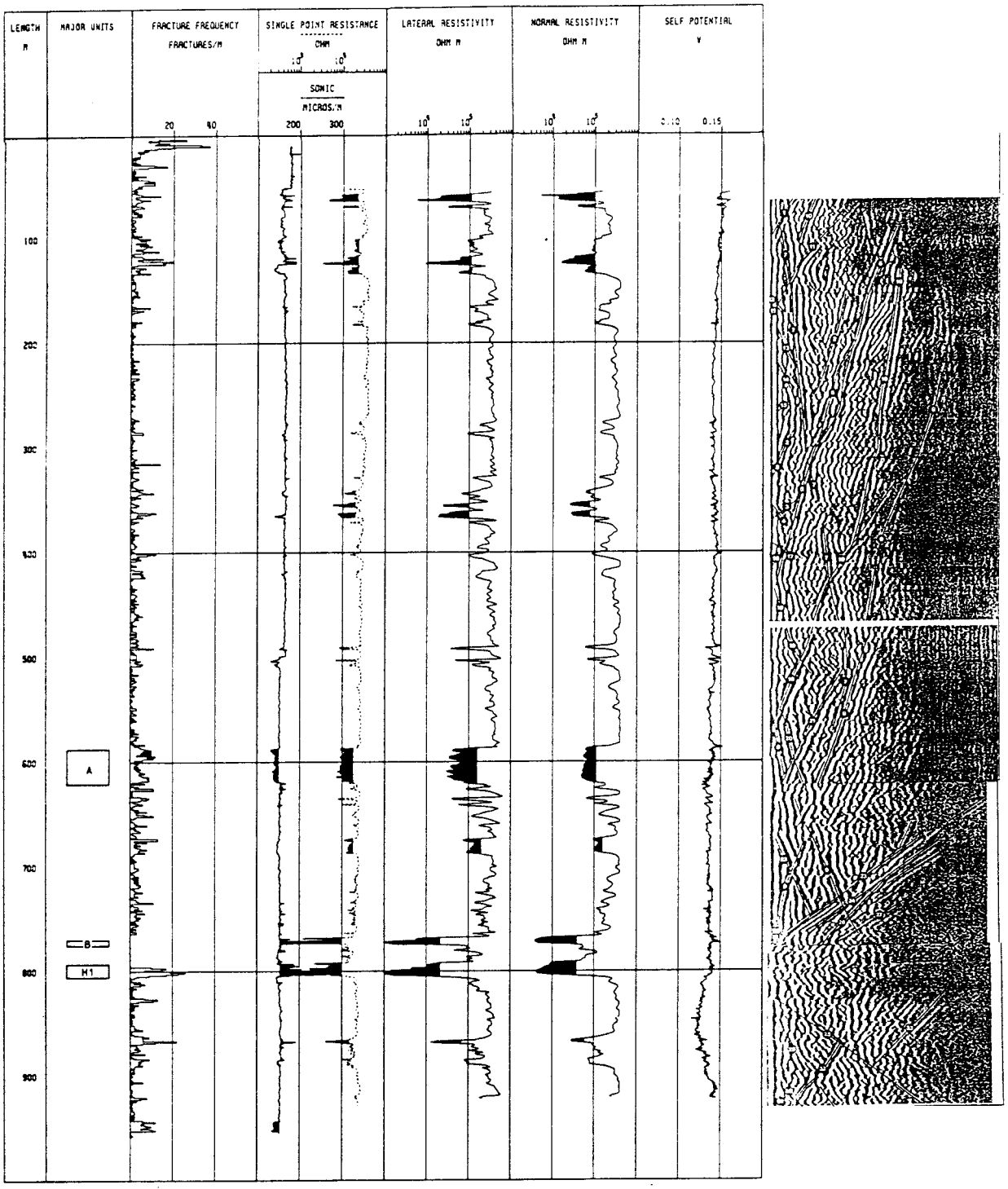


Figure 5.15: Composite plot of borehole K1 2 allowing comparison of the fracture occurrences (interpreted from geophysical logging methods) and radar measurements at 22 Mhz.

variations, i.e. natural gamma, single point resistance and magnetic susceptibility. Although the radar measurements were carried out at both 22 MHz and 60 MHz, only the former are reproduced here.

The number of interpreted radar reflecting structures intersecting the borehole in the 22 MHz measurement is 28 (Table 5.5). Greenstone constitutes 16 of these, mafic (dolerite) 2 and other structures 10. The number of reflectors not intersecting the borehole is 5.

The most prominent radar reflecting structures in the 22 MHz radar map from the borehole are no. 5 (greenstone, low resist.) no. 7 (parallel to the borehole), no. 9 (interpreted as greenstone, low resist., Unit B), no. 19 (greenstone, low resist., Unit A), no. 23 (greenstone, Unit B) and no. 24 (fractured Zone H1). All these reflectors are subparallel to the borehole or intersect at an acute angle except no. 23 and 24 which both intersect at an angle of $58^{o}$. The reflectors subparallel to the borehole can be traced over a length of 400 m along the borehole and at a distance of 75 m outside the borehole. These reflectors exhibit a somewhat bulging or undulating structure. In some cases, for example no. 7 and 9, they seem to converge or split. Reflectors no. 23 and 24 are straight and intersect the borehole at a diverging angle. Together with no. 25 and 27 they indicate the extension of zone H1. However, the radar map also indicates a somewhat shallower formation of the upper parts of the zone H1, namely about 780m. The other reflectors intersecting the borehole are not as prominent. They are short and often seem to cease against, or be cut by, the elongated subparallel reflectors.

Loss of pulse energy occurs between 758-769 m (Unit B) and 778-796 m (Zone H1).

Table 5.5: Radar reflecting structures identified from the borehole K1 2 (22 MHz).

Radar reflecting structures not intersecting the borehole.

| Position (m) | Reflector | Angle Upp/Low | Geological structure | Comments |
|---|---|---|---|---|
| 124 | 1 | 20/ | Greenstone u.s | Low resist. Contact fractured granite /greenstone |
| 132 | 13 | /15 | Greenstone l.s | Low resist (133) Gamma (133) Fract.freq. decrease. |
| 140 | 12 | /35 | (Greenstone l.s)? | - |
| 177 | 14 | /20 | Greenstone? | Somewhat low resist. |
| 280 | 15 | 40/ | Greenstone(285) | Somewhat low resist. |
| 318 | 4 | /25 | ? (315-316) | crushed, core loss |
| 359 | 2 | 14/ | Greenstone(364) Crushed zones(363) | Low resist. |
| 359 | 18 | /14 | | Same as 2 |
| 365 | 17 | /55 | Greenstone | Low resist. Gamma anom. |
| 370 | 3 | 50/ | Greenstone(371) | Somewhat low resist. |
| 422 | 16 | 25/ | Somewhat fractured section | |
| 440 | (20 | $10^{\circ}$ ) | | |
| 480 | 6 | /5-10 | Greenstone same as no.5 | Low resist. (490) |
| 484 | 5 | 10/ | Greenstone(491) | Low resist. (490) |
| 588 | 19 | 15/ | Greenstone u.s Unit A | Same greenstone as 22 Low resist. Gamma anom. Sonic anom. Magnetic an. |
| 609 | 22 | /15 | Within greenstone Unit A | |
| 665 | 21 | 15/ | Greenstone(674) | Low resist. Gamma anom. |
| 685 | 28 | /13 | Greenstone l.s. | Resist.anom. |
| 765 | 23 | 58/ | Dolerite or greenstone, parallel to zone H1 Unit B | Low resist Gamma anom. Magnetic anom |
| 772 | 9 | 10-15/ | Greenstone Unit B | Low resist. (771-773) |
| 780 | 24 | 58/ | Fracture zone H1 | Somewhat low resist. Small sonic Gamma anom. |
| 780 | 25 | /58 | | Same as 24 |
| 791 | 29 | /23 | Fractured l.s. Greenstone u.s. Zone H1 | Resist.anom. Sonic anom. |
| 801 | 27 | 70/ | Greenstone within zone H1 | Strong res. Strong sonic Gamma anom. |
| 818 | 26 | 35/ | | |
| 839 | 30 | /25 | Idiomorphic calcite cryst. in a single fracture | |
| 859 | 31 | /25 | Fractured | |
| 941 | 32 | 30/ | Dolerite | Sonic anom. |

5.1.5.1 Level 326-331 m (approx. 320 m)

This section is characterised by granite with little evidence of fracturing; ten single fractures occur mostly between 328-331 m at intersection angles ranging from 60-80$^{o}$ to the core axis. The main filling minerals are chlorite, calcite and epidote.

Hydrology

The sampled level is located within a 20m section recording a hydraulic conductivity of 4.7 x $10^{-10}$ m/s and a pressure head of +0.6 m. A more precise characterisation of the sampled level is obtained from the only 5m section tested in the near-vicinity, i.e. at 325-330 m. Here the conductivity is 1.9 x $10^{-9}$ m/s and the piezometric head +0.9m. From examination of the detailed core log, it is evident that the one metre which falls outside the sampled section, but included within the hydraulically tested section (325-326 m), cannot be a major conducting borehole length as no fracturing is present, even on a minor scale. Therefore, the water budget presented in Figure 5.16, based on the 5m tested section, should be valid for the sampled level. This is further supported by the tubewave measurements and complementary geophysical logging.

Table 5.6: Physico-chemical parameters of groundwater from borehole KI 2 (level 326-331 m).

| Level/ sample | Depth below surface (metres) | Sampling duration (days) | pH | Eh (mV) | Cond. (mS/m) | $Na^+$ (mg/l) | $K^+$ (mg/l) | $Ca^{2+}$ (mg/l) | $Mg^{2+}$ (mg/l) | $Al^{3+}$ (mg/l) | $Mn^{2+}$ (mg/l) | Fe (tot) (mg/l) | Fe(II) (mg/l) | $HCO_3^-$ (mg/l) | $Cl^-$ (mg/l) | $F^-$ (mg/l) | $Br^-$ (mg/l) | $I^-$ (mg/l) | $PO_4^{3-}$ (mg/l) | $SO_4^{2-}$ (mg/l) | $S^{2-}$ (mg/l) | TOC (mg/l) | $Si^{4+}$ (mg/l) | Drilling water (%) |
|---|---|---|---|---|---|---|---|---|---|---|---|---|---|---|---|---|---|---|---|---|---|---|---|---|
| KI 2 | 326 (320) | 1 | 7.6 | - | 25.5 | 19 | 1.6 | 29 | 2.0 | - | 25 | - | - | 113 | 14 | 3.5 | 0.08 | - | - | 0.8 | 0.21 | - | - | 5.32 |
| | | 2 | 7.6 | -347 | 27.1 | - | - | 30 | 2.0 | 0.17 | 14 | 0.212 | 0.209 | 130 | 15 | 2.8 | - | 0.010 | - | 0.4 | 0.15 | - | - | 1.81 |
| | | 3 | 7.6 | -343 | 27.7 | 29 | 1.5 | 31 | 1.0 | - | - | - | - | 132 | - | - | - | - | - | - | 0.14 | - | - | 0.83 |
| | | 5 | 7.6 | -336 | 27.9 | 29 | - | 31 | 1.2 | - | 0.07 | 0.231 | 0.217 | 132 | 16 | 2.9 | - | - | - | 0.2 | 0.11 | - | - | 0.42 |
| | | 6 | 7.6 | -331 | 27.8 | 29 | 1.5 | 31 | 2.0 | 0.07 | 0.06 | 0.230 | 0.200 | 132 | 16 | 2.9 | 0.09 | 0.010 | - | - | 0.07 | - | 7.0 | 0.32 |
| | | 7 | 7.6 | -327 | 27.9 | 29 | 1.3 | 31 | 2.0 | - | 0.06 | 0.171 | 0.176 | 138 | - | - | - | - | - | 0.2 | 0.10 | - | - | 0.27 |
| | | 8 | 7.6 | -323 | 28.0 | 29 | 1.0 | 31 | 1.0 | 0.08 | 0.05 | - | - | 138 | 17 | 2.9 | 0.02 | 0.010 | - | 0.1 | 0.09 | - | - | 0.24 |
| | | 10 | 7.6 | -316 | 28.0 | - | - | 31 | 1.0 | - | - | 0.203 | 0.162 | - | - | - | 0.05 | - | - | - | - | - | 7.3 | 0.20 |
| | | 12 | 7.6 | -313 | 28.1 | 33 | 0.8 | 30 | 2.0 | - | 0.05 | 0.145 | 0.138 | 139 | 16 | 2.9 | - | - | - | 0.1 | 0.08 | - | 7.9 | 0.16 |
| | | 13 | 7.5 | -312 | 28.2 | 28 | 0.9 | 31 | 1.0 | 0.09 | 0.05 | 0.147 | 0.141 | 135 | 16 | 2.8 | 0.13 | 0.010 | - | 0.1 | 0.08 | - | 7.5 | 0.15 |
| | | 14 | 7.5 | -306 | 28.1 | 27 | 0.9 | 31 | 1.0 | - | 0.05 | 0.133 | 0.130 | 137 | 17 | 2.9 | 0.12 | - | - | 0.1 | 0.06 | - | 7.8 | 0.13 |
| | | 15 | 7.5 | -298 | 28.1 | 29 | 1.1 | 31 | 1.0 | - | 0.06 | 0.140 | 0.134 | 135 | 17 | 2.8 | 0.12 | - | - | 0.1 | 0.06 | - | 7.6 | 0.13 |
| | | 16 | 7.5 | -297 | 28.1 | 31 | 1.1 | 31 | 1.0 | - | 0.06 | 0.130 | 0.123 | 135 | 17 | 2.5 | 0.12 | - | 0.002 | 0.1 | 0.05 | - | 7.8 | 0.12 |
| | | 19 | 7.5 | - | 28.1 | 26 | - | 31 | 1.0 | - | 0.05 | 0.128 | 0.125 | 137 | 16 | - | 0.13 | - | 0.002 | 0.1 | 0.04 | - | 7.6 | 0.10 |
| | | 20 | 7.5 | -289 | 28.1 | 24 | 1.1 | 31 | 1.0 | 0.08 | 0.05 | 0.126 | 0.126 | 136 | 16 | - | - | 0.010 | 0.002 | - | 0.07 | - | 7.6 | 0.11 |
| | | 21 | 7.5 | -287 | 28.2 | 26 | - | 31 | 1.0 | 0.09 | 0.05 | 0.107 | 0.102 | 134 | 17 | - | - | - | 0.002 | - | 0.05 | - | 7.4 | 0.09 |
| | | 22 | 7.5 | - | 28.2 | 27 | 1.1 | 30 | 1.0 | 0.07 | 0.04 | 0.105 | 0.102 | 134 | 18 | - | - | 0.010 | - | - | 0.07 | - | 7.5 | 0.08 |
| | | 23 | 7.5 | -283 | 28.1 | - | - | 31 | 1.0 | - | 0.04 | 0.092 | 0.088 | 132 | 18 | - | - | - | 0.002 | - | 0.02 | - | 7.6 | 0.08 |

Tritium: < 3 TU  Oxygen-18: -12.35 ‰  Uranium: (0.07 ppb)
Carbon-14: -  Deuterium: -  $^{234}U/^{238}U$ ratio:

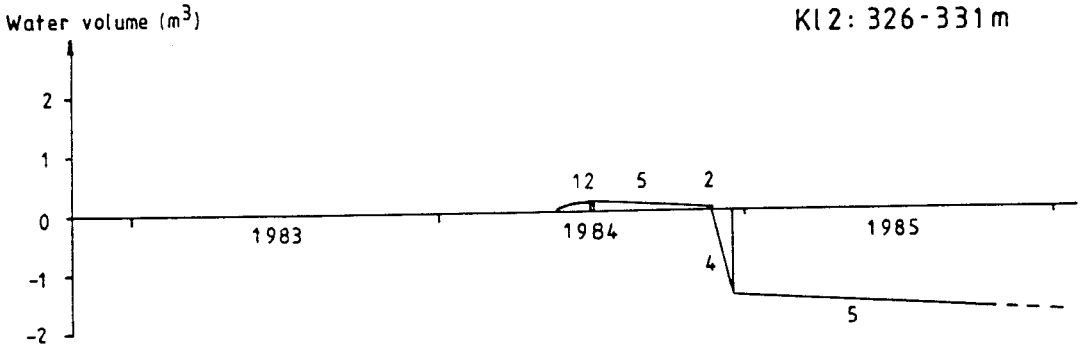


Figure 5.16: Schematic illustration of the calculated water budget for level 326-331m in borehole KI 2.
1 = Drilling water; 2 = Gas-lift pumping;
3 = Hydraulic testing; 4 = Sampling;
5 = Open-hole effect.

The water budget calculations (Table 5.2) take into consideration both the 20m and 5m tested sections. The figures refering to the 20m length have been adjusted by a factor of 0.25 (i.e. 5m/20m) to conform more to the sampled section, based on the assumption that no better data are available for the 5m scale. For example, in the present case the transmissivity ratio ($T_{20}/T_5$) indicates that the 5m section tested (i.e. 325-330 m) is conducting all the water (T-ratio = 1.0). Consequently, calculation of the water budget from the 20m section would not result in the best estimate. However, in the actual case this is of no practical importance as both calculations suggest that a representative groundwater is sampled. This is clearly shown from Figure 5.16.

## Water geochemistry

The sampled water (Table 5.6) has a mean pH value of 7.6 and a major ion range of values typical of a near-surface non-saline water typical for many Swedish crystalline bedrock environments. Na, K, Mg and Mn, often characteristic of deeper waters which have been influenced by rock/water interaction and ion-exchange reactions, are present in low amounts, as are the anions Cl, Br and F. In contrast, Ca and $HCO_3$ are present in greater amounts, as would be expected in a more surface-derived groundwater. Apart from the first 4-5 samples, the drilling water component rapidly falls off during the sampling period until finally only 0.08% is recorded.

## Redox-sensitive parameters

The iron and sulphide contents are low and most of the iron is in the ferrous state. This indication of a reducing groundwater environment is supported by high negative Eh values (-283 to -347 mV).

## Isotope geochemistry

Of the data available, the absence of tritium (<3TU) supports a water devoid of any younger component either due to drilling water or mixing with higher conductive levels along the borehole. The $\delta^{18}O$ value of -12.35 ppt is representative for meteoric waters in this part of Sweden.

## Uranium geochemistry

Little data are available; one analysis records a low uranium content (0.07 ppb) which would suggest a reducing environment.

## Summary

Hydrological considerations have indicated that the sampled section should result in a representative groundwater free from any contamination attributable to drilling fluid, hydro-injection testing, and from open hole effects. This is largely borne out by the chemistry which indicates a groundwater of a near-surface origin, without any younger, modern component, and which is reducing in character. The water budget (Fig. 5.16) is supported by the chemical trends during sampling, which show that the residual drilling water contamination has been fairly rapidly removed from the conductive zones during the sampling period. However, as only the last 3 sampling days record drilling water values of less than 0.1%, in retrospect a longer sampling time would have been desired. Other parameters which show some variation during the sampling period are a reduction of iron and less obviously K, Mn and S(II) and a small increase in Cl and Br.

### 5.1.5.2 Level 623-628 m (approx. 610 m)

The sampled borehole section is located exclusively within the granite and is characterised by a distinct zone of fracturing from approximately 625-627 m; a more isolated thin zone (comprising 4 fractures and 5 cm wide) occurs from 623.05-623.10 m. The main fractured length contains two zones, each of 5 fractures, 10 cm and 20 cm in length respectively (the presence of these are further supported by the geophysical logging and tubewave measurements); otherwise single or double fractures are present (total 14). The intersection angle of the fractures with the dillcore axis ranges mostly from 80-90$^{o}$, with two exceptions of 10$^{o}$ and 50$^{o}$ respectively. The dominant fracture filling minerals are chlorite and calcite with lesser amounts of hydroxy iron oxides and sporadic indications of siderite, gibbsite and kaolinite, the last three phases being identified from the fractured zone at 626.40 m. The presence of iron oxide coatings is a good indication of an active groundwater conducting borehole section.

Table 5.7: Physico-chemical parameters of groundwater from borehole KI 2 (level 623-628 m).

| Level/ sample | Depth below surface (metres) | Sampling duration (days) | pH | Eh (mV) | Cond. (mS/m) | $Na^{+}$ (mg/l) | $K^{+}$ (mg/l) | $Ca^{2+}$ (mg/l) | $Mg^{2+}$ (mg/l) | $Al^{3+}$ (mg/l) | $Mn^{2+}$ (mg/l) | Fe (tot) (mg/l) | Fe(II) (mg/l) | $HCO_3^{-}$ (mg/l) | $Cl^{-}$ (mg/l) | $F^{-}$ (mg/l) | $Br^{-}$ (mg/l) | $I^{-}$ (mg/l) | $PO_4^{3-}$ (mg/l) | $SO_4^{2-}$ (mg/l) | $S^{2-}$ (mg/l) | TOC (mg/l) | $Si^{4+}$ (mg/l) | Drilling water (%) |
|---|---|---|---|---|---|---|---|---|---|---|---|---|---|---|---|---|---|---|---|---|---|---|---|---|
| KI 2 | 623 (619) | 1 | - | - | - | 14.3 | 2.3 | 22.4 | 3.7 | - | - | 0.54 | 0.43 | 101 | 7.9 | 3.0 | 0.04 | - | - | 0.03 | 0.18 | - | - | 4 |
| | | 2 | - | - | - | 17.3 | 2.0 | - | - | - | 0.44 | 0.20 | 0.13 | - | 9.0 | 3.0 | 0.05 | - | - | <0.05 | 0.23 | - | 3.5 | 6 |
| | | 3 | - | - | - | - | - | - | - | - | - | - | - | - | - | - | - | - | - | - | - | - | - | 8 |
| | | 4 | - | - | - | - | - | - | - | - | - | - | - | - | - | - | - | - | - | - | - | - | - | 10 |
| | | 5 | 7.9 | - | 24.1 | - | - | 20.5 | 3.0 | - | - | 0.17 | 0.16 | - | - | - | - | - | - | - | 0.32 | - | 4.7 | 10 |
| | | 6 | 7.9 | - | 25.0 | - | - | 21.1 | 2.5 | - | 0.22 | 0.12 | 0.08 | 93 | 19.9 | 3.6 | 0.23 | - | - | 0.22 | 0.30 | - | - | 10 |

Tritium: -
Carbon-14: -
Oxygen: -
Deuterium: -
Uranium: -
$^{234}U/^{238}U$ ratio: -

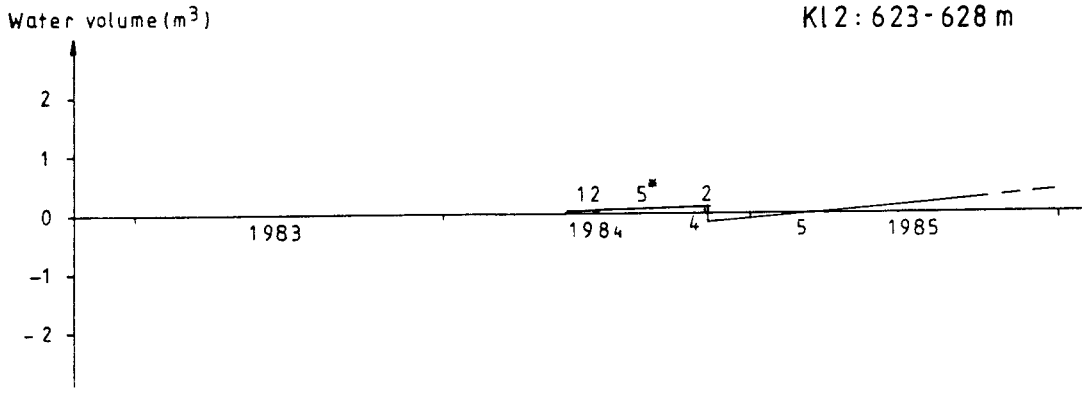


Figure 5.17: Schematic illustration of the calculated water budget for level 623-628 m in borehole KI 2. 1 = Drilling water; 2 = Gas-lift pumping; 3 = Hydraulic testing; 4 = Sampling; 5 = Open-hole effect (* includes 10 weeks with packers emplaced to prevent open-hole effect).

Hydrology

The hydraulic conductivity of the measured 20m borehole section (620-640 m) is $5.5 \times 10^{-10}$ m/s with a piezometric head of -2.8 m (Table 5.2). One of the tested 5m sections (620-625 m) overlaps by 2 m the section sampled, but is not considered to be in any way representative because it does not include the above-mentioned fracture zones at approximately 625 m and 627 m. Furthermore, the potentially conducting fractures most likely to affect the 5m section are located around 620 m, outside the sampled section in question.

The T-ratio ($T_{20}/T_5 = 1.0$) suggests that the 5m section from 620-625 m conducts all the water within the 20 m tested section. However, based on the points of discussion above, the sampled level is assumed to contribute 50% of $T_{20}$. The

water budget presented in Figure 5.17 is based on this assumption and indicates that a representative groundwater sample should be possible.

### Water geochemistry

Only incomplete analyses of this groundwater are available (Table 5.7). These show a pH value of 7.9 and a major ion range typical of a near-surface derived component. A significant proportion of drilling water is present (4-10%) which increases during the sampling period.

### Redox-sensitive parameters

The iron and sulphide contents are low and most of the iron is in the ferrous state. No Eh values are available.

### Isotope geochemistry

No data available.

### Uranium geochemistry

No data available.

### Summary

Hydraulic considerations suggesting a representative groundwater from this level have not been fully realised; the sampled water is near-surface in character and contains a significant drilling water component.

5.1.5.3 Level 741-746 m (approx. 727 m)

This sampled horizon, which once again is dominated by the granite, is moderately fractured comprising 3 fracture zones (respectively represented by 3, 4 and 3 fractures) and the rest as single fractures (total 11).

The intersection angles with the core axis range mostly from $15^{o}$-$75^{o}$, with two exceptions at $90^{o}$; the main filling mineral phases are, in order of decreasing importance, calcite, chlorite, muscovite and hydroxy iron oxides.

Table 5.8: Physico-chemical parameters of groundwater from borehole Kl 2 (Level 741-746 m).

| Level/ sample | Depth below surface (metres) | Sampling duration (days) | pH | Eh (mV) | Cond. (mS/m) | $Na^+$ (mg/l) | $K^+$ (mg/l) | $Ca^{2+}$ (mg/l) | $Mg^{2+}$ (mg/l) | $Al^{3+}$ (mg/l) | $Mn^{2+}$ (mg/l) | Fe (tot) (mg/l) | Fe(II) (mg/l) | $HCO_3^-$ (mg/l) | $Cl^-$ (mg/l) | $F^-$ (mg/l) | $Br^-$ (mg/l) | $I^-$ (mg/l) | $PO_4^{3-}$ (mg/l) | $SO_4^{2-}$ (mg/l) | $S^{2-}$ (mg/l) | TOC (mg/l) | $Si^{4+}$ (mg/l) | Drilling water (%) |
|---|---|---|---|---|---|---|---|---|---|---|---|---|---|---|---|---|---|---|---|---|---|---|---|---|
| Kl 2 | 741 (727) | 1 | 8.6 | - | 20.6 | 14 | 2.0 | 23 | 4.0 | - | 0.88 | 0.199 | 0.151 | 102 | 8 | 2.9 | 0.01 | - | - | 1.1 | 0.04 | - | 3.3 | 4.45 |
| | | 2 | - | - | - | - | - | 18 | 4.0 | - | - | 0.113 | 0.107 | 102 | 14 | 3.6 | 0.08 | - | - | 0.1 | 0.08 | - | 3.4 | 6.44 |
| | | 3 | 7.9 | -327 | 24.0 | 27 | 2.0 | 17 | 3.0 | - | 0.27 | - | - | 97 | 15 | 4.0 | 0.09 | - | - | 0.1 | 0.33 | - | 3.8 | 6.86 |
| | | 4 | 7.9 | -321 | 25.0 | 28 | 1.1 | 16 | 2.0 | - | - | - | - | 97 | 19 | 4.2 | 0.10 | - | - | 0.1 | 0.31 | - | 3.8 | 7.69 |
| | | 5 | 8.0 | -322 | 24.3 | 34 | 1.4 | 16 | 2.0 | - | 0.17 | 0.088 | 0.079 | 98 | 20 | 4.3 | 0.13 | - | - | 0.1 | 0.26 | - | 4.2 | 7.21 |
| | | 6 | 8.0 | -325 | 24.8 | 36 | 2.0 | 16 | 1.0 | - | 0.16 | - | - | 97 | 20 | 4.7 | 0.17 | - | - | 0.1 | 0.24 | - | 3.8 | 7.18 |
| | | 7 | 8.0 | -328 | 25.2 | 35 | 1.8 | 16 | 1.0 | - | 0.16 | - | - | 98 | 21 | 4.4 | 0.17 | - | - | 0.1 | 0.27 | - | 4.0 | 7.01 |
| | | 8 | 8.1 | -332 | 25.5 | 35 | 1.6 | 16 | 1.0 | 0.15 | 0.14 | 0.058 | 0.048 | 97 | 22 | 4.6 | 0.18 | 0.002 | 0.001 | 0.1 | 0.39 | - | 4.0 | 6.97 |
| | | 9 | 8.1 | -337 | 25.8 | 38 | 1.1 | 16 | 1.0 | - | 0.12 | 0.045 | 0.039 | 97 | 23 | 4.4 | 0.19 | - | - | 0.1 | 0.41 | - | 4.3 | 6.90 |
| | | 10 | 8.1 | -342 | 26.2 | - | - | 16 | 1.0 | - | 0.13 | 0.045 | 0.038 | 97 | - | - | - | - | - | 0.1 | 0.41 | - | 4.1 | 7.06 |
| | | 11 | 8.1 | -354 | 26.5 | 39 | 1.6 | 16 | 1.0 | - | 0.11 | 0.068 | 0.067 | 97 | 24 | 4.1 | 0.20 | - | - | - | 0.40 | - | 4.5 | 6.60 |
| | | 12 | 8.1 | -359 | 26.8 | 41 | 1.8 | 16 | - | - | 0.11 | - | - | 99 | 23 | 4.1 | 0.21 | - | - | 0.2 | - | - | 4.4 | 6.47 |
| | | 13 | 8.1 | -364 | 27.0 | 41 | 1.5 | 16 | 1.0 | 0.15 | 0.10 | 0.060 | 0.059 | 99 | 25 | 4.7 | - | 0.002 | 0.001 | 0.1 | 0.36 | - | 4.4 | 5.99 |

Tritium: 13 TU  Oxygen-18: -11.31 ‰  Uranium:
Carbon-14: -  Deuterium: -  $^{234}U/^{238}U$ ratio:

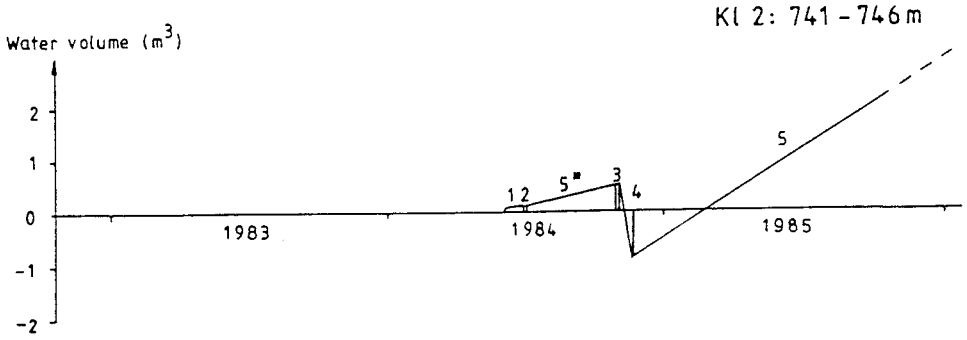


Figure 5.18: Schematic illustration of the calculated water budget for level 741-746 m in borehole Kl 2.
1 = Drilling water; 2 = Gas-lift pumping;
3 = Hydraulic testing; 4 = Sampling;
5 = Open-hole effect (* includes 10 weeks with packers emplaced to prevent open-hole effect).

## Hydrology

For this sampled level a hydraulic conductivity of $1.1 \times 10^{-8}$ m/s and a piezometric head of -2.5 m was determined from the 20 m test section. From the core log it can be concluded that the 5 m tested section from 740-745 m is representative for the sampled level; some fractures do occur at either side of the 5m section, but are of a minor nature. This section gives a K-value of $8.2 \times 10^{-9}$ m/s and a head of -2.6 m. This corresponds to a T-ratio, $T_5/T_{20} = 0.19$, for the 5m section. The water budget values calculated for both the 20m and 5m section lengths are presented in Table 5.2 and generally illustrated in Figure 5.18. Even though there is a negative piezometric head, the open-hole effect is considered small so that any contaminants should be speedily removed. Both sections therefore should result in a representative groundwater sample after sufficient sampling time.

## Water geochemistry

The sampled water (Table 5.8) has a mean pH of 8.0; of the major cations, Na, Ca, K, Mg, Fe and Mn are present in low amounts, likewise for the major anions $HCO_3$, Cl, Br and $SO_4$. Fluorine, in contrast, shows a small increase. Compared to the previous level at 326-331 m, this groundwater, whilst still exhibiting features of a near-surface character, indicates a deeper origin, as would be expected. This is seen as reductions in Ca, $HCO_3$ and S and small increases in Na, K, Cl and S(II). A significant component of residual drilling water is indicated by values of 4.45-7.69%.

## Redox-sensitive parameters

Markedly negative Eh values, together with most of the iron being in the ferrous state and the presence of small amounts of S(II), show this sampled groundwater to be reducing, to a similar degree as level 326-331 m.

## Isotope geochemistry

The presence of 13TU of tritium indicates a significant component of young, near-surface derived groundwater; no $^{14}C$ data are available. The $\delta^{18}O$ value of -11.31ppt is normal for meteoric water.

## Uranium geochemistry

No data are available.

## Summary

Borehole hydraulics and water budget calculations indicated that whilst the sampled section was characterised by a relatively high conductivity, in combination with a negative piezometric head, the open-hole effect should not have amounted to excessive groundwater contamination, but rather to small volumes which would readily be removed during sampling. The sampled groundwaters should therefore have been representative. The chemistry shows, however, that although the sampled waters suggest an intermediate to shallow origin, there is a sizeable near-surface young component, ultimately confirmed by detectable tritium (13TU). The percentage of the drilling water tracer (uranine) shows, during sampling, an initial increase from 4.45-7.69%, and then a systematic decrease to 5.99% at the end of the sampling period. Many of the chemical parameters also showed trends, e.g. a steady increase in salinity, Br, S(II) and sulphur, and initial decreases in Ca, K, Mg, Mn, Fe and $HCO_3$. This all points to an initial removal of water of similar character to level 326-331 m, and presumably the drilling water, followed by the gradual build-up of groundwater representative for the intermediate sampled level. However, as the results show, not enough sampling time was allowed to remove all of the contaminating influence, especially the drilling water fraction. Even though the borehole was plugged at 720 m directly after drilling, sufficient contamination had already been caused.

### 5.1.5.4 Levels 761 m (approx. 746 m)-hole bottom
### 777 m (approx. 762 m)-hole bottom

These sections of the borehole are hydraulically dominated by the sub-horizontal fracture Zone H1 extending from 792-804 m. This geological description will therefore refer to Zone H1 and its immediate vicinity.

Zone H1 (Fig. 5.12) is recognised from geophysical logging, and also from strong responses during tubewave and radar measurements. Its sub-horizontal extension ($30^{o}$ to the horizontal) was confirmed by radar. Unfortunately, a long section of the core within and around the zone was lost. The sections remaining consist of highly fractured granite mixed with compressed greenstone. The conductive nature of the zone is indicated by the intense fracturing and the abundant hydroxy iron-oxide coatings on the fracture planes. From 796.50 m to the end of the zone at 804 m there occur three zones of highly crushed material ranging in width from 5-30 cm, nine zones of intense fracturing (e.g. from 800.10-801.20 m there occur 23 fractures), and a total of 12 single fractures. The angle of intersection of the fractures with the core axis range from $20\text{-}80^{o}$; the major filling minerals are calcite, chlorite, hydroxy iron-oxides and subordinate pyrite. Epidote occurs sporadically.

Table 5.9: Physico-chemical parameters of groundwater from borehole KI 2 (levels 761m-hole bottom and 777m-hole bottom).

| Level/ sample | Depth below surface (metres) | Sampling duration (days) | pH | Eh (mV) | Cond. (mS/m) | $Na^{+}$ (mg/l) | $K^{+}$ (mg/l) | $Ca^{2+}$ (mg/l) | $Mg^{2+}$ (mg/l) | $Al^{3+}$ (mg/l) | $Mn^{2+}$ (mg/l) | Fe (tot) (mg/l) | Fe(II) (mg/l) | $HCO_3^{-}$ (mg/l) | $Cl^{-}$ (mg/l) | $F^{-}$ (mg/l) | $Br^{-}$ (mg/l) | $I^{-}$ (mg/l) | $PO_4^{3-}$ (mg/l) | $SO_4^{2-}$ (mg/l) | $S^{2-}$ (mg/l) | TOC (mg/l) | $Si^{4+}$ (mg/l) | Drilling water (%) |
|---|---|---|---|---|---|---|---|---|---|---|---|---|---|---|---|---|---|---|---|---|---|---|---|---|
| KI 2 | 761-hole bottom (746) | 1 | - | - | - | - | - | 23 | 5.0 | - | 0.86 | 0.430 | 0.410 | 107 | 6 | 2.0 | - | - | - | 0.8 | 0.04 | - | 2.8 | 5.32 |
| | | 2 | - | -199 | - | 11 | 3.1 | 23 | 4.0 | - | 0.77 | 0.365 | 0.365 | 100 | 6 | - | 0.02 | - | - | 0.8 | 0.04 | - | 2.8 | 3.15 |
| | | 3 | - | -249 | - | - | - | - | - | - | - | 0.435 | 0.445 | - | 6 | 2.1 | 0.03 | - | - | 0.6 | - | - | 2.8 | 4.39 |
| | | 4 | - | -268 | - | 12 | 3.0 | 23 | 4.0 | - | 0.73 | 0.430 | 0.430 | 106 | 7 | 1.9 | 0.04 | - | - | 0.6 | 0.03 | - | 2.7 | 4.74 |
| | | 5 | - | -280 | - | 13 | 3.3 | 23 | 4.0 | - | 0.72 | 0.405 | 0.410 | 105 | 6 | 2.0 | 0.03 | - | - | 0.5 | - | - | 2.7 | 6.02 |
| | | 6 | 8.0 | -290 | 20.4 | 13 | 3.4 | 23 | 4.0 | - | 0.69 | 0.340 | 0.320 | 106 | 7 | 2.3 | 0.02 | - | - | 0.5 | 0.04 | - | 2.5 | 6.87 |
| | | 7 | 8.0 | -299 | 20.5 | 13 | 3.3 | 22 | 4.0 | - | 0.63 | 0.310 | 0.285 | 106 | 8 | 2.7 | 0.04 | - | - | 0.4 | 0.05 | - | 2.5 | 4.78 |
| | | 8 | - | -307 | - | 13 | 2.5 | 22 | 4.0 | - | 0.57 | 0.350 | 0.345 | 106 | 7 | 2.5 | 0.04 | - | - | 0.3 | 0.05 | - | 2.4 | 5.23 |
| | | 9 | - | -313 | - | 13 | 3.1 | 22 | 4.0 | - | 0.60 | 0.259 | 0.253 | 105 | 7 | 2.4 | 0.02 | - | - | 0.2 | 0.05 | - | 2.6 | 5.09 |

Tritium: 25 TU  Oxygen-18:  Uranium:
Carbon-14:  Deuterium:  $^{234}U/^{238}U$ ratio:

| Level/ sample | Depth below surface (metres) | Sampling duration (days) | pH | Eh (mV) | Cond. (mS/m) | $Na^+$ (mg/l) | $K^+$ (mg/l) | $Ca^{2+}$ (mg/l) | $Mg^{2+}$ (mg/l) | $Al^{3+}$ (mg/l) | $Mn^{2+}$ (mg/l) | Fe (tot) (mg/l) | Fe(II) (mg/l) | $HCO_3^-$ (mg/l) | $Cl^-$ (mg/l) | $F^-$ (mg/l) | $Br^-$ (mg/l) | $I^-$ (mg/l) | $PO_4^{3-}$ (mg/l) | $SO_4^{2-}$ (mg/l) | $S^{2-}$ (mg/l) | TOC (mg/l) | $Si^{4+}$ (mg/l) | Drilling water (%) |
|---|---|---|---|---|---|---|---|---|---|---|---|---|---|---|---|---|---|---|---|---|---|---|---|---|
| Kl 2 | 777-hole bottom (762) | 1 | - | - | - | 9 | 2.2 | 24 | 5.5 | - | 1.10 | - | - | 105 | 6 | 1.3 | 0.02 | - | - | 2.4 | - | - | - | - |
| | | 2 | 8.1 | - | 20.7 | 9 | 2.0 | 24 | 5.5 | - | 0.94 | - | - | 107 | 6 | 1.9 | 0.03 | - | - | 1.5 | - | - | 3.0 | 4.20 |
| | | 15 | 8.1 | -325 | 20.8 | 15 | 3.1 | 23 | 4.0 | - | 0.54 | - | - | 103 | 8 | 2.7 | 0.05 | - | - | 0.1 | 0.05 | - | 2.6 | 4.56 |
| | | 16 | - | -328 | - | - | - | 22 | 4.0 | - | - | 0.209 | 0.201 | 103 | 8 | 2.8 | 0.05 | - | - | 0.2 | 0.05 | - | 2.5 | 4.39 |
| | | 17 | - | -329 | - | 16 | 3.1 | 22 | 4.0 | - | 0.51 | 0.173 | 0.159 | 103 | 8 | 2.9 | 0.03 | - | - | 0.2 | 0.05 | - | 2.6 | 5.01 |

Tritium:
Carbon-14:

Oxygen-18:
Deuterium:

Uranium:
$^{234}U/^{238}U$ ratio:

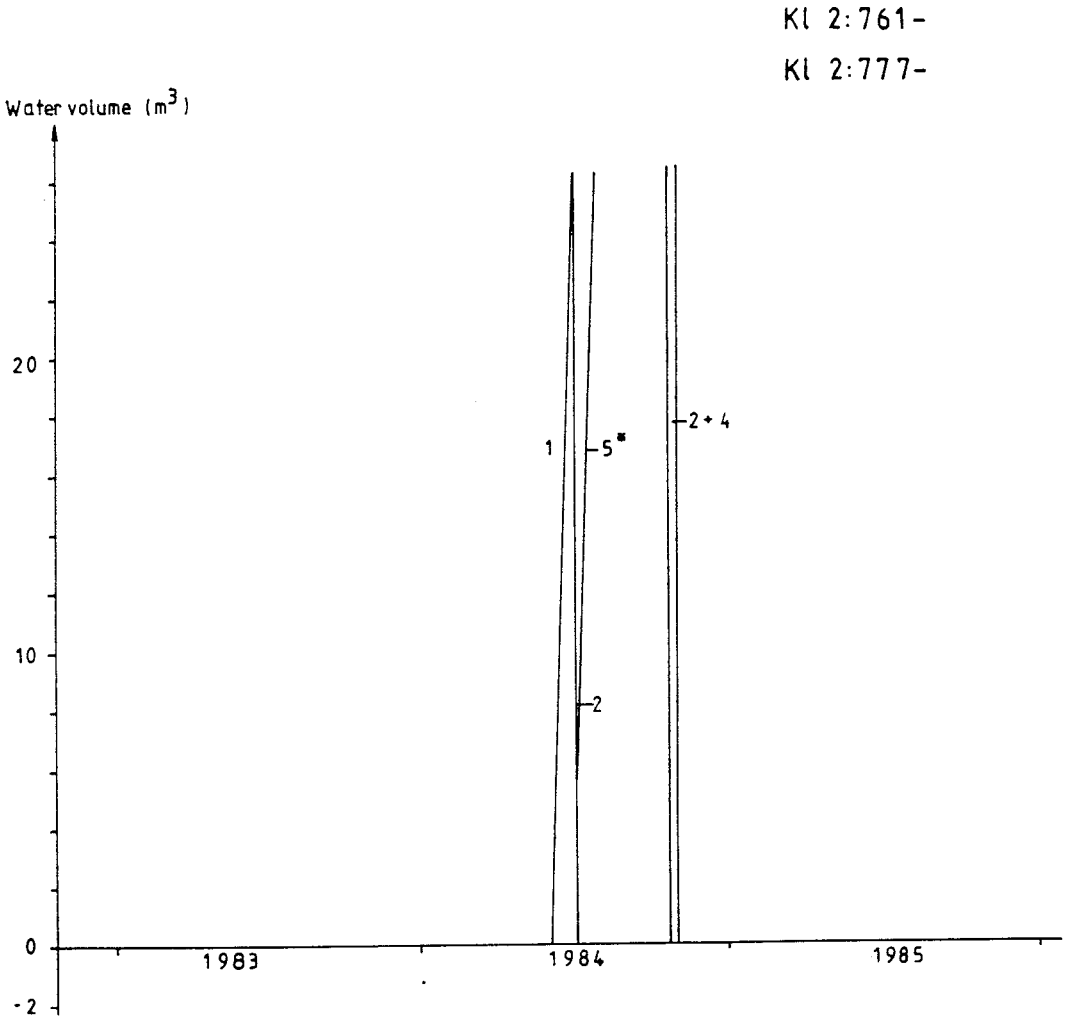


Figure 5.19: Schematic illustration of the calculated water budget for levels 761m-hole bottom and 777m-hole bottom in borehole Kl 2.
1 = Drilling water; 2 = Gas-lift pumping;
3 = Hydraulic testing; 4 = Sampling;
5 = Open-hole effect (* includes 10 weeks with packers emplaced to prevent open-hole effect).

## Hydrology

As mentioned above, sampling from these two levels is dominated by the extremely high hydraulic conductivity of the sub-horizontal Zone H1 present within the tested 20m borehole section from 790-810 m. The conductivity is $1.2 \times 10^{-6}$ m/s and the piezometric head is -2.2 m (Table 5.2). The water budgets were calculated from a mean hydraulic conductivity of the sampled section lengths of approximately $1 \times 10^{-7}$ m/s, with an estimated head of -2.2 m. The water budget (Fig 5.19) shows extreme conditions with little chance of achieving a representative groundwater sample. Even if gas-lift pumping were to remove considerable volumes of water, the open hole conditions would be so effective that not even a year of continuous pumping would extract more than 105 $m^3$ of water. For the actual sampled sections, only approximately 4.5 times the borehole water volume in the sectioned-off portion of the borehole has been removed during sampling. Plugging the borehole at 720 m, 800 m and at 860 m following drilling has not either been successful enough, although it has prevented some 300 $m^3$ of additional water from flowing into the sampled levels.

## Water geochemistry

Because of the dominance of Zone H1, both sets of analyses will be treated collectively (Table 5.9). The water sampled from the respective sections has a pH 8.0, and low concentrations of the major cations and anions strongly indicate a near-surface derived young water. The very low salinity (cond. 20.4-20.8 mS/m) and the high percentage of drilling water (4.20-6.87%) essentially support this conclusion.

## Redox-sensitive parameters

In both cases the iron content is low but significantly higher than the other described levels; almost all iron is in the ferrous state. This indication of a reducing groundwater

environment is supported by the negative Eh values (-199 to -329 mV).

## Isotope geochemistry

Only one analysis is available; 25TU has been measured in the groundwater from the 761m-hole bottom section. This shows, beyond doubt, a very major portion of surface-derived water, i.e. in this case drilling water.

## Uranium geochemistry

No data available.

## Summary

The two sampled sections, even though extending down for some 200 m from the installed packer, are hydraulically dominated by the sub-horizontal fracture Zone H1 which intersects the borehole from 792-804 m. This zone is characterised by a high conductivity coupled with a marked negative piezometric head. This has enabled large volumes of contaminating waters (ie. from drilling water and from higher conducting levels within the borehole) to flow out, along the fracture for considerable distances. The normal clearing procedure of the hole by gas-lift pumping, the installation of packers to plug the hole prior to sampling, and the removal of water during sampling, has been totally ineffective in controlling and removing the large volumes of accumulated contaminating waters. This is strongly reflected by the groundwater chemistry and the tritium value (25TU) which point to a surface- to near-surface derived young water. The continuous presence of uranine, the drilling water tracer, shows that a major contaminating component is from the drilling water.

5.1.5.5 Level 860m-hole bottom

The sampled borehole length consists mainly of granite and the section considered to be hydraulically dominant extends from 865-870 m. Present within this section is one highly crushed zone some 10 cm wide characterised by hydroxy iron-oxide coatings and fracture fillings of calcite, chlorite, epidote and pyrite. In addition, there is a broad more moderately fractured zone adjacent to the crushed section, comprising a total width of 110 cm and containing 23 fractures; several single fractures, mostly occurring between 865-867 m and 868.50-870.00 m also occur. Hydroxy iron-oxide is only present in those fractures adjacent to the crush zone; otherwise the main filling minerals are epidote, chlorite and calcite.

Hydrology

Along the total length of sampled section, the hydraulic characteristics of the tested 5m section from 865-870 m are considered to dominate. Here the hydraulic conductivity is 6.9 x $10^{-9}$ m/s and the piezometric head is -2.0 m (Table 5.2). The calculated water budget presented in Figure 5.20 indicates that with sufficient extraction of water during the sampling period, a representative groundwater sample should be possible. The pumped volume removed by sampling has been shown to exceed the sealed-off borehole section by 8 times. Furthermore, without plugging of the borehole at 800 m following drilling, the water budget calculations show that an additional 130 litres would have remained to have been extracted after the sampling period, before a representative sample could have been collected.

Table 5.10: Physico-chemical parameters of groundwater from borehole Kl 2 (Level 860m-hole bottom).

| Level/ sample | Depth below surface (metres) | Sampling duration (days) | pH | Eh (mV) | Cond. (mS/m) | $Na^+$ (mg/l) | $K^+$ (mg/l) | $Ca^{2+}$ (mg/l) | $Mg^{2+}$ (mg/l) | $Al^{3+}$ (mg/l) | $Mn^{2+}$ (mg/l) | Fe (tot) (mg/l) | Fe(II) (mg/l) | $HCO_3^-$ (mg/l) | $Cl^-$ (mg/l) | $F^-$ (mg/l) | $Br^-$ (mg/l) | $I^-$ (mg/l) | $PO_4^{3-}$ (mg/l) | $SO_4^{2-}$ (mg/l) | $S^{2-}$ (mg/l) | TOC (mg/l) | $Si^{4+}$ (mg/l) | Drilling water (%) |
|---|---|---|---|---|---|---|---|---|---|---|---|---|---|---|---|---|---|---|---|---|---|---|---|---|
| Kl 2 | 860-hole bottom (843) | 1 | - | -291 | - | 57 | 1.6 | 8.4 | 1.9 | - | 0.11 | 0.043 | 0.031 | 106 | 37 | 5.4 | 0.25 | - | - | 1.6 | 0.15 | - | 3.9 | 4.54 |
| | | 2 | 8.6 | -298 | 34.0 | 59 | 1.7 | 8.6 | 1.8 | 0.09 | 0.10 | 0.050 | 0.045 | 103 | 37 | 5.4 | 0.25 | 0.012 | 0.002 | 1.6 | 0.15 | 5.3 | 3.8 | - |
| | | 3 | 8.6 | -296 | 35.0 | 63 | 1.6 | 8.3 | 1.8 | - | 0.10 | 0.043 | 0.041 | 102 | 49 | 5.8 | 0.35 | - | - | 1.5 | 0.14 | - | 4.9 | 4.17 |
| | | 4 | 8.6 | -295 | 36.0 | 65 | 1.6 | 8.2 | 1.8 | - | 0.07 | 0.042 | 0.037 | 101 | 51 | 5.3 | 0.42 | - | - | 1.5 | 0.12 | - | 5.0 | 3.80 |
| | | 17 | 8.7 | - | 38.5 | 72 | 1.4 | 7.9 | 1.9 | - | 0.06 | 0.060 | 0.045 | 87 | 53 | 4.8 | 0.48 | - | - | 1.3 | 0.11 | - | 4.9 | 3.50 |

Tritium:
Carbon-14:

Oxygen-18:
Deuterium:

Uranium:
$^{234}U/^{238}U$ ratio:

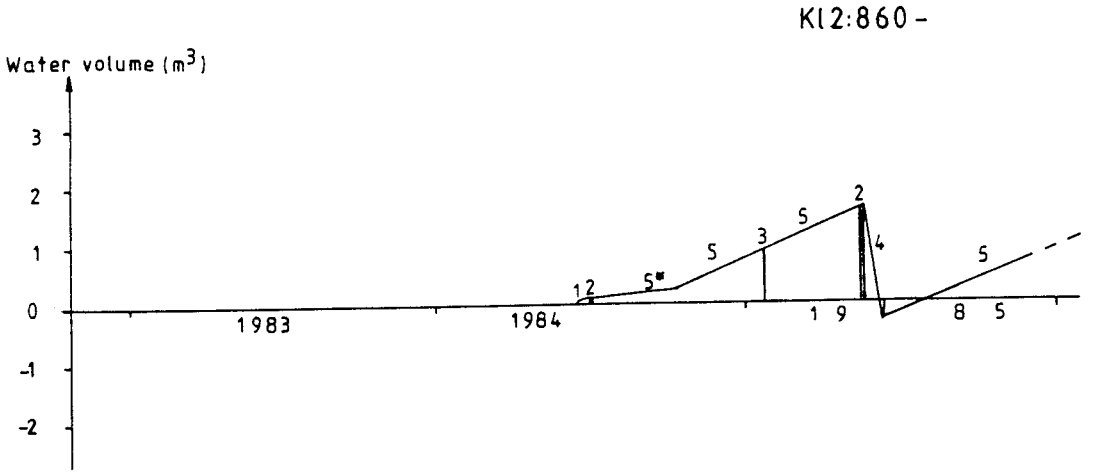


Figure 5.20: Schematic illustration of the calculated water budget for level 860m-hole bottom in borehole Kl 2.
1 = Drilling water; 2 = Gas-lift pumping;
3 = Hydraulic testing; 4 = Sampling;
5 = Open-hole effect (* includes 10 weeks with packers emplaced to prevent open-hole effect).

## Water geochemistry

The sampled water (Table 5.10) has a pH of 8.6; the major ions, with the exception of Na, Cl, Br and $SO_4$, are all present in low amounts, when compared to the other analysed levels. The chemistry, especially the higher Na, and Cl, and the decrease in Ca and to a lesser extent $HCO_3$, shows a water mainly of intermediate origin. However, the significant drilling water percentage (3.50-4.54%) indicates a sizeable component of contamination.

## Redox-sensitive parameters

Iron, mainly in the ferrous state, is present in low amounts; the sulphide content is significantly higher than the other levels. These two reducing characteristics are further supported by the negative Eh values ranging from -291 to -298 mV.

## Isotopic geochemistry

No data available.

## Uranium geochemistry

No data available.

Summary

The hydraulic characteristics of the tested section predicted an uncontaminated groundwater sample, even though a moderately high conductivity is coupled with a negative piezometric head. It was considered that plugging of the borehole after drilling, together with the pre-sampling extraction of water by gas-lift pumping and pumping prior to sampling, would be adequate to remove all traces of residual contaminating water. This, however, was not fulfilled, and the collected sample shows the presence of a significantly high drilling water component, even though the general water chemistry suggests a groundwater of intermediate origin. More water extraction would have been necessary prior to sampling.

5.1.5.6 Borehole summary and discussion

Geological and hydrological investigations within borehole Kl 2 have resulted in establishing the presence of the sub-horizontal fracture Zone H1, together with four other, more minor horizons, of increased hydraulic conductivity. Apart from the uppermost 150-200 m, which typically is highly conductive at this and other Swedish test-site areas, the chosen zones for sampling purposes are quite clearly demarcated in an otherwise low fracture density bedrock (mean about 2 fractures/m). With the exception of level 326-331 m, all the other conductive horizons investigated are characterised by a negative piezometric head, no more so than the Zone H1 with values of $1.2 \times 10^{-6}$ m/s for conductivity and -2.2 m for piezometric head. The water flow direction in the borehole is thus dominantly downwards and out into the bedrock mainly via Zone H1. Open hole effects would therefore be expected to pose serious problems to a potential groundwater sampling programme. In an attempt to minimise such effects, the borehole was plugged following drilling to await future groundwater sampling. This has undoubtedly helped, as the water budget calculations have shown. On basis of the hydraulics, levels 326-331 m and 741-746 m and to a lesser extent level 623-628 m and 860m-hole bottom, were considered promising to obtain

representative groundwater samples. Borehole sections 761m-hole bottom and 777m-hole bottom, both of which include the sub-horizontal Zone H1, were expected to be unsuitable.

On the basis of general chemistry, all the collected groundwaters represented an intermediate to a near-surface meteoric origin; no saline waters were encountered. With the exception of the uppermost level (326-331 m) all groundwaters exhibited degrees of drilling water contamination which was still present even after the sampling period, although in level 741-746 m and section 860m-hole bottom, the drilling water component was systematically decreasing, and over a longer pumping period may have disappeared altogether. Contamination by a young water component is also supported by the few tritium analyses which ranged from 13-25TU; once again only level 326-331 m showed no evidence of contamination.

Combining the hydrology and chemistry of the groundwater, it would appear that only level 326-331 m is representative, and the main determining factor for this is the positive piezometric head which has negated possible contamination from a younger water component deriving from higher conductive levels in the borehole (i.e. upper 100-150 m). At the other extreme, those sampled sections which included the sub-horizontal Zone H1 stood little chance, given the combination of high conductivity and high negative head. This fracture zone has served as a sump for much of the drilling water and higher-level younger waters which have flowed down the borehole. These contaminating waters have spread for considerable distances along the zone and no amount of pump extraction would achieve a representative sample given the time available. For the other levels, which theoretically showed promise because of less serious open-hole effects, more time would be required to rid the conductive horizons of the residual groundwater contaminants introduced (aided by negative head characteristics) into the conductive horizons under investigation.

Irrespective of contamination or not, all the sampled groundwaters were highly reducing and therefore iron was mainly in the ferrous state and uranium contents were low. A contributary reason for this, when it is obvious that a considerable volume of oxidising drilling water was introduced into the system, is the time lag between drilling and sampling, i.e. some 3-6 months, more than adequate for the introduced water to become reduced.

Investigation of this hole showed the value of both tubewave and radar measurements. All zones identified by tubewave to be potentially conductive, were, on sampling, proven to be correct. In addition, the value of the radar measurements was particularly seen in the characterisation of the sub-horizontal Zone H1 as well as confirmation of many of the mapped fracture zones.

### 5.1.6 Borehole Kl 9

Borehole Kl 9, drilled at an angle of 56° in an WNW direction is located within the north central part of the Klipperås test site area (Fig. 5.6). The total length of the hole is 801.03 m (vertical depth of approx. 670 m) and the primary objective was to penetrate the granite bedrock limited by the local fracture zones, Zones 1 and 2. As a result, Zone 2 was intercepted between 120-160 m and Zone 1 between 615-665 m (Fig. 5.21).

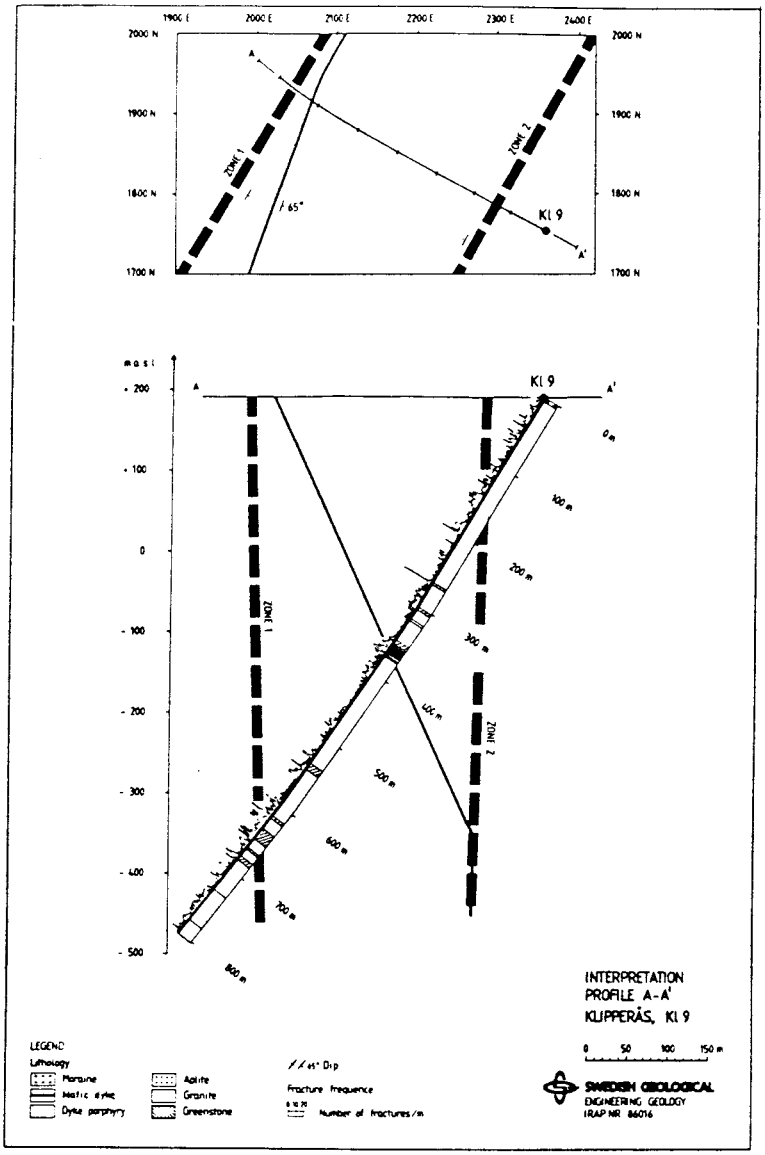


Figure 5.21: Schematic lithology and fracture frequency with interpretation of the borehole Kl 9.

The dominant rock-type along the borehole length is granite (81.22%) followed by 10.00% porphyry, 6.68% greenstone, 1.85% mafic dolerite dyke, and 0.25% aplite. The uppermost part of the hole (down to approx. 270 m) is dominantly granite, after which porphyry, and especially greenstone occurrences, increase towards the hole bottom; a distinct dolerite dyke occurs around 370 m (Fig. 5.6). The granite is principally medium-grained, massive and macroscopically homogeneous. The mobile textural nature of the granite is due mainly to the presence of microfracturing or compressional structures. Numerous bands of greenstone of variable thickness and unknown orientation occur, together with subordinate narrow dykes of aplite and veins of quartz.

The dolerite dyke, striking NNE and dipping towards the east, has retained its primary ophitic texture and forms a strong feature on the magnetic map. The porphyry dykes traversing the granite have a somewhat different macroscopic appearance. The porphyry at 280 m is reddish-brown with quartz and feldspar phenocrysts, which contrasts with 750 m whereupon a dark-grey plagioclase porphyry occurs. Their orientation is in some doubt.

The distribution of fracturing in the hole is illustrated in Figure 5.22a. The mean fracture density is 4.50 fractures/m. The greatest fracture frequency is associated with the aplite (9.00 fractures/m), followed by greenstone (8.59), mafic dolerite material (6.24), porphyry (5.27) and finally granite (4.02). The variation in fracture frequency along the core gives the impression of a regular alternation of moderate to dense fracturing in the bedrock.

The interception of the two local fracture zones dominate the major structural characteristics of the borehole. Zone 2 was traversed between 120-160 m; this was initially observed by a marked increase in fracture frequency and a 0.2 m wide crushed granite section. This was followed between 142-156 m by repeated zones of fracturing until another 10cm section of crushed granite occurred. The most common fracture filling

minerals are chlorite, calcite and quartz, with considerable hydroxy iron-oxide coatings on fracture surfaces.

Zone 1 was intercepted between 615-665 m; the zone is characterised by schistose greenstone and deformed granite. Often the contacts are compressional or brecciated. Both rock-types are fractured and thicknesses of crushed material (up to 15 cm) and clay alteration products (up to 1cm bands) occur. Coatings of clay alteration products and hydroxy iron-oxides are commonly present on the fracture surfaces.

Increased mylonitisation of the granite was observed from 760 m down to the hole bottom.

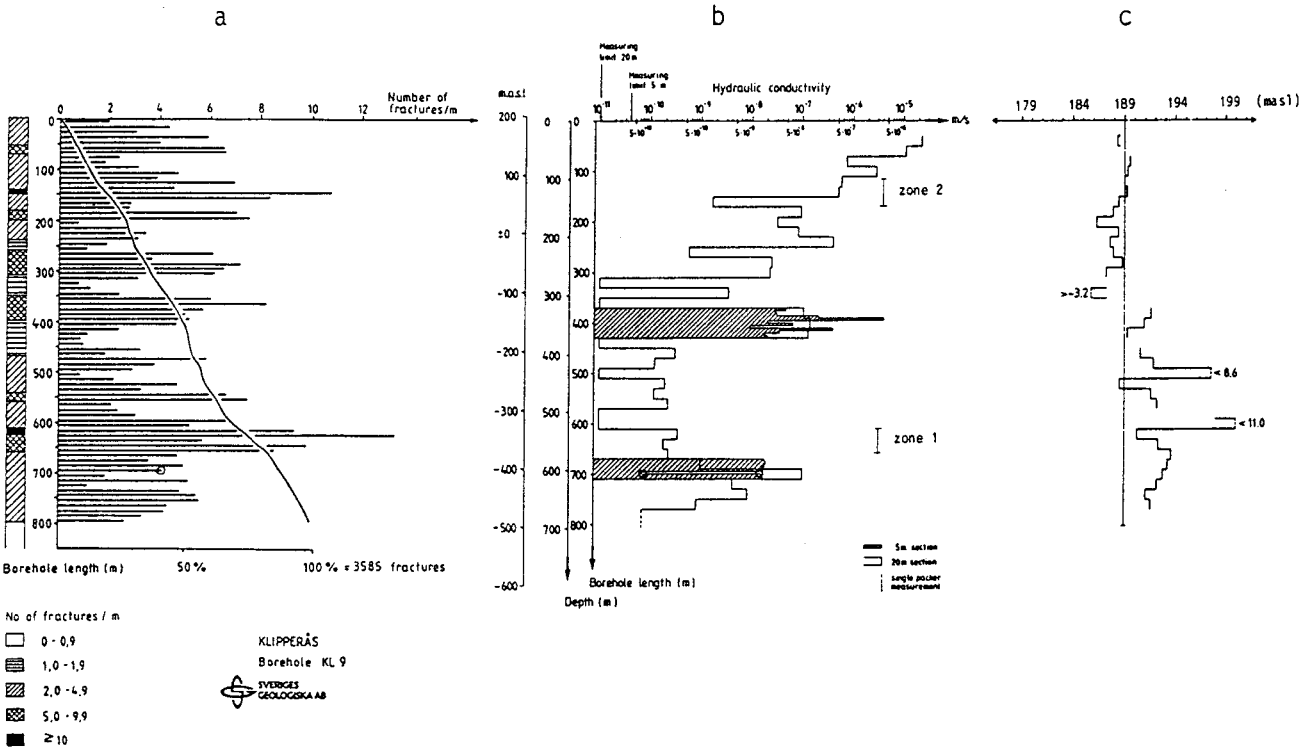


Figure 5.22: Hydrogeological characteristics for borehole Kl 9.
a) Fracture frequency (for 10m sections)
b) Hydraulic conductivity
c) Piezometric head distributions and hydrostatic head in the borehole.

The background hydrological characterisics of the borehole (Figs. 5.22b and c) show normal variations for a Swedish bedrock situation, i.e. high hydraulic conductivities in the uppermost bedrock portion, decreasing in value with increasing depth. This idealistic pattern is disturbed by two main horizons of higher conductivity; one occurring at around 400m which correlates with a tectonic horizon associated with and orientated parallel to a mafic dyke structure, and the other located below the local fracture Zone 1 at 700 m. The piezometric head along the borehole shows excess pressures below 370 m and negative pressure above, although from 70-150 m small positive heads also occur. This pattern implies a general upward transport of the groundwater within the hole. The negative head values correspond to the bedrock portion between Zone 2 and the dolerite dyke at 370 m. The two relatively high positive head values (<8.6 m and <11.0 m) correspond to sections with conductivities below the limit of measurement and can thus be ignored.

No tubewave measurements were carried out in borehole Kl 9. Results of the radar investigations at 22 MHz are presented in Table 5.11 and illustrated in Figure 5.23; the results for 60 MHz are reported by Carlsten et al (1987).

The number of interpreted radar reflecting structures intersecting the borehole in the 22 MHz measurement is 32. Greenstone constitutes 14 of these, mafic (dolerite) 3 and other structures 15. The number of radar reflectors not intersecting the borehole is 7.

The most prominent radar reflecting structures in the 22 MHz radar map from the borehole are no. 1 (fractured section incl. greenstone, low resist.), no. 5 (greenstone, low resist.), no. 6 (greenstone, somewhat low resist.), no. 7 (greenstone, low resist.), no. 8 (greenstone, low resist.), no. 9 (dolerite, low resist., Unit A), no. 11 (greenstone, low resist.), no. 13 (dolerite, low resist., Unit A), no. 27 (fractured geenstone), no. 32 (fractured greenstone) and no. 38 (not intersecting). They all intersect the borehole, except no. 38, and all of them, except three, are interpreted as greenstone. The

reflectors are rather straight and can be traced over 100 m along the borehole and up to 80 m outside the borehole. There is a marked loss of radar pulse energy between the reflectors no. 8 and no. 9. This is clearly indicated by the bulging shape of the black line representing arrival time of the direct pulse. The section between these reflectors (Unit A, 356-374 m) contains a fractured dolerite and a greenstone. The dolerite dyke has a NNE strike and dips towards E. The geophysical logs exhibit strong decrease in resistivity in this section.

Loss of radar pulse energy occurs between 138-161 m (Zone 2), 257-273 m (somewhat fractured), 347-377 m (Unit A) and 755-768 m (Unit B).

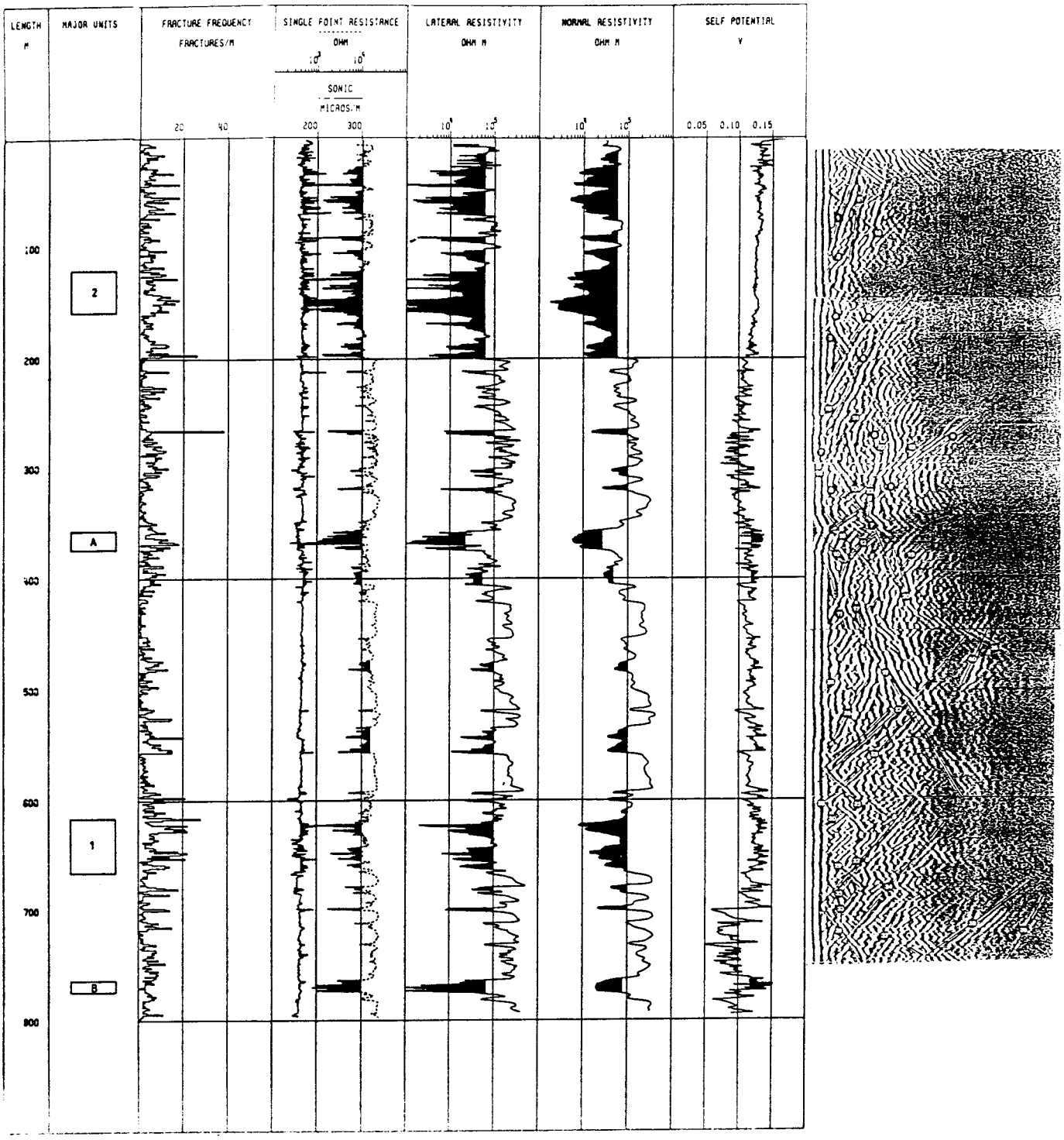


Figure 5.23: Composite plot of borehole K1 9 allowing comparison of the fracture occurrences (interpreted from geophysical logging methods) and radar measurements at 22 MHz.

# Table 5.11: Radar reflecting structures identified from the borehole K1 9.

Radar reflecting structures intersecting the borehole.

| Position (m) | Reflector | Angle Upp/Low | Geological structure | Comments |
|---|---|---|---|---|
| 32 | 15 | /40 | Altered fracture zone(31-33) | Somewhat low resist. Sonic anom. |
| 122 | 4 | /25 | Crushed and altered section upper parts Zone 2 | Low resist. Sonic anom. |
| 149 | 2 | 30/ | Altered breccia, clay, incl. a crushed zone Zone 2 | Strong decr. resistivity |
| 149 | 3 | /28 | | Same as no.2 |
| 179 | 1 | 10/ | Fractured and altered section incl.greenstone | Low resist. |
| 179 | 16 | / 10 | | Same as no.1 |
| 262 | 5 | 23/ | Greenstone u.s. (265) | Low resist. Gamma anom. Sonic anom. |
| 263 | 7 | /24 | | Same as no.5 |
| 307 | 6 | 20/ | Greenstone l.s. (303) | Somewhat low resist. Somewhat low sonic |
| 313 | 18 | /23 | Greenstone u.s. (317) | Somewhat low resist (317) Gamma anom. |
| 328 | 11 | /10 | Greenstone l.s. (323) | Low resist. (320) |
| 333 | 14 | 22/ | | |
| 355 | 8 | 30/ | Greenstone l.s. | Low resist. |
| 357 | 13 | 55/ | Dolerite u.s. Unit A | Low resist. |
| 362 | 36 | 90/ | Unit A | Low resist. |
| 374 | 9 | 60/ | Dolerite l.s. (373) fractured Unit A | Low resist. (355-373) |
| 394 | 17 | /33 | Greenstone (393) | Somewhat low resist. |
| 478 | 23 | 20/ | Fractured | Somewhat low resist. |
| 480 | 12 | 14/ | Altered fractures (481-482) | |
| 522 | 24 | 30/ | | Small sonic Somewhat low resist. |
| 555 | 25 | /40 | Greenstone, fractured | Sonic anom. Somewhat low |
| 589 | 26 | 20/ | Fractured (592-594) | |
| 598 | 27 | 40/ | Greenstone, fractured | Somewhat low resist. Gamma anom. |
| 618 | 28 | 45/ | Greenstone l.s. fractured Zone 1 | Gamma anom. |
| 625 | 29 | /35 | Fractured, crushed, altered Zone 1 | Sonic anom. Gamma anom. |
| 638 | 30 | 50/ | Greenstone Zone 1 | Gamma anom. |
| 674 | 31 | /38 | Greenstone u.s. (678) | |
| 713 | 32 | 33/ | Greenstone, fractured | |
| 727 | 35 | 28/ | Dolerite | |
| 742 | 33 | 30/ | Within porph., fractured (740) | |
| 772 | 34 | 30/ | Within porph., fractured Unit B | Low resist. |
| 790 | 40 | 15/ | Greenstone, fractured | Somewhat low resist. |

5.1.6.1 Level 696-701 m (approx. 581 m)

The sampled level lies within the granite and is characterised by two zones of fracturing, one 90 cm wide (containing 15 fractures) and the other 30 cm wide (7 fractures). Otherwise a total of 7 single fractures are present. The main fracture filling minerals are chlorite with subordinate muscovite; more detailed investigations within the larger of the two fracture zones (698.3-699.2 m) revealed the presence of epidote, siderite, gibbsite and goethite.

Hydrology

The hydraulic conductivity for the 20m section from 690-710 m is $9.4 \times 10^{-8}$ m/s and the piezometric head is +3.7 (Table 5.2). The 5m section tests in this case have been ignored because it is not considered possible that section 695-700 m, which from the core log and geophysical measurements shows evidence of conducting fractures, should have recorded a hydraulic conductivity below the detection limit. Consequently, the water budget calculations are based on the 20m test section (Table 5.2; Fig. 5.24). The water budget shows that a representative groundwater should be easily obtained from this level.

Water geochemistry

The water sampled (Table 5.12) records a pH of 8.0; the major ions are present in generally low amounts; only sulphur shows some slight anomaly. These characteristics, together with a low conductivity of 23 mS/m, classify this water as near-surface in origin. No drilling water contamination is present as indicated by the absence of the tracer uranine.

Table 5.12: Physico-chemical parameters of groundwater from borehole Kl 9 (Level 696-701 m).

| Level/ sample | Depth below surface (metres) | Sampling duration (days) | pH | Eh (mV) | Cond. (mS/m) | $Na^+$ (mg/l) | $K^+$ (mg/l) | $Ca^{2+}$ (mg/l) | $Mg^{2+}$ (mg/l) | $Al^{3+}$ (mg/l) | $Mn^{2+}$ (mg/l) | Fe (tot) (mg/l) | Fe(II) (mg/l) | $HCO_3^-$ (mg/l) | $Cl^-$ (mg/l) | $F^-$ (mg/l) | $Br^-$ (mg/l) | $I^-$ (mg/l) | $PO_4^{3-}$ (mg/l) | $SO_4^{2-}$ (mg/l) | $S^{2-}$ (mg/l) | TOC (mg/l) | $Si^{4+}$ (mg/l) | Drilling water (%) |
|---|---|---|---|---|---|---|---|---|---|---|---|---|---|---|---|---|---|---|---|---|---|---|---|---|
| Kl 9 | 696 (581) | 1 | - | - | 22.9 | 15 | 1.1 | 28 | 2 | - | 0.03 | 0.074 | 0.066 | 119 | 6.0 | 3.6 | - | - | - | 4.4 | 0.01 | 0.5 | 9.6 | - |
| | | 2 | 7.9 | - | 22.9 | 16 | 1.4 | - | - | - | - | 0.084 | 0.071 | 120 | - | - | - | 0.002 | - | 4.5 | 0.01 | - | 9.7 | - |
| | | 3 | 7.9 | - | 22.9 | 16 | 1.4 | - | - | - | 0.03 | 0.071 | 0.063 | 120 | 5.9 | - | - | - | - | 4.4 | 0.01 | - | 9.7 | - |
| | | 4 | 7.9 | - | 23.0 | 16 | - | - | - | - | - | 0.077 | 0.069 | 120 | 6.2 | - | - | - | - | 4.1 | 0.01 | - | 9.7 | - |
| | | 5 | 7.9 | - | 23.0 | 16 | 1.2 | - | - | - | - | 0.081 | 0.071 | 120 | 6.1 | - | - | - | - | 4.1 | 0.01 | - | 10.0 | - |
| | | 6 | 7.9 | - | 23.0 | 16 | 1.3 | - | - | - | 0.03 | 0.080 | - | 119 | 6.2 | 3.5 | - | 0.002 | 0.003 | - | 0.01 | 0.5 | 9.8 | - |
| | | 7 | 7.9 | - | 23.0 | - | - | - | - | - | 0.03 | 0.085 | 0.079 | 121 | 6.2 | - | - | - | - | 4.0 | 0.01 | - | 10.0 | - |
| | | 8 | 7.9 | - | 23.0 | 16 | 1.2 | 29 | 3 | - | 0.04 | 0.088 | 0.082 | 120 | 6.1 | 3.2 | - | - | - | 4.5 | 0.01 | - | 10.0 | - |
| | | 10 | 8.0 | -217 | 23.0 | 16 | 1.2 | 28 | 3 | - | - | 0.092 | 0.094 | 119 | 6.0 | 3.2 | - | - | - | 4.4 | 0.01 | - | 10.0 | - |
| | | 12 | 8.0 | -280 | 22.9 | 15 | 1.3 | 29 | 3 | - | 0.04 | 0.092 | 0.087 | 120 | - | - | - | - | - | 4.4 | 0.01 | - | 10.0 | - |
| | | 13 | 8.0 | -297 | 23.0 | 15 | 1.3 | 29 | 3 | 0.025 | 0.04 | 0.100 | 0.096 | 120 | 5.9 | 3.2 | - | 0.002 | 0.003 | 4.4 | 0.01 | 1.2 | 9.7 | - |
| | | 14 | 8.0 | -324 | 23.0 | 16 | 1.3 | 29 | 3 | - | 0.03 | 0.098 | 0.097 | 120 | 5.8 | 3.1 | - | - | - | 4.3 | 0.02 | - | 9.9 | - |
| | | 15 | 8.0 | -340 | 23.0 | 16 | 1.3 | 29 | 3 | - | 0.04 | 0.096 | 0.092 | 120 | 5.9 | 2.9 | - | - | - | 4.1 | 0.02 | - | 9.9 | - |
| | | 16 | 8.0 | -283 | 23.0 | 16 | 1.3 | 29 | 3 | - | 0.04 | 0.096 | 0.094 | 120 | 5.8 | 3.0 | 0.05 | - | - | 4.0 | 0.02 | - | 9.9 | - |
| | | 19 | 8.0 | -276 | 23.0 | 16 | 1.1 | 29 | 3 | - | 0.05 | 0.098 | 0.082 | 121 | 5.7 | 2.9 | 0.05 | 0.002 | 0.001 | 3.9 | 0.01 | 0.5 | - | 0.01 |
| | | 20 | 8.0 | -276 | 23.0 | 16 | 1.0 | 30 | 3 | - | 0.04 | 0.098 | 0.091 | 121 | 5.5 | - | 0.05 | - | - | 4.0 | 0.01 | - | 9.6 | - |
| | | 21 | 8.0 | -278 | 23.0 | 15 | 1.0 | 29 | 3 | - | 0.04 | 0.092 | 0.085 | 121 | 5.5 | 3.0 | 0.04 | - | - | 4.3 | 0.01 | - | 10.0 | - |
| | | 22 | 8.0 | - | 23.0 | 15 | 1.0 | 30 | 2 | - | 0.04 | 0.090 | 0.082 | 119 | 6.3 | 3.1 | 0.05 | - | - | 4.4 | 0.01 | - | 10.0 | - |

Tritium: < 3 TU Oxygen-18: -11.93 ‰ Uranium: (0.01 ppb)
Carbon-14: 30295 years Deuterium: $^{234}U/^{238}U$ ratio:

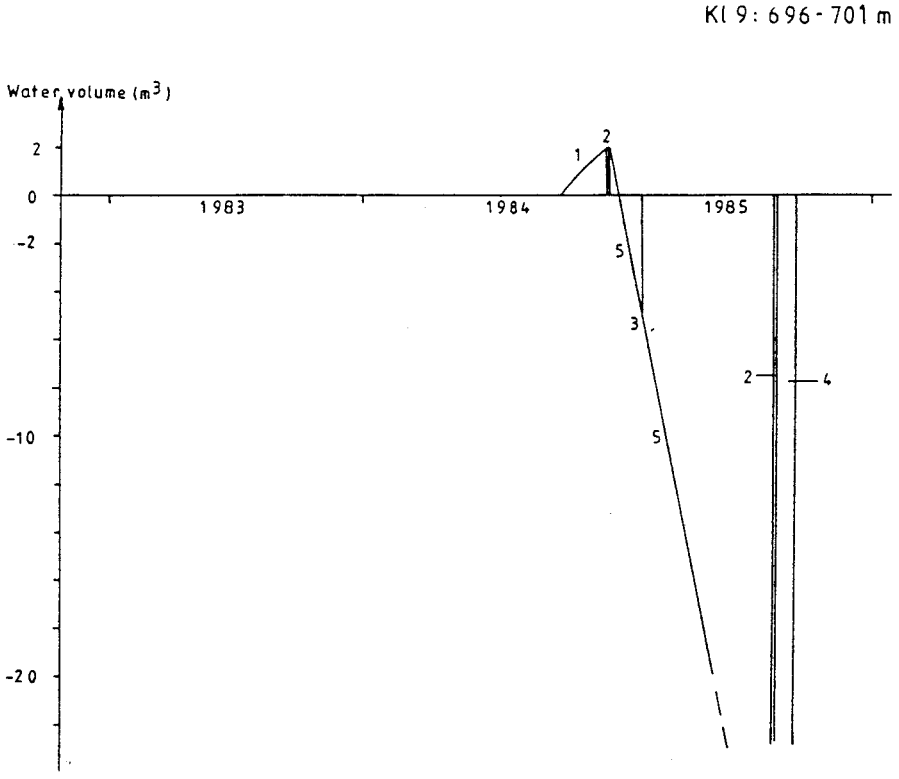


Figure 5.24: Schematic illustration of the calculated water budget for level 696-701 m in borehole Kl 9.
1 = Drilling water; 2 = Gas-lift pumping;
3 = Hydraulic testing; 4 = Sampling;
5 = Open-hole effect.

## Redox-sensitive parameters

Iron, although present in small amounts, is mostly in the ferrous state. S(II) is also barely detectable. In addition to the ferrous iron, the overall reducing nature of the groundwater is supported by the redox potential meaurements (Eh = -217 to -324 mV).

## Isotope geochemistry

Tritium is below the level of detection (<3TU) which indicates the absence of a young, surface derived component; this is also supported by the apparently very old age of the water ($^{14}C$ = 30295 years). No deuterium value is available; the $\delta^{18}O$ value of -11.93ppt indicates a meteoric origin to the groundwater.

## Uranium goechemistry

The dissolved uranium content of 0.01ppb suggests a reducing groundwater environment.

## Summary

Hydrological considerations, in this case a combination of high hydraulic conductivity and positive piezometric head, were predicted to result in a representative groundwater sample from this level. This has been borne out by the water chemistry which shows a meteoric water free from any drilling contamination or surface-derived water from conducting levels higher up in the borehole. This last point is supported by the both the tritium (<3TU) and radiocarbon data (30295 years).

5.1.6.2 Borehole summary and discussion

Geological and geophysical investigations of borehole Kl 9 have confirmed the intersection of the two local fracture Zones 1 and 2. The area between these zones is considered to represent an inter-block contact, sheared and mylonitised due to periodically activated vertical movements. The presence of Zone 2 and other fracture zones, has also been confirmed by borehole radar measurements. As borehole Kl 9 represents an inter-block contact, then two differing geological environments, and possibly groundwater environments, may be represented.

Apart from high conductivity values for the upper 300m bedrock, common for many Swedish environments as a response to tensional fracturing due to the ice-melt, the hydrogeological investigations have revealed two additional highly conductive horizons; one at around 400 m and the other just below Zone 1 at 700 m. The hydrologic pattern implies a general upward transport of water within the borehole, from a deeper (>350 m) bedrock environment characterised by positive head values, to a shallow bedrock environment (<350 m) of negative piezometric head.

Only one level was sampled, from 696-701 m. Water budget calculations predicted a representative groundwater free from any contamination that may have resulted from borehole activities; this was borne out by the groundwater chemistry. Surprisingly, however, the chemistry suggests a near-surface origin to the groundwater, especially when the sampled level is located at 700 m depth. As near-surface contamination can be ruled out, then the sampled conductive zone must eventually have some hydraulic connection with higher groundwater horizons in the bedrock. The very old age of the groundwater would initially appear to preclude this, although one can question the validity of groundwater dating by radiocarbon methods (see below, Section 6).

# 6. SUMMARY AND DISCUSSION

This report on the Klipperås test-site area represents a continuation of earlier site investigations reported by Smellie et al (1985). Because of some time overlap between the Klipperås investigation and the earlier studies, it has only been possible to implement some of the recommendations as set out in the above report.

From a total of 14 cored boreholes drilled at Klipperås, three have been selected for hydrochemical characterisation; boreholes Kl 1, Kl 2 and Kl 9. From these holes, 7 conductive borehole sections have been isolated and sampled, one each from Kl 1 and Kl 9, and the remaining 5 from Kl 2. Over and above the normal detailed geological, geophysical and hydrological site investigation programmes, the following additional studies have also been taken into consideration:

- borehole tubewave investigations (Kl 2)
- borehole radar investigations (Kl 1, Kl 2 and Kl 9)
- borehole plugging to minimise open-hole effects during the time-lag between drilling and sampling (Kl 2)
- application of hydrochemical and mineralogical data to chemical equilibrium modelling

## 6.1 Quality of the Sampled Groundwaters

From a combination of geological, geophysical and hydrological methods, suitable conductive sections were selected from the boreholes for groundwater sampling. In most cases, the hydraulically tested 20 m and 5 m sections were satisfactorly located relative to the conductive horizons in question, and the majority of the resulting water budget calculations and predictions have therefore been based on quantitative criteria.

Of the 7 borehole sections sampled, the water budget calculations predicted that four should result in representative groundwaters (Kl 1 level 406m-hole bottom; Kl 2

level 326-331m and level 741-746 m; Kl 9 level 696-701 m), one possible representative groundwater (Kl 2 level 860m-hole bottom), and two unrepresentative waters (Kl 2 level 761m-hole bottom and level 777m-hole bottom). One other section tested hydraulically, but not fully sampled (Kl 2 level 623-628 m), also indicated a possible representative groundwater. Groundwaters which are here considered representative are defined as those which show no evidence of mixing with other water sources, whether from drilling water, younger, near-surface water, or other deeper groundwaters.

Taking into consideration the groundwater chemistry and available isotopic data, it was possible to support the water budget calculations for three of the 4 representative sections; Kl 1, Kl 9 and level 326-331 m in Kl 2. Inadequate pumping time to remove all the residual drilling water (as indicated by the uranine content) was the most obvious reason for the unacceptance of Kl 2 level 741-746 m. At this level there seems to have been an underestimation of the injection of drilling water employed in the water budget calculations. This is a consequence of the calculation method used; for example, it was assumed that when drilling intercepted the highly conductive Zone H1, no further drilling water was injected in bedrock sections above this Zone during subsequent drilling. It was considered that Zone H1 had the necessary conductivity capacity to more than accomodate the total amount of drilling water pumped down. In retrospect this was not quite the case but to make a more accurate estimation of the drilling water distribution along the 20m sections may be even more precarious.

What all three representative levels (Kl 1, Kl 9 and level 326-331 m in Kl 2) have in common is a positive head deviation and moderate hydraulic conductivities between $7.10^{-10}$ to $9.10^{-8}$ m/s. As indicated by Kl 2 level 741-746 m, characterised by high conductivity but a negative head, such horizons may eventually yield a representative sample, but only after considerably longer pumping intervals than the 13 days employed in this case.

Plugging of borehole K1 2 to minimise open-hole effects during the time-lag between drilling and sampling, which in this case amounted to 3-6 months, was considered to be worthwhile for some of the sampled sections, especially those of moderate conductivity (and low negative head) characteristics. The advantages of plugging would obviously be more beneficial over longer time intervals, i e years. However, for those sections incorporating the sub-horizontal Zone H1, the combination of high conductivity and negative head showed that even though plugging was carried out only two weeks after drilling, the degree of contamination established during drilling and subsequent open-hole effects (total 1 month comprising 2 weeks prior to plugging and 2 weeks for Tubewave measurements and hole preparation before sampling) was already too substantial for representative groundwater sampling purposes. This exercise underlines the importance of rapid plugging of high-conductive zones in order to be in any way effective.

## 6.2 General Hydrochemical Characteristics of the Groundwaters

The representative chemistries for the sampled sections are summarised in Table 6.1. Two groundwater types are indicated: groundwaters of near-surface origin, and of intermediate origin (Smellie et al, 1985; Wikberg et al, 1987). No deep saline varieties were encountered. In comparison with the near-surface groundwaters, the intermediate type contains slightly enhanced contents of Na, Cl, Br and F, and reduced contents of Ca, Mg(?) and $HCO_3$; slightly higher pH is also suggested (mean of 8.2 vs 7.9). These characteristics would be expected for a deeper groundwater type whereupon typical near-surface Ca - $HCO_3$ groundwaters have gradually become depleted in Ca and $HCO_3$ (due to mineral/water reactions, and/or ion exchange reactions between Ca and Na on the clay minerals lining the conducting fractures). The source of Cl is more problematical, with several possibilities existing such as alteration of Cl-bearing minerals, leakage from fluid inclusions, and relict sea-water; sea-water is not considered to be a major factor in these samples.

Table 6.1: Summary of the physico-chemical parameters of the groundwaters from the Klipperås test-site.

| Borehole | Kl 1+ | Kl 2+ | Kl 2 | Kl 2 | Kl 2 | Kl 2 | Kl 9+ |
|---|---|---|---|---|---|---|---|
| Sampled level (m) | 406-* | 326 | 741* | 761- | 777- | 860-* | 696 |
| Na | 47 | 29 | 38 | 13 | 15 | 60 | 15 |
| K | 1.0 | 1.1 | 1.6 | 3.1 | 3.1 | 1.6 | 1.3 |
| Ca | 14 | 31 | 16 | 22 | 22 | 8.3 | 29 |
| Mg | 2.3 | 1.0 | 1.0 | 4.0 | 4.0 | 1.8 | 3.0 |
| Fe(tot) | 0.010 | 0.14 | 0.09 | 0.35 | 0.21 | 0.04 | 0.10 |
| Fe(II) | 0.008 | 0.13 | 0.08 | 0.33 | 0.20 | 0.04 | 0.09 |
| $HCO_3$ | 80 | 140 | 97 | 106 | 103 | 102 | 120 |
| Cl | 45 | 17 | 21 | 7 | 8 | 51 | 5.9 |
| F | 3.8 | 2.9 | 4.4 | 2.5 | 2.8 | 5.3 | 3.0 |
| Br | 0.4 | 0.12 | 0.18 | 0.04 | 0.05 | 0.35 | 0.05 |
| I | 0.008 | 0.010 | 0.002 | - | - | 0.012 | 0.002 |
| $PO_4$ | 0.001 | 0.002 | 0.001 | - | - | 0.002 | 0.003 |
| $SO_4$ | 1.5 | 0.1 | 0.1 | 0.5 | 0.2 | 1.5 | 4.3 |
| S(tot) | 0.10 | 0.06 | 0.40 | 0.04 | 0.05 | 0.14 | 0.01 |
| Si | 4.4 | 7.6 | 4.0 | 2.6 | 2.6 | 5.0 | 9.9 |
| TOC | 3.7 | 2.0 | 12.0 | - | - | 5.3 | 1.2 |
| $^{14}C$ (pmc) | 4.29 | - | - | - | - | - | 2.18 |
| $^{14}C$ (yrs) | 28500 | - | - | - | - | - | 30295 |
| $^{13}C$ (‰) | -17.0 | - | - | - | - | - | -15.7 |
| $^{3}H$ (TU) | <3 | <3 | 13 | 25 | - | - | <3 |
| $^{2}H$ | -86.5 | - | - | - | - | - | - |
| $^{18}O$ | -12.11 | -11.93 | -12.35 | -11.31 | - | - | -11.90 |
| U (ppb) | 0.01 | 0.01 | 0.07 | - | - | - | 0.04 |
| pH | 8.3 | 7.6 | 8.2 | 8.1 | 8.2 | 8.2 | 7.6 |
| Eh | -300 | -290 | -360 | -310 | -320 | -300 | -270 |
| Drilling water (%) | <0.1 | <0.1 | 5-6 | 5-7 | 4 | 4 | - |

Measured elements are in mg/l unless otherwise stated.

$^{2}H$ and $^{18}O$ are expressed to deviations in per mill from SMOW (Standard Mean Oceanic Water).

* Waters considered intermediate in type. (see text).
+ Waters considered representative.

A further characteristic feature of all the sampled horizons, irrespective of groundwater contamination, is the consistently negative redox potential values (-360 to -270 mV). These consistent values, supported also by uniform pH measurements may indicate that it is the fracture minerals that are determining the Eh. The overall reducing nature of the groundwaters is further supported by most of the analysed total iron being in the ferrous state. In fact, the absence of any marked redox trends, together with relatively little chemical variation in the groundwaters, bearing in mind that sampling has been systematically conducted to considerable depths, underlines the caution necessary when sampling is mainly carried out within highly active, relatively isolated hydraulic fracture systems, which traverse through the bedrock. Mixing of groundwaters from different sources has undoubtedly occurred, and may be a contributory reason why there are no marked changes in groundwater composition from the sampled holes. Obviously, near-surface groundwater contamination has strongly influenced 4 of the 5 sampled sections in borehole Kl 2, but not Kl 1 and Kl 9, both of which have been sampled from considerable depths, and yet are still characterised by relatively fresh groundwater. These features indicate that much of the groundwater collected during sampling has originated from groundwater reservoirs at substantially higher levels than those depths actually sampled, and their presence at greater depths is due to downward hydraulic gradients along active fracture zones, many of which have been shown through drilling to be mainly sub-vertical in orientation through the bedrock.

Some attempt was made to correlate groundwater composition with the regional geological model. As local fracture Zones 1 and 2 are considered to represent one of the interblock boundaries in the region, then the sampled groundwaters originate from two differing geological environments. Borehole Kl 1 lies well within the western block, and Kl 2 within the eastern block; borehole Kl 9 traverses the contact but the actual sampled level is within the western block and therefore may show some affinity with Kl 1. Comparison of the groundwater compositions, however, do not show any definitive trends that would support two distinct groundwater types. Two exceptions are the Mg and

especially the $SO_4$ contents which differentiate Kl 2 from both Kl 1 and Kl 9. Whether this is general, and can be attributed to differing hydrogeological environments requires additional data.

Future investigations should involve a considerable number of potential sampling sites, both at varying depths along the major conductive fracture zones, and from less conductive minor fracture zones yielding more representative ground/pore waters locally derived from the bedrock. This would provide a much more quantitative appraisal of the hydrochemistry which could be better correlated with younger groundwaters of short residence time (i.e. mixed waters within the highly conductive zones) and older groundwaters of long residence time (i.e. from minor fracture zones of low conductivity in the bedrock). As the latter waters should be relatively unmixed, chemical variations with depth, and/or variations due to differing bedrock geochemistries, should be more easily discernible.

## 6.3 Chemical Equilibrium Modelling of the Klipperås Groundwaters

Initially, geochemical modelling of the groundwater data was to be restricted to those waters considered to be representative. Later, it was decided to use all data to see if such modelling approaches could in any way help to detect degrees of water mixing (i e contamination). As the program deals with the saturation state of minerals, additional complementary sampling of some of the relevant fracture horizons for mineralogical identification was carried out to supplement the data already reported by Tullborg (1986). These new data are presented in Table 6.2. Furthermore, calcite, when present in these samples, was analysed for $\delta^{13}C$ and $\delta^{18}O$ (see Table 6.3).

Table 6.2: Supplementary fracture mineral identification from selected conductive zones in the Klipperås area.

| Sampled Level (m) | | Kl 1 438-80 | Kl 1 440-30 | Kl 2 329-65 | Kl 2 625-05 | Kl 2 620-30 | Kl 2 626-40 | Kl 9 698-35 |
|---|---|---|---|---|---|---|---|---|
| Å | Mineral | | | | | | | |
| 2.45<br>4.18<br>4.98 | Goethite | | | | | | | x |
| 2.51<br>2.69 | Hematite | | x | | | xx | | |
| 2.68<br>2.90 | Epidote | | | | | | | xx |
| 2.79<br>3.60 | Siderite | | | | | | x | x |
| 3.03<br>2.28 | Calcite | | x | xx | xx | (x) | x | |
| 3.21-<br>3.28 | K-feldspar | xx | x | x | x | x | ? | (x) |
| 3.35<br>4.12 | Quartz | x | x | x | x | x | x | x |
| 4.06 | Stilbite | (x) | | | | | | |
| 4.37<br>4.85 | Gibbsite | | | (x) | | | x | x |
| 3.12<br>4.7 | Talc | | | | | (x) | | |
| 7.0<br>3.5 | Kaolinite | | | x | x | | xx | |
| 10.0<br>5.0<br>3.33 | Mica | xx | xx | xx | | | | |
| 14<br>7 | Chlorite | | | x | x | xx | (x) | |

N.B. Some of the reported K-feldspar and quartz may be derived from residual drilling debris and/or the surrounding granite.

Table 6.3: $\delta^{13}C$ and $\delta^{18}O$ analyses of calcites from selected conductive zones in the Klipperås area.

| Sample (metres) | $\delta^{13}C$ (PDB) | $\delta^{18}O$ (PDB) |
|---|---|---|
| Kl 2 : 329.50 | -13.4 | -10.0 |
| Kl 2 : 620.30 | - 6.7 | -19.4 |
| Kl 2 : 625.05 | -10.9 | -17.5 |
| Kl 2 : 625.30 | - 8.9 | -21.3 |
| Kl 2 : 626.40 | -11.5 | -16.9 |
| Kl 2 : 744.40 | -10.1 | -18.4 |

As stated in section 2.3, the calculations conducted include the concentrations of all species in the aqueous solution (metal complexes etc), the redox potentials according to all chemical couples, the mineral saturations, and the gas fugacities.

### 6.3.1 Gas Fugacities

The calculated gas fugacities (for a hypothetical gas phase in equilibrium with the groundwaters) are reported in Table 6.4. It is worth noting that methane is (at least thermodynamically) rather stable in the waters sampled. This is confirmed by the gas analyses reported by Laurent (1986), and illustrated in Fig. 6.1, where the limit between bicarbonate and methane (at 1 atmos. pressure) is compared with the experimental redox potentials. It is thus possible, in theory, to generate methane from calcite by changing the pH slightly.

Table 6.4: Calculated gas fugacities in atm (from EQ3NR runs).

| Sample (vertical depth) | $log\ f_{CH_4(g)}$ | $log\ f_{CO_2(g)}$ |
|---|---|---|
| K101, 398m | -2.92 | -3.38 |
| K102, 320m 84-11-30 | | |
| surface pH | -0.71 | -2.96 |
| bottom pH | +2.88 | -2.58 |
| K102, 727m | | |
| 84-10-25 | -0.64 | -3.05 |
| K102, 746m | -2.07 | -3.03 |
| K102, 762m | -0.72 | -3.19 |
| K102, 843m | -3.72 | -3.19 |
| K109[a], 581m | -0.73 | -2.60 |

Note: a: bottom (down hole) pH.

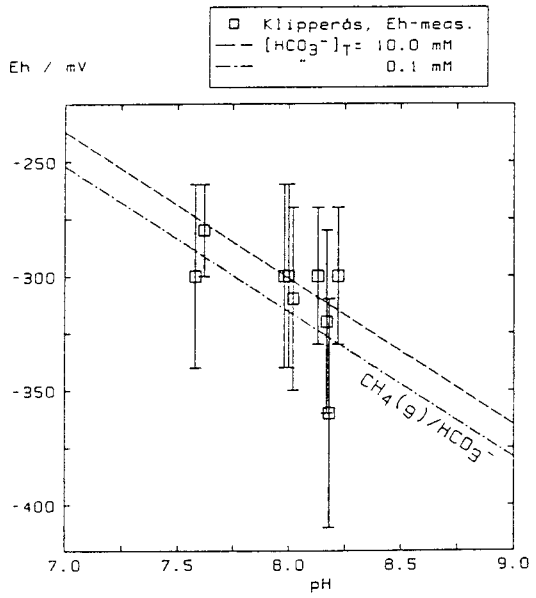


Figure 6.1: Redox potentials (measured in situ) plotted against their corresponding pH values. Theoretical stability fields for methane and bicarbonate are shown as dashed lines for two different total $HCO_3^-$ concentrations in the groundwaters. The dashed lines correspond to Eh/pH values at which the partial pressure for methane is 1 atm. Under each line, the partial pressure of $CH_4(g)$ is >> 1 atm, and above it, it is << 1 atm.

The interaction of calcite and methane is known to strongly affect the $\delta^{13}C$ in calcite. Isotopic fractionation between $CH_4/CO_2$, in addition to bacterial reduction of $CO_2$, yields $CO_2$ enriched in $\delta^{13}C$ resulting in calcite also enriched in heavy isotopes (Fritz et al, 1978). Such distinctive signatures have been reported in calcites from Gideå (Gi2:172.8m; $\delta^{13}C$ + 18) (Tullborg and Larson, 1983) and from Stripa (SBH2: 103.8m and 104.3m; $\delta^{13}C$ values of +15 and +13 respectively) (Fritz et al, 1979).

In contrast, reoxidation of light methane results in extremely low or negative $\delta^{13}C$ values within many fracture filling calcites. For example, fracture calcites from the centre of the Siljan Ring complex record low values (-18‰ to -20‰); one sample from Kråkemåla even lower (-25‰). These have been interpreted as the result of reoxidation of isotopically light methane (Smellie and Tullborg, 1985).

The two complexes cited above show that interaction between $CH_4$ and $CO_2$ mostly results in extremely high (>0) or low ($\leq$-20) $\delta^{13}C$ values in fracture calcites. Comparison with this present study show that at Klipperås the calcites fall within the interval of -14 to -2‰; one exception of -17.7‰ occurs (Tullborg, 1986). These values do not indicate any methane related calcite.

### 6.3.2 Redox potentials

The redox characteristics of groundwaters, as well as pH, have a direct impact on the speciation and solubility limits of trace metal elements. Therefore, an understanding of the processes that regulate the redox state of groundwaters is necessary in order to estimate possible effects of radioactive contamination from a nuclear repository.

In the Klipperås site, the redox potential (Eh) has been measured in situ by three different types of electrodes, gold, platinum and glassy carbon. In Table 6.5 the maximum difference

in values between the three electrodes is given as ± the average value.

As the electrode readings are expected to be controlled by the iron redox couple (Wikberg et al, 1987), the Eh has been calculated with the EQ3NR computer code from the analytical data of the total and ferrous iron content in the water (see Table 6.5). The large discrepancy between measured and calculated Eh values reflects the uncertainty in the Fe(III) concentrations. This can be explained by the extremely small difference between the measured total and ferrous iron (= ferric iron) concentrations (Table 6.1). This makes the calculation very uncertain since a change of a few percent in the analytical data will result in a change of several hundred mV in the calculated Eh values. Table 6.9 shows the effect of individual changes of total and ferrous iron, pH etc. on the calculated Eh.

Table 6.5: Measured and calculated (with EQ3NR) redox potentials in mV. and Fe(III) concentrations.

| Sample (vertical depth) | Eh (meas.) | analyzed $[Fe^{3+}]_T$ *mg/l* | calculated Eh $Fe^{3+}/Fe^{2+}$ | $HS^-/SO_4^{2-}$ | S(c)/HS- |
|---|---|---|---|---|---|
| K101, 398m | -300±30 | 0.003±0.001 | +70 | -274 | -142 |
| K102[a], 320m 84-11-30 | | | | | |
| surface pH | -300±40 | 0.004±0.004 | +53 | -267 | -127 |
| bottom pH | -300±40 | " " | +118 | -241 | -113 |
| K102, 727m | | | | | |
| 84-10-25 | -310±40 | 0.048 | +74 | -266 | -121 |
| 84-11-06 | -360±40 | 0.055±0.030 | +13 | -294 | -155 |
| K102, 746m | -300±40 | 0.014±0.020 | +24 | -268 | -118 |
| K102, 762m | -320±30 | 0.011±0.008 | +4 | -283 | -129 |
| K102, 843m | -300±40 | 0.008±0.010 | +30 | -281 | -139 |
| K109[b], 581m | -280±20 | 0.006±0.008 | +115 | -229 | -91 |

Notes a: Data from 84-11-30, except for Fe, and $S^{2-}$ values which are from 84-12-07 (they decrease with time).
b: bottom (down hole) pH.

The Eh values have also been calculated by using the analytical data for the sulphate/sulphide redox couple (Table 6.5). It should be noted from the table that these values are in fairly good agreement with the measured values. This is thought to be a pure coincidence, as it is well known that the electrode reactions are not controlled by the highly irreversible sulphide/sulphate transformation (Drever, 1982, p. 258; Lindberg and Runnells, 1984). Considering the reaction

$$SO_4^{2-} + 9\ H^+ + 8\ e^- \rightarrow HS^- + 4\ H_2O$$

the calculated redox potential for the groundwaters becomes

$$Eh(HS^-/SO_4^{2-}) = E^\circ + 55 \cdot (1/8\ \log[\{SO_4^{2-}\}/\{HS^-\}] - 9/8\ pH)$$

From this equation it is clear that "a change of 1000 in the ratio of $SO_4^{2-}$ to $HS^-$ results in a change of only about 20 mV in the corresponding computed Eh" (Lindberg and Runnells, 1984). However, a change of 0.5 pH units gives a change of about 30 mV in the computed Eh. In fact, the computed $Eh(HS^-/SO_4^{2-})$ is almost entirely dependent on $E^\circ$ and pH only.

Therefore, a comparison of the measured Eh with the calculated $Eh(HS^-/SO_4^{2-})$ values is only useful in the sense that it gives an indication of the chemical stability of sulphate in the groundwaters.

The redox couple element sulphur/hydrogen sulphide has been shown to control the measured Eh readings (in the range +50 to -200 mV) in earlier SKB's site investigations (Nordstrom and Puigdomenech, 1986). Now the Eh values are much more negative and seem to be controlled by the minerals in the bedrock (Wikberg and Grenthe, 1987). The reason for this difference can be found in the way the data was obtained. The data reported here have been obtained by down-hole Eh measuring probes, and are therefore considered to be undisturbed. The earlier data were obtained from measurements in flow-through cells on the ground surface. Contamination by small amounts of oxygen caused an oxidation of part of the sulphide. Therefore the Eh values

were controlled by the sulphur-hydrogen sulphide system. As oxygen contamination is no longer present, neither Fe(III) nor polysulphide has been formed in the sampled groundwaters. And as expected, the calculated values in Table 6.5 show that there is no longer an agreement between the experimental Eh and the $S(c)/HS^-$ values.

### 6.3.3 Mineral-water equilibria

Knowledge on the saturation state of mineral-water equilibria is necessary in order to make any assessment on the future evolution of a groundwater body. Furthermore, the saturation state of spend fuel and barrier components (like actinide oxides, canister metal, clays, etc), give an indication about the long term stability of a nuclear repository.

The mineral saturation indices that result from the computer calculations (reported in Tables 6.6-6.10) are defined as $\log(IAP/K_{sp})$ where IAP is the ion activity product, and $K_{sp}$ is the solubility product constant (see Drever, 1982, or Nordstrom and Munoz, 1985). Saturation indices greater than zero indicate that the mineral under consideration might precipitate from the groundwater, while saturation indices lower than zero indicate that the mineral, if in contact with the groundwater, would have a tendency to dissolve. However, the calculations give no indication about the rate at which such processes might occur.

The carbonate chemical system, because of its acid-base properties, is one of the most important for the regulation of pH, and also because of its complexing abilities, it affects trace metal concentrations. Most carbonate minerals are near to equilibrium with the groundwaters (c.f. Table 6.6).

The hydroxides of $Al^{3+}$ (gibbsite, Table 6.8) and $Fe^{3+}$ (Table 6.7) are also near to saturation. The same is true for fluorite (Table 6.6) and the Fe(II)-sulphide troilite (Table 6.9).

Table 6.6: Saturation indices ($\log(IAP/K_{sp})$) for some minerals (from EQ3NR calculations). Positive values indicate oversaturation. Negative values indicate undersaturation.

| Sample (vertical depth) | Calcite $CaCO_3$ | Rhodochr. $MnCO_3$ | Siderite $FeCO_3$ | $UO_2$(am) | Uranophane[a] | Fluorite $CaF_2$ |
|---|---|---|---|---|---|---|
| K101, 398m | -0.19 | -0.90 | -1.79 | -0.54 | 32.5 | 0.09 |
| K102[b], 320m 84-11-30 | | | | | | |
| surface pH | +0.15 | -0.89 | -0.69 | -0.64 | 31.9 | 0.08 |
| bottom pH | -0.26 | -1.30 | -1.09 | -0.54 | 29.7 | 0.08 |
| K102, 727m | | | | | | |
| 84-10-25 | 0.00 | 0.42 | -0.44 | --- | --- | 0.01 |
| 84-11-06 | +0.03 | -0.35 | -0.70 | --- | --- | 0.27 |
| K102, 746m | +0.03 | 0.36 | -0.12 | --- | --- | -0.36 |
| K102, 762m | +0.15 | 0.34 | -0.20 | --- | --- | -0.02 |
| K102, 843m | -0.29 | -0.53 | -0.86 | --- | --- | 0.04 |
| K109[c], 581m | -0.27 | -1.25 | -1.09 | -19.8 | -6.9 | 0.13 |

Notes a: uranophane: $Ca(UO_2)_2(SiO_3)_2(OH)_2$.
b: Data from 84-11-30, except for Fe and Mn values which are from 84-12-07 (they decrease with time).
c: bottom (down hole) pH.

Table 6.7: Saturation indices ($\log(IAP/K_{sp})$) for some iron minerals (from EQ3NR calculations). Positive values indicate oversaturation. Negative values indicate undersaturation.

| Sample (verticl depth) | $Fe(OH)_3$ amorph. | Troilite FeS | Pyrite $FeS_2$ | Magnet. $Fe_3O_4$ | Hemat. $Fe_2O_3$ | Goethite FeOOH | Siderite $FeCO_3$ |
|---|---|---|---|---|---|---|---|
| K101, 398m | 0.08 | -0.62 | 4.76 | 8.56 | 10.14 | 4.61 | -1.79 |
| K102[a], 320m | | | | | | | |
| surface pH | 0.21 | -0.06 | 4.81 | 9.50 | 10.43 | 4.76 | -0.69 |
| bottom pH | 0.19 | -0.54 | 3.83 | 8.67 | 10.38 | 4.73 | -1.09 |
| K102, 727m | | | | | | | |
| 84-10-25 | 1.20 | 0.03 | 4.22 | 11.92 | 12.28 | 5.67 | -0.44 |
| 84-11-06 | 0.29 | 0.77 | 4.43 | 10.07 | 10.47 | 4.77 | -0.70 |
| K102, 746m | 0.66 | 0.20 | 4.62 | 11.15 | 11.19 | 5.13 | -0.12 |
| K102, 762m | 0.55 | 0.36 | 4.47 | 11.01 | 19.97 | 5.02 | -0.20 |
| K102, 843m | 0.39 | 0.08 | 5.23 | 10.07 | 10.63 | 4.85 | -0.86 |
| K109[b], 581m | 0.31 | -1.34 | 2.86 | 9.01 | 10.55 | 4.81 | -1.09 |

Notes a: Data for 84-11-30, except for Fe and sulfide values which are from 84-12-07 (they decrease with time).
b: bottom (down hole) pH.

Table 6.8: Saturation indices ($\log(IAP/K_{sp})$) for some alumino-silicate minerals (from EQ3NR calculations). Positive values indicate oversaturation. Negative values indicate undersaturation.

| Sample | Gibbsite / Kaolinite | K-felspar / Muskovite | Illite / Laumontite | Clinocl.[a] / Chamos.[b] | Epid.[c] |
|---|---|---|---|---|---|
| K101, 398m | 0.68 | 2.58 | 1.18 | 3.87 | 2.31 | 0.76 | -4.71 | -2.50 | 2.35 |
| K102[d], 320m | | | | | | | | | |
| surface pH | 1.53 | 4.82 | 2.71 | 7.10 | 4.92 | 3.41 | -6.32 | 0.77 | 4.77 |
| bottom pH | 1.90 | 5.55 | 2.68 | 7.80 | 5.33 | 3.35 | <-8 | -0.07 | 3.88 |
| K102, 727m | | | | | | | | | |
| 84-10-25 | -- | -- | -- | -- | -- | -- | -- | -- | -- |
| 84-11-06 | 1.23 | 3.54 | 1.75 | 5.58 | 3.46 | 1.90 | -4.08 | 0.91 | 4.14 |
| K102, 746m | -- | -- | -- | -- | -- | -- | -- | -- | -- |
| K102, 762m | -- | -- | -- | -- | -- | -- | -- | -- | -- |
| K102, 843m | 0.95 | 3.04 | 1.54 | 4.82 | 2.98 | 1.15 | -3.31 | 0.08 | 3.15 |
| K109[e], 581m | 1.16 | 4.20 | 2.13 | 5.80 | 4.02 | 2.29 | -7.32 | -1.11 | 3.07 |

Notes a: 14Å-clinochlore: $Mg_5Al(Si_3Al)O_{10}(OH)_8$

b: 7Å-chamosite: $Fe_4^{(II)}Al_2(Si_2Al_2)O_{10}(OH)_8$

c: epidote: $Ca_2Fe^{(III)}Al_2(SiO_4)_3(OH)$

d: Data for 84-11-30, except for Fe values which are from 84-12-07 (they decrease with time).

e: bottom (down hole) pH.

Iron equilibria are of importance because they affect the redox state of the waters and therefore also affect the solubility of other trace metal elements. As mentioned above, $Fe(OH)_3$ (amorph) is near to saturation with the groundwaters, and because this is the most soluble mineral of Fe(III), all other minerals of Fe(III) are oversaturated (c.f. Table 6.7). In contrast, $Fe^{2+}$ ions in the groundwaters seem to be nearly at equilibrium with both the carbonate (siderite) and the sulphide troilite (c.f. Table 6.7). The uncertainties associated with the calculated saturation indices for iron minerals can be estimated from an inspection of Table 6.9, where individual variations are made in the parameters pH, measured Eh, and total iron concentrations.

In the case of aluminium, most minerals appear to be far from equilibrium, except for gibbsite (identified from the fracture zones; Table 6.2) and chamosite (a chlorite containing Fe(II)). This reflects both the chemical inertness (slow reaction rates for dissolution/precipitation) of many alumino-silicate minerals, and substantial uncertainties in the EQ3NR data base for these minerals.

Table 6.9: Sensitivity analysis for iron saturation indices calculated by varying individually Eh, pH and total iron contents. Results from EQ3NR calculations on a sample from borehole K11, at 398 m vertical depth. Iron concentrations are given in mg/l.

| | Eh-calc. (mV) $Fe^{3+}/Fe^{2+}$ | $Fe(OH)_3$ amorph. | Troil. FeS | Pyrite $FeS_2$ | Magnet. $Fe_3O_4$ | Hemat. $Fe_2O_3$ | Goeth. FeOOH | Sider. $FeCO_3$ |
|---|---|---|---|---|---|---|---|---|
| original[a] | +70 | 0.08 | -0.62 | 4.76 | 8.56 | 10.14 | 4.61 | -1.79 |
| Eh=-375 mV | +70 | 0.08 | -0.62 | 2.11 | 8.56 | 10.14 | 4.61 | -1.79 |
| Eh=-225 mV | +70 | 0.08 | -0.62 | 7.41 | 8.56 | 10.14 | 4.61 | -1.79 |
| pH=9.2 | -95 | +0.01 | +0.26 | 6.68 | 10.26 | 10.00 | 4.54 | -0.98 |
| pH=7.2 | +233 | -0.01 | -1.89 | 2.20 | 6.41 | 9.96 | 4.52 | -2.82 |
| $[Fe^{3+}]_T$=0.03 | +127 | 1.08 | -0.62 | 4.76 | 10.56 | 12.14 | 5.61 | -1.79 |
| $[Fe^{3+}]_T$=0.0003 | +13 | -0.92 | -0.62 | 4.76 | 6.56 | 8.14 | 3.61 | -1.79 |
| $[Fe^{2+}]_T$=0.03 | +34 | 0.08 | 0.01 | 5.39 | 9.20 | 10.14 | 4.61 | -1.16 |
| $[Fe^{2+}]_T$=0.0003 | +148 | 0.08 | -1.99 | 3.39 | 7.20 | 10.14 | 4.61 | -3.16 |

Notes a: Eh=-300 mV, pH=8.2, $[Fe(II)]_T$=0.007, $[Fe(III)]_T$=0.003

In accordance with these calculations, it can be noted that except for calcite, which is frequently found in the fractures, siderite (see Table 6.2) and also rodochrosite have been observed (Tullborg, 1986). XRD studies also prove the occurrence of Fe-oxyhydroxide (goethite) and Al-hydroxide (gibbsite); see Table 6.2. Fluorite, however, has not been observed.

Chlorite, identified in the fracture samples as 14Å-chlorite, and probably of hydrothermal origin, dominates. However, small amounts of 7Å chlorite cannot be excluded. Another Al-mineral somewhat surprisingly found is kaolinite. This mineral is mostly regarded as a clay mineral favoured by near-surface conditions.

Calcites have been sampled from some of the hydraulically conductive zones described in this report. These have been analysed isotopically (Table 6.3) and compared to the isotopic composition of the groundwaters believed to be in contact with them, in order to determine if any modern precipitation of calcite in equilibrium with the groundwater analysed has occurred. The results show varying isotope ratios not only in $\delta^{13}C$ (-6.7 to -13.4 ‰) but also in $\delta^{18}O$ (-10 to -21.3‰). This means that calcites of quite different origin occur within the sampled sections.

If the isotopic composition of the waters within borehole Kl 2 is supposed to be in accordance with the values measured in Kl 1 and Kl 9 ($\delta^{18}O$ -12 ‰, $\delta^{13}C$ -15 to -17 ‰) the only sample showing an isotopic composition close to eqilibrium with the water analysed is sample K12 - 329,5 m. The $\delta^{18}O$ values of the samples from deeper levels point to an hydrothermal origin of these calcites. This means that no extensive calcite formation occurs at present at the sampled depths, or that the sampled calcites are not in contact with the sampled waters, e.g. due to channeling in the fractures.

Table 6.10: Sensitivity analysis for uranium saturation indices calculated by varying each of the parameters Eh, pH and total uranium individually. Results from EQ3NR calculations on a sample from borehole K11, at 398 m vertical depth. Uranium concentrations are given in mg/l.

| Calculation | Uraninite $UO_2$(cr) | $UO_2$(am) | $U_3O_8$ | $U_4O_9$ | Schoepite $UO_3 \cdot 2H_2O$ | Uranophane[a] | Coffinite[b] |
|---|---|---|---|---|---|---|---|
| original[c] | +4.41 | -0.54 | -11.56 | +7.81 | -9.38 | +32.51 | +4.45 |
| Eh=-375 mV | +4.41 | -0.54 | -16.85 | +5.17 | -12.03 | +27.24 | +4.45 |
| Eh=-225 mV | +4.40 | -0.55 | -6.29 | +10.42 | -6.74 | +37.78 | +4.44 |
| pH=9.2 | +3.69 | -1.26 | -9.72 | +6.93 | -8.10 | +36.92 | +3.67 |
| pH=7.2 | +4.65 | -0.30 | -14.84 | +6.77 | -11.14 | +27.02 | +4.70 |
| $[U]_T=3.2 \cdot 10^{-3}$ | +5.01 | +0.06 | -9.75 | +10.22 | -8.78 | +33.72 | +5.05 |
| $[U]_T=0.5 \cdot 10^{-3}$ | -12.58 | -17.52 | -62.50 | -60.12 | -26.36 | -1.45 | -12.53 |

Notes a: Uranophane: $Ca(UO_2)_2(SiO_3)_2(OH)_2$(c)
b: Coffinite: $USiO_4$(c)
c: Eh=-300 mV, pH=8.2, $[U]_T=1.73 \cdot 10^{-3}$ mg/l

### 6.3.4 Uranium geochemistry

The case of uranium is specially interesting. The calculations show that of the aqueous complexes, the most stable is the phosphate $UO_2(HPO_4)_2$. This emphasizes the importance that the phosphate system has on uranium speciation, and also indicates that a thermodynamic data base revision of the uranium-phosphate system is highly desirable.

Due to weathering reactions, secondary uranium minerals (i.e. U(VI) minerals) should be forming at the expense of uraninite and other U(IV) minerals. For the sampled groundwaters of the Klipperås area, only 4 uranium analyses are available: K11, 406 m, both Dec. 1983 and June 1985, K12, 326 m, and K19, 696 m. In two of the samples (K11 from June 1985 and K12), the calculations show (Table 6.6) that $UO_2$(amorph) is near saturation. Unfortunately, no solid uranium mineral phases have been identified in the site (neither in the rock matrix, nor in the fracture filling materials), and the results of the EQ3NR calculations can not be supported by mineral identification. However, Löfvendahl (1981) has shown that silicates (specially, uranophane) are the most common secondary minerals of uranium in Sweden.

The other two samples (K11 from Dec. 1983 and K19) have lower uranium contents and are saturated or even undersaturated with uranophane (see Table 6.6 and 6.10); K11 from Dec. 1983 has a $(U)_T$ in the range $(0.2 - 0.6) \times 10^{-3}$ mg/l.

The tritium levels (Laurent, 1986) found in borehole K12 and in K11 during June-July 1985 (the time during which the second uranium sample was taken), indicate that high U-concentrations (that correspond to saturation with $UO_2$(amorph)) might be the result of weathering/oxidation, during the open hole effect, of either uraninite (from the rock matrix) or secondary uranium minerals (present as fracture filling minerals).

There is therefore the possibility that high uranium concentrations (>1ug/l) are due to the mixing of superficial and groundwaters at the sampled depths. This mixing might be

natural (due to water transport through highly conductive fractures) or, more probably, due to the perturbation that borehole activities introduce into the geological environment. These observations essentially are borne out by the hydrogeology and hydrochemistry of the site.

The saturation indices calculated by the EQ3NR code can be very sensitive to variations in the parameters employed. Table 6.10 gives an illustration of the variation in the saturation index for several uranium containing minerals when the Eh, pH and total uranium concentration are individually varied.

### 6.3.5 Conclusions of geochemical modelling

Three groundwaters (K11 406 m, K12 326 m and K19 696 m) have been sampled with little contamination of superficial (oxygen and tritium rich) waters. This results in very low Fe(III) concentrations and redox potentials below -300 mV. The calculated fugacities for methane are also rather high.

The down hole pH probe has given high quality pH values that show that the groundwaters are nearly saturated with calcite and other carbonate minerals.

Both $Fe^{3+}$ and $Al^{3+}$ ions appear to be saturated with their hydroxides ($Fe(OH)_3$(amorph) and gibbsite respectively).

The uranium concentration levels for two of the four available uranium samples are regulated by the precipitation of $UO_2$(amorph). For the other two samples the uranium concentrations indicate saturation with some secondary uranium mineral (possibly uranophane). The tritium analyses indicate that the open-hole effect might be the reason for the high (>1µg/l) uranium concentrations in two of the samples.

## 6.4 Evaluation of Borehole Tubewaves and Radar Measurements

As described under section 2, these two borehole techniques are complementary to one another. Tubewave measurements are considered to provide data relating:

- to a measure of the elastic properties of a large volume of rock
- to the detection of borehole sections of high or increased hydraulic conductivity. In general terms, it appears that tubewaves may be detected from zones with a hydraulic conductivity exceeding $10^{-10}$ m/s.
- to the detection of impermeable fracture zones filled with clay. Tubewaves from clay-filled zones have, in general, smaller amplitude than tubewaves obtained from hydraulically conductive zones.

Radar measurements are considered to result in:

- the ability to detect structural (or lithological, such as dykes) patterns (orientation and extension) within the host bedrock outside (or between) the measured boreholes, thus providing a two- or three-dimensional detailed construction of the tectonic characteristics of the bedrock. The more holes available, the better the construction.
- a general picture of the anisotropy of the total rock mass
- the identification of structures seen outside the borehole which do not intersect or should intersect the extension of the borehole.

Tubewave measurements were only carried out in borehole Kl 2 (Stenberg and Olsson, 1985). Comparison of these measurements with drillcore mapping and geophysical logging from the same hole showed a good correlation with the intersection of supposed conductive fracture zones. There is also a good correlation between tubewave sources and sections of high or increased hydraulic conductivity in the borehole. In general terms, tubewaves were detected from zones with a hydraulic conductivity exceeding $10^{-10}$ m/s (based on 20 m test

section lengths). The detection limit depends on the background hydraulic conductivity (i.e. the frequency and distribution of the conductive fracture zones), and also on the packer spacing used for the hydraulic tests, with which the tubewave data are compared.

If there is a single hydraulically conductive fracture which acts as a source of the tubewave, a distinct tubewave is obtained, and it is relatively easy to localize the source in the borehole. However, if there are several open fractures, close to each other, the tubewaves generated will interfere with each other, and a broader, less specific waveform will result. Thus, in the regions of the boreholes close to the ground surface, a large number of tubewaves are normally generated. This is probably due to a larger number of open fractures in the rock mass close to the surface, where in-situ rock stresses are lower.

There are also several cases in which tubewaves are generated in sections where no increase in hydraulic conductivity was detected. Some of these are caused by fracture zones filled with clay, making them impermeable. Tubewaves from clay-filled zones have, in general, smaller amplitude than tubewaves from hydraulically conductive zones.

The calculations of the hydraulic conductivity from tubewave data generally give values which are two orders of magnitude larger than those obtained from the hydraulic injection tests. The principal reason for this discrepancy is the difference in concepts upon which the calculation of the hydraulic conductivities is based. A further complication in the determination of hydraulic conductivity from tubewave amplitudes arises because tubewaves may be generated either by single open fractures or by a group of fractures. If there are several tubewave generating fractures close to each other, they will interfere with each other, sometimes giving constructive and sometimes destructive interference. It may be concluded from theoretical considerations and experimental data that it will be difficult to establish a quantitative relationship between hydraulic injection test results and the tubewave data.

In summary, as borehole Kl 2 has clearly shown, the tubewave method is a good tool for detecting permeable fracture zones. The method can only give qualitative results, however, but gives a wider hydrogeological perspective and is considerably quicker than hydraulic injection tests. The tubewave data, for example, may therefore be used for the selection of sections for detailed hydraulic tests or for the selection of sampling points for hydrogeochemical studies. It should be noted that tubewaves may also be generated by clay-filled impermeable fracture zones. However, this possibility can easily be checked from the core logs.

Of the 14 cored boreholes drilled in the Klipperås site area, 10 have been investigated by borehole radar; these include the three holes selected for hydrochemical characterisation. Of the many different geophysical methods for detecting inhomogenities in the rock mass, such as fracture zones or dykes, borehole radar is the only method that besides the position, also indicates the extension of zones and dykes outside the borehole. However, the determination of position in the borehole is not as exact as other geophysical methods. Other methods have only assumed that the structures have an extension in the rock mass. The radar gives a geometrical image of the area surrounding the borehole. The range of the radar in the investigated rock from single hole measurements is 100-120 m from the borehole.

Thus, from the radar map information it is possible to obtain a detailed picture of single zones and dykes and their orientation and extension, as well as a general picture of the anisotropy of the total rock mass. Also, several structures can be seen outside the borehole which do not intersect or should intersect the extension of the borehole.

The anisotropy of the rock mass is clearly seen on the radar maps from the different boreholes depending on the direction and inclination of the borehole. Inclined boreholes (see Figure 5.6) directed towards north exhibit a very characteristic pattern of almost exclusively parallel structures intersecting more or less perpendicular to the boreholes. Inclined boreholes

directed towards east or west (which include those hydrochemically described in this report) exhibit another characteristic pattern from the radar maps. Radar reflecting structures with an acute angle of intersection and several parallel structures outside the borehole is a dominating feature in these holes. This contributes to the suggestion of vertical east-west striking zones and dykes in the area. The subvertical boreholes also support the suggestion of vertical east-west striking zones and dykes.

However, there is still a possibility of the existence of horizontal structures in the area. It should be noted that structures perpendicular to the borehole only exhibit weak reflections, if any reflection at all. Taken together, these facts indicate that horizontal structures in the area are not a common feature, but cannot be excluded as single features. One example of this is the Zone H1 in Kl 2 which seems to be more or less horizontal.

The detailed investigation of the radar maps shows that the greenstones can be considered as extensive structures and usually constitute the longest radar reflecting structures. They also exhibit a somewhat undulating structure which might be caused by slight folding where the fold-axis is subvertical. Detailed investigations of encountered dolerite and ultramafic dykes show that they usually exhibit a marked loss of the direct radar pulse energy.

Comparison with the results of geophysical logging and core mapping show an expected strong correlation with low resistivity or high porosity, criteria traditionally used to identify fracture zones by geophysical logging, as well as the fracture density obtained by visual inspection of the core. A majority of the interpreted radar reflecting structures intersecting the borehole are coupled together with low resistivity. This is of course expected, since the propagation and reflection of a radar pulse is directly related to the electrical properties of the medium. In fact, the radar reflections are probably caused by rapid variations in the resistivity. It should be noted that all greenstones and mafic

dykes (dolerite and basalt) which are characterized by low resistivity also give rise to radar reflections. Most of the porphyries do not have a contrast in resistivity to the surrounding granite. As expected it was difficult to observe radar reflections from the porphyries. In fact, the reflections observed are correlated to the greenstones which appear at the margin of the porphyries or to mylonites within the porphyries. Both these features are characterized by contrasting low resistivity. Wider fracture zones and other units, e g mafic dykes (dolerite and basalt), with a very low resistivity give a strong loss in radar pulse energy.

Fracturing is a common feature associated with the different dykes detected by the radar. There is a possibility that they can be associated with higher hydraulic conductivity than dykes not detected by radar. Additional work concerning hydraulic conductivity of the dykes will be required for a complete understanding.

In general, the predicted orientation of the fracture zones from earlier investigations agree well with the orientation calculated from radar crossing angles. One of the major problems concerning the evaluation of the tectonic model for study site Klipperås was the orientation and extent of fracture Zone H1 encountered in borehole K1 2 at 792-804 m borehole length. According to the radar investigation different orientations of the fracture Zone H1 have been analyzed. The best correlation with independent information is obtained when the strike direction of fracture Zone H1 is between $180^{o}$-$210^{o}$ and the dip is $20^{o}$ to the west. With an orientation of $180^{o}/20^{o}$, the outcrop of the fracture zone correlates well with a geophysical anomaly obtained along profiles extended outside the investigated area.

The radar investigations performed in the boreholes with different directions show that a majority of the structures causing reflections are straight and elongated in one predominating direction. This would imply a relatively simple geological model of structures striking east-west. This anisotropy will probably have a great effect also on the water

movements within the bedrock. The hydraulic anisotropy depends also on the three-dimensional rock stress distribution in the rock volume. This has not been investigated within the area and warrants further studies.

In summary, the borehole radar has been a useful instrument for detection and characterization of zones and dykes in this geological environment. It has also been found to be useful for obtaining a general picture of the anisotropy of the rock mass and the geometry of the dykes and zones in the surroundings of the boreholes. It can be concluded that the borehole radar measurements have given a valuable contribution to the evaluation of the geological, geophysical and hydrogeological conditions at the Klipperås study site. In some aspects the earlier investigations gave an incomplete picture of the tectonic model of the site. The borehole radar measurements have confirmed the tectonic model and have also given complementary information for the construction of a three-dimensional model of the site. This in turn facilitates interpretation of the hydrochemistry in relation to large-scale conductive fracture zones and to differing hydrogeological environments represented by different tectonic blocks. Unfortunately the hydrochemical data are inadequate to fully exploit the potential of the hydrogeological model of the Klipperås test-site.

## 6.5 Isotopic Characteristics and origin of the Klipperås Groundwaters

Not all isotopic measurements are available, however there are sufficient available data to enable some preliminary discussion of the general groundwater isotopic characteristics.

### Radiocarbon and Tritium Isotopes

The radiocarbon results (Fig. 6.1) are presented as percentage modern derived carbon-14 (pmc) and as apparent ages (years). Also presented are the stable isotope carbon-13 values in parts per thousand (‰) which can indicate the origin of the dissolved carbonate in the water.

Carbon-14 correction methods are notoriously uncertain; the evaluation of the dilution of soil $CO_2$ originally containing 100% of modern C-14 with C-14-free carbonate to estimate the initial C-14 concentration in recharge water reaching the water table constitutes the most difficult problem of the C-14 age determination of water.

The $\delta^{13}C$ values (-17.0 and -15.7 ‰) of the waters analysed for $^{14}C$ in Klipperås indicate that carbonate minerals have been dissolved and added to the water. Water in equilibrium with the soil $CO_2$ produces $\delta^{13}C_{HCO_3^-}$ close to -20 ‰ or slightly lower in recharge areas with a pH below 6. In order to correct for this dissolution of $^{14}C$-free carbonates, $\delta^{13}C$ of the dissolved carbonate, carbonate minerals, and the soil $CO_2$, can be used. The following correction factor (q) is given by Fritz in Nordstrom et al (1985).

$$q = \frac{\delta^{13}C_{TIC} - \delta^{13}C_{carb}}{\delta^{13}C_{soil} - \varepsilon - \delta^{13}C_{carb}}$$

$\delta^{13}C_{TIC}$ is the dissolved carbonate in the water sample.

$\delta^{13}C_{carb}$ is the value for the dissolving carbonate mineral

$\delta^{13}C_{soil}$ is the isotopic composition of the soil-$CO_2$. Mostly close to -23 ‰ in areas like Klipperås.

$\varepsilon$ is the pH dependent isotopic difference between soil-$CO_2$ and inorganic carbon (TIC) under open system equilibrium conditions. The value will be close to 0 ‰ for recharge environments with pH close to 5 which can be expected in the Klipperås area.

However, to use this correction a reliable value of the dissolving carbonate has to be established. In Klipperås where the $\delta^{13}C$ values of the calcite from open fissures range from -2 to -17.7 this is somewhat problematic and the estimated q factor varies between 0,05 to 0,7.

Another unknown factor is the uptake of $^{14}C$ on calcite surfaces which would further deplete the $^{14}C$ content in the groundwater. In order to study this, calcite samples from hydraulically conductive zones in Klipperås are at present being analyzed for $^{14}C$.

The tritium results are expressed in tritium units (TU), defined as the concentration of one tritium atom per $10^{-18}$ atoms of the light hydrogen isotope ($^{1}H$). In Sweden today, the average concentration of tritium in rain water from natural sources is about 30-35 TU in a continental environment. Taking into account the inception of nuclear bomb tests in 1952, any groundwater containing more than 2 TU, i e the present-day decay value of 5 TU recharge rain water which occurred prior to 1952, indicates a post-1952 component. Similarly, any carbon-14 value higher than 80 pmc (i e the accepted amount of naturally accumulated carbon-14 reaching the water table prior to 1952) probably also indicates a post-1952 component. Following the

thermonuclear tests the carbon-14 increased in Europe to 120-160 pmc in the period 1960-65.

One of the major discrepancies of the isotopic results from the Klipperås test-site is the very old age (28000-30000 yrs; 2.18-4.29 pmc respectively) of the groundwaters which exhibit near-surface to intermediate characteristics. Furthermore, their association with major penetrating conductive fracture zones inclined sub-vertically through the bedrock, would suggest a highly active hydraulic environment. Such groundwaters are pre-1952 in age (evidenced by below detection limits (<3 TU) of tritium), but whether they can be up to 30000 years in age is not considered realistic. The question now arises as to what degree of reliability can one apply to such carbon-14 dating techniques? Hopefully, new information from the $^{14}C$ analysis of fracture calcites at present under investigation, will help to shed some light on this problem.

## Stable Isotopes

The stable isotopes deuterium and oxygen-18 are expressed as permille (‰) deviations from an international oceanic standard. They are used to distinguish waters from different origins when $\delta^{2}H$ and $\delta^{18}O$ contents are conservative. For practical purposes one usually considers two cases:

- non evaporated waters before or during recharge. Here the stable isotope content decreases with the number of condensation stages of the initial vapour, i e mainly with temperature (altitude effect, seasonal effect, paleoclimatic effect) following a slope of 8 in the $\delta^{2}H$ - $\delta^{18}O$ diagram.
- evaporated waters before or during the recharge. Here the stable isotope content increases with the amount of evaporated water, following a slope which is variable but lower than 8 in the $\delta^{2}H$ - $\delta^{18}O$ diagram.

The analytical data are few, but stable isotopic values confirm that the analysed groundwaters are meteoric in origin and have not undergone any modification due to evaporation processes.

Uranium-series Isotopes

The analytical data are as yet too few for a meaningful discussion.

## 7. ACKNOWLEDGEMENTS

This report represents a compilation of data obtained through the efforts of colleagues, both at the Swedish Geological Company and at the Royal School of Technology, Stockholm. These many persons are acknowledged. Fred Karlsson (SKB) is thanked for his continual support and critical reading of the report.

# 8. REFERENCES

Åberg, G., 1978. Precambrian geochronology of south-eastern Sweden. Geol. Fören. Stockh. Förh., 100: 125-154.

Almén, K-E., Andersson, O., Fridh, B., Johansson, B-E., Sehlstedt, M., Hansson, K., Olsson, O., Nilsson, G. and Wikberg, P., 1986. Site investigation - equipment for geological, geophysical, hydrogeological and hydrochemical characterization. SKB Technical Report TR 86-16. Stockholm.

Ask, K. and Carlsson, L., 1984. Groundwater influence by boreholes and borehole activities in crystalline rocks - preliminary studies. SKBF/KBS Status Report AR 84-27. Stockholm.

Carlsten, S., Olsson, O., Sehlstedt, S. and Stenberg, L., 1987. Radar measurements performed at the Klipperås study site. SKB Technical Report TR 87-01. Stockholm.

Drever, J.I., 1982. The Geochemistry of Natural Waters, Prentice Hall Inc., 338 pp.

Fritz, P., Reardon, E.J., Barker, J., Brown, R.M., Cherry, J.A., Killey, R.W.D., and Mc Naughton, D. 1978. The carbon isotope geochemistry of a small watershed in northeastern Ontario. Wat. Resources. Res. 14, 1059-1067.

Fritz, P., Barker, J.F. and Gale, J.E. 1979. Geochemistry and isotope hydrology of groundwaters in the Stripa granite. Univ. of California, LBL-8285, Berkeley.

Gentzschein, B., 1986. Hydrogeological investigations at the Klipperås study site. SKB Technical Report TR 86-08. Stockholm.

Holst, N.O., 1876. Geological description of map sheet Lessebo. (In Swedish). Swedish Geological Survey (SGU). Ab 4. Stockholm.

Holst, N.O., 1893. Geological description of map sheet Lenhofda. (In Swedish). Swedish Geological Survey (SGU). Ab 15. Stockholm.

Huang, C.F. and Hunter, J.A.M., 1981. A sesmic "tube wave" method for in-situ estimation of rock fracture permeability in boreholes. In S.E.G. Preprint Series, 51 st Annual International Meeting, Los Angeles, Vol. 1, E1.4, pp 23-46.

Knutsson, G. and Fagerlind, T., 1977. Groundwater supplies in Sweden. (In Swedish). Swedish Geological Survey (SGU) Reports and Notices No. 9. Stockholm.

Laurent, S., 1986. Analysis of groundwater from deep boreholes in Klipperås. SKB Technical Report TR 86-17. Stockholm.

Lindberg, R.D. and Runnells, D.D., 1984. Ground Water Redox Reactions: An Analysis of Equilibrium State Applied on Eh Measurements and Geochemical Modelling. Science, 225 (1984) 925-927.

Löfvendahl, R. 1981. Secondary uranium minerals in Sweden. Sveriges Geologiska Undersökning, Serie C, Nr 779, Avhandlingar och Uppsatser, Årsbok 74, Nr 7; Uppsala.

Lundqvist, T., 1979. The Precambrian of Sweden. SGU Ser C 768. Uppsala.

Nordstrom, D.K., and Ball, J.W. 1984. Chemical models, computer programs and metal complexation in natural waters in Complexation of trace metals in natural waters (eds. C.J.M. Kramer and J.C. Duinker); Martinus Nijhoff/Dr J.W. Junk Publishers, p. 149-164.

Nordstrom, D.K., Andrews, J.N., Carlsson, L., Fontes, J.C., Fritz, P., Moser, H. and Olsson, T. 1985. Hydrogeological and hydrochemical investigations in boreholes - Final report of the phase 1 geochemical investigations of the Stripa groundwaters. Stripa Project Technical Report 85-06.

Nordstrom, D.K. and Munoz, J.L. 1985. Geochemical Thermodynamics, Benjamin/Cummings, 477 p.

Nordstrom, D.K., and Puigdomenech, I. 1986. Redox chemistry of deep groundwaters in Sweden. SKB Technical Report TR 86-03, Stockholm.

Olkiewicz, A., Magnusson, K-Å., Tirén, S.A. and Gentzschein, B., 1984. Geological, geophysical and hydrogeological investigations of the Klipperås area (Map Sheet 4F NE Småland). (In Swedish). Swedish Geological Company (SGAB) Internal Report. Uppsala.

Olkiewicz, A. and Stejskal, V., 1986. Geological and tectonical description of the Klipperås study site. SKB Technical Report TR 86-06. Stockholm.

Olsson, O., Sandberg, E. and Nilsson, B., 1983. The use of borehole radar for the detection of fractures in crystalline rock. Stripa Project, IR-83-06, SKBF/KBS. Stockholm.

Olsson, O. and Sandberg, E., 1984. Preliminary design of a new borehole radar system. Stripa Project, IR-84-04, SKBF/KBS. Stockholm.

Olsson, O., Forslund, O., Lundmark, L., Sandberg, E. and Falk, L., 1985. The design of a borehole radar system for the detection of fracture zones. In Proc. on "In situ experiments in granite associated with the disposal of radioactive waste". OECD. Stockholm.

Pousette, J., Müllern, C-F, Engqvist, P. and Knutsson, G., 1981. Description and appendices to the hydrogeological map of Kalmar county. SGU Serie Ah 1. Uppsala.

Sehlstedt, S. and Stenberg, L., 1986. Geophysical investigations at the Klipperås study site. SKB Technical Report TR 86-07. Stockholm.

Swedish Geological Survey, 1960. Geological map of Sweden. Ba 16. Stockholm.

Smellie, J.A.T. and Tullborg, E-L. 1985. Geochemical investigations in the Siljan area, Sweden. SGAB Internal Report, IRAP 85214, Uppsala/Göteborg.

Smellie, J., Larsson, N-Å., Wikberg, P. and Carlsson, L., 1985. Hydrochemical investigations in crystalline bedrock in relation to existing hydraulic conditions: Experience from the SKB test-sites in Sweden. SKB Technical Report TR 85-11. Stockholm.

Stenberg, L. and Olsson, O., 1985. The tubewave method for identifying permeable fracture zones intersecting a borehole. SKB Status Report AR 85-14. Stockholm.

Stenberg, L. 1984. Tubewavemätning i borrhål K102, Klipperås. SGAB Internal Report, IRAP 84105.

Stenberg, L. 1986. Geophysical laboratory investigations on core samples from the Klipperås study site. SKB Technical Report TR 86-09. Stockholm.

Swedish Geological Survey (SGU): Geological Map of Sweden. Ba 16. Stockholm.

Tullborg, E-L. and Larson, S.Å. 1983. Fissure fillings from Gideå, central Sweden. SKB Technical Report TR 83-74. Stockholm.

Tullborg, E-L., 1986. Fissure fillings from the Klipperås study site. SKB Technical Report TR 86-10. Stockholm.

Wikberg, P., Axelsen, K. and Fredlund, F. 1987. Deep groundwater chemistry. SKB Technical Report TR 87-07. Stockholm.

Wikberg, P. and Grenthe, I. 1987. Redox Conditions of deep groundwaters. Submitted to Geochim. Cosmochim. Acta.

Wolery, T.J. 1979. Calculation of chemical equilibrium between aqueous solution and minerals: the EQ3/6 software package, UCRL-52658. Lawrence Livermore Nat. Lab., California 94550, 41 pp.

Wolery, T.J. 1983. EQ3NR, a computer program for geological aqueous speciation-solubility calculations: User´s guide and documentation UCRL-53414. Lawrence Livermore Nat. Lab., California 94550, 191 pp.

# *List of SKB reports*

## Annual Reports

*1977–78*
TR 121
**KBS Technical Reports 1 – 120.**
Summaries. Stockholm, May 1979.

*1979*
TR 79–28
**The KBS Annual Report 1979.**
KBS Technical Reports 79-01 – 79-27.
Summaries. Stockholm, March 1980.

*1980*
TR 80–26
**The KBS Annual Report 1980.**
KBS Technical Reports 80-01 – 80-25.
Summaries. Stockholm, March 1981.

*1981*
TR 81–17
**The KBS Annual Report 1981.**
KBS Technical Reports 81-01 – 81-16.
Summaries. Stockholm, April 1982.

*1982*
TR 82–28
**The KBS Annual Report 1982.**
KBS Technical Reports 82-01 – 82-27.
Summaries. Stockholm, July 1983.

*1983*
TR 83–77
**The KBS Annual Report 1983.**
KBS Technical Reports 83-01 – 83-76
Summaries. Stockholm, June 1984.

*1984*
TR 85–01
**Annual Research and Development Report 1984**
Including Summaries of Technical Reports Issued during 1984. (Technical Reports 84-01–84-19)
Stockholm June 1985.

*1985*
TR 85-20
**Annual Research and Development Report 1985**
Including Summaries of Technical Reports Issued during 1985. (Technical Reports 85-01-85-19)
Stockholm May 1986.

*1986*
TR86-31
**SKB Annual Report 1986**
Including Summaries of Technical Reports Issued during 1986
Stockholm, May 1987

## Technical Reports

*1987*
TR 87-01
**Radar measurements performed at the Klipperås study site**
Seje Carlsten, Olle Olsson, Stefan Sehlstedt, Leif Stenberg
Swedish Geological Co, Uppsala/Luleå
February 1987

TR 87-02
**Fuel rod D07/B15 from Ringhals 2 PWR: Source material for corrosion/leach tests in groundwater**
**Fuel rod/pellet characterization program part one**
Roy Forsyth, Editor
Studsvik Energiteknik AB, Nyköping
March 1987

TR 87-03
**Calculations on HYDROCOIN level 1 using the GWHRT flow model**
**Case 1 Transient flow of water from a borehole penetrating a confined aquifer**
**Case 3 Saturated-unsaturated flow through a layered sequence of sedimentary rocks**
**Case 4 Transient thermal convection in a saturated medium**
Roger Thunvik, Royal Institute of Technology, Stockholm
March 1987

TR 87-04
**Calculations on HYDROCOIN level 2, case 1 using the GWHRT flow model**
**Thermal convection and conduction around a field heat transfer experiment**
Roger Thunvik
Royal Institute of Technology, Stockholm
March 1987

TR 87-05
**Applications of stochastic models to solute transport in fractured rocks**
Lynn W Gelhar
Massachusetts Institute of Technology
January 1987

TR 87-06
**Some properties of a channeling model of fracture flow**
Y W Tsang, C F Tsang, I Neretnieks
Royal Institute of Technology, Stockholm
December 1986

TR 87-07
**Deep groundwater chemistry**
Peter Wikberg, Karin Axelsen, Folke Fredlund
Royal Institute of Technology, Stockholm
June 1987

TR 87-08
**An approach for evaluating the general and localized corrosion of carbon steel containers for nuclear waste disposal**
GP March, KJ Taylor, SM Sharland, PW Tasker
Harwell Laboratory, Oxfordshire
June 1987

TR 87-09
**Piping and erosion phenomena in soft clay gels**
Roland Pusch, Mikael Erlström,
Lennart Börgesson
Swedish Geological Co, Lund
May 1987

TR 87-10
**Outline of models of water and gas flow through smectite clay buffers**
Roland Pusch, Harald Hökmark,
Lennart Börgesson
Swedish Geological Co, Lund
June 1987

TR 87-11
**Modelling of crustal rock mechanics for radioactive waste storage in Fennoscandia—Problem definition**
Ove Stephansson
University of Luleå
May 1987

TR 87-12
**Study of groundwater colloids and their ability to transport radionuclides**
Kåre Tjus* and Peter Wikberg**
*Institute for Surface Chemistry, Stockholm
**Royal Institute of Technology, Inorganic Chemistry Stockholm
March 1987

TR 87-13
**Shallow reflection seismic investigation of fracture zones in the Finnsjö area method evaluation**
Trine Dahl-Jensen
Jonas Lindgren
University of Uppsala, Department of Geophysics
June 1987

TR 87-14
**Combined interpretation of geophysical, geological, hydrological and radar investigations in the boreholes ST1 and ST2 at the Saltsjötunnel**
Jan-Erik Andersson
Per Andersson
Seje Carlsten
Lars Falk
Olle Olsson
Allan Stråhle
Swedish Geological Co, Uppsala
1987-06-30

TR 87-15
**Geochemical interpretation of groundwaters from Finnsjön, Sweden**
Ignasi Puigdomènech[1]
Kirk Nordstrom[2]
[1]Royal Institute of Technology, Stockholm
[2]U S Geological Survey, Menlo Park, California
August 23, 1987

TR 87-16
**Corrosion tests on spent PWR fuel in synthetic groundwater**
R S Forsyth[1] and L O Werme[2]
[1]Studsvik Energiteknik AB, Nyköping, Sweden
[2]The Swedish Nuclear Fuel and Waste Management Co (SKB), Stockholm, Sweden
Stockholm, September 1987

TR 87-17
**The July – September 1986 Skövde aftershock sequence**
Conny Holmqvist
Rutger Wahlström
Seismological Department, Uppsala University
August 1987

TR 87-18
**Calculation of gas migration in fractured rock**
Roger Thunvik[1] and Carol Braester[2]
[1]Royal Institute of Technology
Stockholm, Sweden
[2]Israel Institute of Technology
Haifa, Israel
September 1987

TR 87-19

**Calculation of gas migration in fractured rock – a continuum approach**

Carol Braester[1] and Roger Thunvik[2]
[1]Israel Institute of Technology
Haifa, Israel
[2]Royal Institute of Technology
Stockholm, Sweden
September 1987

TR 87-20

**Stability fields of smectites and illites as a function of temperature and chemical composition**

Y Tardy, J Duplay and B Fritz
Centre de Sédimentologie et de Géochimie de la Surface (CNRS)
Institut de Géologie Université Louis Pasteur (ULP)
1 rue Blessig, F-67084 Strasbourg, France
April 1987